



<https://theses.gla.ac.uk/>

Theses Digitisation:

<https://www.gla.ac.uk/myglasgow/research/enlighten/theses/digitisation/>

This is a digitised version of the original print thesis.

Copyright and moral rights for this work are retained by the author

A copy can be downloaded for personal non-commercial research or study,  
without prior permission or charge

This work cannot be reproduced or quoted extensively from without first  
obtaining permission in writing from the author

The content must not be changed in any way or sold commercially in any  
format or medium without the formal permission of the author

When referring to this work, full bibliographic details including the author,  
title, awarding institution and date of the thesis must be given

Enlighten: Theses

<https://theses.gla.ac.uk/>  
[research-enlighten@glasgow.ac.uk](mailto:research-enlighten@glasgow.ac.uk)

M. Sc. Thesis

MODAL ANALYSIS OF COMPLEX STRUCTURES USING

THE FINITE ELEMENT METHOD

C Graham Cook 1986

ProQuest Number: 10948148

All rights reserved

INFORMATION TO ALL USERS

The quality of this reproduction is dependent upon the quality of the copy submitted.

In the unlikely event that the author did not send a complete manuscript and there are missing pages, these will be noted. Also, if material had to be removed, a note will indicate the deletion.



ProQuest 10948148

Published by ProQuest LLC (2018). Copyright of the Dissertation is held by the Author.

All rights reserved.

This work is protected against unauthorized copying under Title 17, United States Code  
Microform Edition © ProQuest LLC.

ProQuest LLC.  
789 East Eisenhower Parkway  
P.O. Box 1346  
Ann Arbor, MI 48106 – 1346

## Summary

The subject dealt with concerns Finite Element analyses of complex structures. In particular the area studied is the determination of the natural frequencies and mode shapes of centrifugal-type impellers and the impact of this analysis on human and computer resources.

This investigation was carried out during a Teaching Company project between Glasgow University and James Howden and Company Ltd, involving optimisation of modal analysis of James Howden impeller products using the PAFEC FE package. The object was to maximise the accuracy of the analysis results whilst minimising both computer effort and man effort required for the analysis.

As well as investigations of simple structures, several impeller structures were modelled and analysed, and some results verified experimentally. Different modelling techniques were used and several element types considered. The full analysis was considered, ie pre-modelling steps; modelling the structure; analysing the structure; and interpreting the results.

The accumulation of specific results on good modelling practice allowed a Design Guide to be produced for James Howden which could lead an inexperienced FE analyst to produce an accurate model of a centrifugal impeller and from this produce natural frequency results in an accuracy band of +14% to -3.5%, utilising the minimum computer effort.

The examples of good modelling practice and considerations required in complex FE analyses are transferrable to many different types of analysis and many different types of FE package. The main conclusions of the investigation include the careful considerations necessary for different stages of an FE analysis, particularly when a complex structure is being analysed. Results from simple analyses are not transferrable to complex analyses and often methods and element types used do not produce the required results. However objective evaluations such as this one on a "family" of structures such as centrifugal impellers can produce guidelines which do not rely on the "art" or expertise of the FE analyst.

As computing time becomes an increasingly precious resource in engineering companies, labour-saving aids and minimisation of computer effort required are actively sought. This investigation considers and advises on both of these.

## Acknowledgements

I would like to thank James Howden and Company Ltd. for their patience in allowing me to command use of their computing facilities at will.

In particular I would like to thank Dr. R. G. Mulholland, who guided me through the mysticisms of mechanical engineering.

## Contents

<u>Section</u>	<u>Page</u>
Introduction	1
1. Initial Steps	4
2. Modelling the Structure	9
3. Carrying out the Analysis	25
4. Interpreting the Results	29
5. Discussion of Results	40
6. Conclusion	49
Figures	53
References	74
Appendix A	75
Appendix B	95
Appendix C	103

## Introduction

This investigation was carried out during a Teaching Company Associate post at the University of Glasgow and James Howden and Company Limited, (Manufacturers of air and gas handling equipment). The Teaching Company project involved optimising and rationalising the determination of natural frequencies and mode shapes of James Howden impeller products, using the PAFEC F.E. suite.

The F.E. method has been used widely in the past 20 years in both industry and research fields. With the relatively recent availability of large capacity computing resources at relatively low cost the ability to analyse complex structures has become widespread in many engineering companies. However for engineers with relatively little experience in the techniques of F.E. modelling, there is limited practical and objective advice on how to carry out complex analyses. There are texts which suggest good modelling practice (5) including the respective software manufacturers' literature, although these are usually validated by results on simple structures and consider only one part of the analyses eg. comparisons of element formulations. The results of this investigation have shown that recommendations based on the results of simple structure analyses are not always prudent for more complex structures.

This investigation seeks to give practical and objective advice on the complete F.E. analysis from approaching the construction of the model to analysing the results produced, and is validated by testing both simple and complex structures.

It is therefore set out according to the stages encountered in any F.E. analysis :

1. Initial steps (pre-modelling decisions)

2. Modelling the structure

3. Carrying Out the Analysis

4. Interpreting the Results

It includes a component of the F.E. analysis that is seldom considered - the computing effort required. Central Processing Unit time i.e. time spent actually computing, is becoming a scarce resource in today's engineering companies as more departments utilise the company's computers. This study considers ways to minimise the amount of computing effort required to produce acceptable results.

By covering 1 facet of F.E. analysis - natural frequency determination - and comparing it with other types eg. stress calculations, the investigation seeks to serve two purposes :

1. To provide a general guide for users analysing complex structures using F.E. software packages. This study indicates how to prepare an objective modelling strategy that will produce consistent analyses. Without such an objective strategy to follow, the results of an F.E. strategy depend on the users' 'art' or expertise, to produce a satisfactory model. The study also seeks to stimulate the users' awareness of the extra problems faced when dealing with the F.E. analysis of a complex structure. F.E. analyses of simple structures can be checked theoretically or practically. Measuring the behaviour of a complex structure can be difficult and can place more emphasis on numerical techniques such as the F.E. method.

By following the layout of this investigation and considering the types of points raised, the user is in a position to model a complex structure and be aware of those features requiring investigation before a reliable modelling method is proposed for

that structure.

2. For those engineers involved in using F.E. packages to analyse centrifugal-type impellers for natural frequency and mode shape determination, this investigation can be used directly to prepare, analyse and interpret an F.E. model.

Obviously this study concerns one F.E. package - PAFEC - and the results will not be directly comparable to every F.E. software suite. However the numerical methods - see Appendix A - used in PAFEC are common in many F.E. packages.

Many of the general and specific points raised in this investigation are points regarding good F.E. practice and do not relate solely to the PAFEC natural frequency analyses of centrifugal impellers.

GENERAL PRINCIPLES

Any F.E. analysis will be carried out in response to a request for some type of information - a 'problem'. cursory consideration of the problem can lead to at best wasted time and effort and at worst incorrect results accepted as correct. The very first step therefore in an F.E. project is to consider the problem very carefully.

Some questions that require answering before an analysis is attempted are :

A. Exactly What is Required ? - if for example a stress analysis of a part is required ; is the maximum stress required ? Is the highest stress in a particular area required ? Are displacements also required ?

B. What Accuracy is Required ? - can an F.E. type analysis be expected to produce this type of accuracy ? Does it require a special approach to achieve this accuracy ?

C. Can the Software Package Carry out the Analysis ? - ensure that the package to be used is robust enough to handle the problem type, size and accuracy required.

D. Can the Computer Carry Out the Calculation ? - Many software packages can carry out calculations approaching infinite size - computers cannot ! How long will the analysis take ? Constraints may be placed on when the results are required and some calculations can take days of continuous computer use to complete.

The means of finding answers to the above questions are not contained in this investigation but are highlighted to ensure that they are given the attention they deserve, as without answers to them no F.E. analysis should proceed.

investigation - determination of natural frequencies of centrifugal-type impellers - the above questions are now considered.

### The Problem

A. Natural frequencies of a centrifugal impeller are required. As will be explained later, the natural frequencies will be those of a static impeller mounted on infinitely stiff supports. The range of natural frequencies of interest are from 0 Hz. to an upper frequency which can be detailed for each individual analysis.

B. Bearing in mind the increasing numerical innaccuracy inherent in the ability of the software package (PAFEC) used to calculate the higher natural frequencies, results will be taken to the nearest Hz. and in conjunction with test data will determine the accuracy which can be achieved. The PAFEC solution method is outlined in appendix A.

C. The software package used for this investigation is adequate for calculating natural frequencies of unloaded structures.

D. Computing time is a precious resource in engineering companies and this type of analysis consumes large amounts of it. One of the aims of this investigation is to ensure that it is minimised.

### The Structure

Once the problem has been defined, the structure to which it is addressed must also be carefully considered before a modelling strategy can be formulated. The structure should be examined to identify features which may affect the constraints of time taken to perform the analysis and accuracy required. With respect to the centrifugal impeller structure, such features are :

1. supports,

2. symmetry,

3. 'special' features

4. revolving or stationary impeller.

1. Supports- considered in a later section, but the nature of support of any structure will obviously affect particular natural frequencies of it.

2. Symmetry- use of symmetry and appropriate boundary conditions can greatly reduce the amount of computing effort required to obtain results. Unfortunately seldom will a real structure have ideal, pure symmetry and a decision has to be taken on whether the approximation of symmetry is valid. For an impeller, slight misalignments in fabrication of blades, application of balance patches and other features, produce a structure which has no perfect symmetry. However these imperfections do not affect the natural frequencies significantly and the recommendation is to treat the impeller as being made up of a number of identical segments each containing a blade.

However we now have a situation which again has to be referred back to 'The Problem'. If the analysis were a static one, simple boundary conditions may be applied to the segment model to produce results for the full model. However as the analysis is a natural frequency one, more complex boundary conditions are required to produce the anti-symmetric modes. Referring to the software limitations point mentioned earlier, an add-on to the main PAFEC suite, called RABBITS, can be used to apply the appropriate boundary conditions automatically. Without this RABBITS package, modelling and analysing the full impeller would prove a task so large that the computer used to run the PAFEC

to do it ! Other large software suites also contain cyclic symmetry packages eg. NASTRAN, ABAQUS.

### 3. 'Special' Features

This can be considered as areas within the structure requiring special attention - perhaps stress raising sections of a structural analysis - or any parts of the structure which may have a significant effect on the behaviour of the structure . The method of supporting the impeller structure has already been identified, but as shall be explained later, the inclusion of the shaft or omission of it in the impeller model can also directly affect some natural frequencies of the impeller.

### 4. Revolving or Stationary Impeller

Centrifugal stiffening and gyroscopic-type effects mean that the natural frequencies of a revolving impeller are different to those of the static impeller. For low rotational speeds the effect on the natural frequencies is negligible. This is highlighted in the relation shown by Den Hartog<sup>①</sup> for centrifugal stiffening effects of simple discs. However to take account of such effects in complex structures such as centrifugal impellers requires the use of sophisticated packages such as ABAQUS or SNAKES (part of the PAFEC suite). As centrifugal impellers rotate at relatively low speeds and because the inclusion of rotational effects vastly increases the problem size, the impeller is taken to be static.

### Information Required Prior to Modelling

At this point , with the problem well defined and the structure fully considered, assembly of relevant information to be able to construct an F.E. model would be the next requirement.

As well as overall dimensions of the structure detailed on suitable engineering drawings, plate thicknesses and material properties such as density, Youngs Modulus and Poissons ratio, must also be obtained. Even if the model building process utilises 'drawings' passed automatically via some C.A.D. interface, all parameters should be checked to ensure correlation with the real structure. The time taken to manually create an F.E. model of a centrifugal impeller can be longer than the time taken to carry out the analysis on the model and produce the results, and as such should be given very careful consideration.

Time saving aids such as digitising profiles direct from scale drawings or using mesh generation facilities should therefore be used where available. This investigation has demonstrated the need for careful 'double-checking' of information, as in one instance engineering drawings used to create a model of an impeller did not contain information of blade liners which had been attached (effectively increasing the plate thickness of a portion of a blade). The results obtained were 20% lower than the true results and had taken 4 man days to obtain.

A further piece of information that can prove useful to the modeller is an estimate of the real mass of the structure to compare to the F.E. model mass, as this can often be a powerful first check on the accuracy of the F.E. model.

## What to Model ?

This question often poses a problem to the F.E. modeller interested in the behaviour of large complex structures.

If the natural frequencies of the flat disc in figure 1 are required then the problem is relatively simple, as the complete structure can be geometrically represented by appropriately shaped elements and the resulting model is fixed at the centre.

If the natural frequencies of a complex structure such as a centrifugal impeller are required, an immediate problem arises as to what should be modelled - is the impeller casing required? do the support structures, bearings, foundations etc., affect the results? will the shaft be required in the model? is exact geometrical representation required? etc.

This section takes the centrifugal-type impeller as an example of a complex structure, examines areas where doubts may exist and indicates practice which will ensure acceptable results.

### General Structure

In the case of the centrifugal-type impeller the requirement is to calculate the impeller natural frequencies to ensure that no exciting force frequencies coincide and result in fatigue problems. For example the impeller casing would not affect the natural frequencies of the impeller and should not be modelled.

### Impeller Shaft and Supports

Although when determining the load/deflections, stresses etc. of an impeller there is no need to model the shaft, it is well known that the shaft, and supports for the shaft affect natural frequency calculations. Such effects are well documented and will not be quantified in this investigation. What will be highlighted are the effects produced when the impeller is modelled with and

without the shaft.

If the shaft is not modelled and the appropriate infinite stiffness supports applied to the hub, then those modes such as in figure 2 in which the shaft displaces, would not be obtained. Also the diaphragming-type modes such as figure 3 would not have the correct frequency due to the axial restraint on the hub and the omission of the shaft mass. Thus if the modeller is not interested in these groups of frequencies then the shaft need not be modelled. The remaining impeller side and centreplate 'ripple' modes would be correct and would be obtained with less computer effort due to the smaller model.

If however the diametral-type (shaft modes) and diaphragming-type modes are of interest then the shaft would have to be modelled and the supports given attention.

For the in-service condition of a centrifugal-type impeller, the shaft rotates on a flexible oil-film, resting on a finite stiffness bearing housing, foundations etc. and a value for the finite stiffness support can be calculated. To obtain accurate values for the natural frequencies of the modes in which the shaft displaces the finite stiffness support conditions would have to be modelled, even though the shaft supports would not affect the impeller 'ripple' modes or the diaphragming modes. Because of the many methods available to calculate shaft critical speeds accurately and simply and in view of the earlier recommendation on modelling the impeller as a static structure it is not recommended to model the shaft supports as finite stiffness supports but to restrain the shaft from moving in the plane perpendicular to the shaft centre-line at nodal points on the bearing centres as shown in figure 4. This leaves the

the axial direction and providing the correct natural frequency results for diaphragming and torsional modes.

### Shrink-Fitted Hubs

Much work has been done on the stress raising effects of shrink-fitted hubs on shafts. <sup>③</sup> <sup>④</sup> The effects on natural frequencies were investigated by comparing a single inlet impeller with a fully connected hub as in figure 5 , with a model containing a shrink-fitted hub as in figure 6. This shrink-fit was approximated by connecting the hub to the shaft at the ends only leaving the interior hub nodes unconnected to the shaft.

The results in Table 1 below show that the effect of the shrink-fit approximation on the natural frequencies is negligible.

(Hz.)	<u>Fully Connected Hub</u>	<u>Shrink-Fit Hub</u>
	42	42
	82	82
	119	119
	197	196
	286	287
	304	302

Table 1

However the shrink-fit model uses less brick elements for the analysis and reduces the computing effort appreciably as shall be explained later. The recommendation therefore is to model the impeller with the shrink-fitted hub.

With the abundance of large F.E. packages there are often a bewildering array of element types seemingly suited to modelling a particular situation. Guidelines are often presented by the package manufacturers on uses of their element types and of their limitations. Care should be taken however to determine the limitations as often the guidelines suggested can produce incorrect results. Theoretical formulations of elements should also be sought to determine an elements' applicability to a particular situation. It is not the purpose of this report to analyse different element formulations but to highlight general principles by using a set of common element formulations found in the PAFEC F.E. package suite.

For natural frequency analysis of structures such as impellers where the majority of the structure is platework, 2D elements which can undergo membrane and bending deformations are necessary.

The general advice of many user guides such as NAFEMS<sup>⑤</sup> is to use high order elements (more complex) for better results; to avoid using triangular 2D elements as they are in general poor elements; and to avoid distorted elements as they again produce poor results. However the findings of this investigation are that such generalisations can be misleading.

#### High Order Elements

In general high order elements tend to be more expensive to use in terms of computing time, than low order simple elements. The strategy proposed therefore is to use the simplest element type available that will definitely produce acceptable results. i.e. the decision on which element types to use should only be based on previous experience in similar situations. Problems

encountered and recommendations for which element types should be used for natural frequency analyses of impeller models are indicated below.

Beams v Bricks

Consider the arrangement of the free structure of a thin disc mounted on a long shaft as in figure 7. The investigation of the natural frequencies of this structure using the PAFEC F.E. suite highlighted the problem in assuming that high order elements will always produce better results than the simpler element types.

The first model created used solid ( 3D ) elements throughout the shaft and hubs and 2D shell elements for the plate. The unsupported F.E. model results are shown below in Table 2.

Brick Element Shaft Model (Hz.)

140

244

625

737

Table 2

Resonance testing of the structure was carried out by placing the shaft in a flexible sling and using a calibrated hammer and spectrum analyser to record the natural frequencies. The results obtained for Table 3 below, clearly differ appreciably from those in Table 2.

84

144

468

496

Table 3

A second F.E. model was created by replacing the shaft brick elements by beam ( 1D ) elements . The results below in Table 4 show that the beam element model is far superior to the brick element model.

Beam Element Shaft Model

83

141

465

493

Table 4

On investigation of the brick element model the reason found for its unsuitability was the inability of 'straight-sided' bricks used in the shaft to represent the modes with curved displacements in the shaft. As these 6 noded wedge shaped elements have no mid-side nodes there is a linear displacement assumption between the nodes and the cumulative effect of this in the shaft produces the large discrepancies in frequency results. The beam elements on the other hand have a cubic bending assumption along their length which can describe the displacement curvature well and produces the correct frequencies.

In terms of centrifugal impellers the shaft , when modelled ,

shaft bending frequencies without the expense of brick elements with mid-side nodes.

#### 8 Noded Quadrilaterals v 4 Noded Quadrilaterals

In structures such as impellers plate-like members often meet at angles and bending in one plate is usually coupled to bending and membrane effects in an adjacent plate meeting it at an angle. To describe such a situation flat elements with both membrane and bending effects are required. PAFEC contains such a family of facet shell elements which have only five degrees of freedom at each node (no in-plane rotation of element nodes) at the element level although after transformation to a general shell the extra freedom is introduced. These element types must however be flat and also are based on thin plate theory. Within this family there is a 4 noded quadrilateral, and an 8 noded quadrilateral with mid-side nodes. In view of the aforementioned limitations of straight-sided elements a model of the flat disc as in figure 1 was examined. Using the cyclic symmetry of a disc a 60 segment of curved elements and a 60 segment of straight-sided elements was created. To try and have a useful comparison in terms of numbers of degrees of freedom describing the model, 4 curved elements and 8 straight-sided elements were used. The results of Table 5 below, clearly show the curved element model (higher order element) to be superior.

The theoretical frequencies were calculated from Timoshenko formulae. ⑥

<u>Straight-Sided Element Model</u>	<u>Curved Element Model</u>	<u>Theoretical Frequencies</u>
304	224	---
703	671	655
1645	1557	1525
2807	2467	2607

Table 5

A similar examination of these shell elements was made on an impeller model, replacing two 4 noded shell elements with one 8 noded curved shell element. However using curved shell elements in the model required attaching curved bricks at the appropriate parts of the model and the result was that the curved element model contained many more degrees of freedom than the straight-sided element model even though the number of elements was smaller. The two models created are shown in figures 8 and 9 with a sample of the frequencies obtained shown below in Table 6.

<u>Straight-Sided Element Model (Hz.)</u>	<u>Curved Element Model (Hz.)</u>	<u>Resonance Test Results (sample) Hz.</u>
42	41	64
78	77	96
158	160	176

Table 6

Bearing in mind the small effect on the frequencies obtained using curved shell elements and the fact that no reduction in the mesh density of either model would be practicable, there is no evidence to support using curved shells in the impeller models and that straight-sided shells should be used. This is further supported by the difference in computing times necessary to produce the natural frequencies of the two models.

Straight-Sided Shells : 152 Elements (Total in model)

941 Degrees of Freedom

18 hrs. Central Processing Unit Time

Curved Shells 72 Elements (Total in Model)

1469 Degrees of Freedom

46 hrs. Central Processing Unit Time

The recommendation for impeller natural frequency analysis using the PAFEC suite is therefore to use the straight-sided shell elements. This clearly illustrates the fact that 'validation' of methods on simple structures such as the flat disc will not necessarily reflect the best methods of analysing complex structures, and there is no substitute for experience of analysing similar structures.

Recommendations for Centrifugal Impellers  
(Impeller parts identified in figure 10)

Based on the investigations into three different types of centrifugal impeller and the preceding comments, an F.E. model capable of producing an efficient analysis in terms of time taken to perform it and resulting accuracy should contain the following element types :

Backplate/Centreplate/Sideplate/  
Coneplate/Blade(hollow or plate) -

Basically regular 4 noded thin shell (2D) elements capable of transmitting bending and membrane effects. Triangular elements can be used with confidence to describe complex geometries, or to prevent the use of many small quadrilaterals.

Hub/Inlet Ring -

8 noded brick (3D) elements . Triangular prisms should not be used. Appropriate coupling mechanisms may be necessary to link

Shaft -

2 noded beam (1D) elements are sufficient to describe the flexural shaft movements, and the distributed mass of the shaft.

How to Arrange Mesh ?

F.E. Stress calculations can be very sensitive to mesh density and areas such as changes of section should contain finer mesh detail than areas of no interest. However when calculating natural frequencies of structures a more regular mesh is desirable , and in fact for a package such as PAFEC which uses a reduced eigenvalue type solution method , fine mesh detail can lead to problematic numerical errors. With this in mind the minimum mesh density required to produce acceptable results was considered. There are basic rules applied to the impeller which apply to any structure for which the natural frequencies are being calculated.

1. The element types placed in any region must be able to transmit accurately the type of modal deformations of interest to the modeller.
2. There must be sufficient nodal points in any area of the model to describe the relative displacements of points on the structure in each mode of interest.

Two impeller meshes are shown in figure 11. Clearly the mesh densities and thus the time taken to perform the analyses will be different in each case. A sample of the frequencies obtained are shown below in Table 7 along with the resonance test results for comparison.

Results (Hz.)	Results (Hz.)	Resonance test Results (Hz.)
41	40	42
82	79	72
135	145	140
198	196	190
331	317	296
401	395	376

C.P.U.= 7.5 hrs.      C.P.U.=14.5 hrs.

Table 7

From the above results which show a small increase in accuracy in the fine mesh model for a large increase in computer effort, there is clearly little benefit in this fine mesh being used to obtain these natural frequencies.

However if the modeller was interested in the high frequency modes, the fine mesh with its greater number of degrees of freedom would produce more accurate results for these higher frequencies, due to the numerical solution method of PAFEC.

As well as the number of elements in a model, their arrangement or relative size, is also important. As mentioned earlier the F.E. modeller should arrange the mesh so that regions where most deflection takes place have a suitable number of appropriate elements. eg. In the impeller model there is virtually no deformation of the hub section therefore the minimum number of elements possible to describe the geometry of the section should be placed there. However at the edge of the centreplate between the blades there are large deflections in many of the modes. Therefore in this region more than 1 element is necessary, and the use of distorted elements should be avoided.

### Centreplate/Sideplate/Backplate :

Often the complex geometries of the blade sections will dictate the mesh arrangement in these regions. However in order to describe the 'ripple' type modes where these plate sections deform, at least 2 straight-sided elements are required leaving at least one nodal point between each blade. Typical backplate mesh is shown in figure 12 , using triangular elements to describe the complex parts of the geometry.

### Blade :

Flexure of the blade takes place in many of the modes of interest to the F.E. modeller of centrifugal impellers, and a minimum of 2 elements across the blade from side to centreplate is required to describe the simplest flexure.

### Shaft:

Sufficient beam elements must be used to describe the geometrical changes in section along the shaft. Also there must be sufficient elements to describe the most complex shaft modes of interest to the modeller, although normally sufficient will be included when the shaft geometry is described. (see figure 9)

### Inlet Ring:

The inlet ring forms a seal at the inlet to the impeller and is not a critical area in terms of the impellers' structural strength. However its representation in the F.E. model is critical to the values of natural frequency obtained. The number of brick elements used to describe it should simply reflect the number of sideplate shell elements to which it is to be attached. The thickness of these brick elements should be as detailed below.

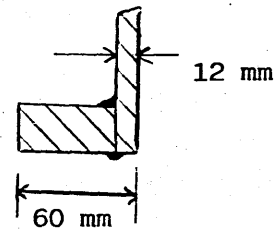
The inlet ring forms basically a stepped plate arrangement onto

the sideplate, although the thickness of the ring is too great to be modelled efficiently using the thin shell elements of the sideplate. The brick elements in the PAFEC suite have to be coupled to the shell elements in the sideplate as will be explained later in this section, and the method of coupling recommended is to use extra, thin shell elements. This introduces the problem of whether to include the coupling element thickness in the geometry of the model as highlighted below.

**Resonance Test Results  
( Sample )**

64  
176

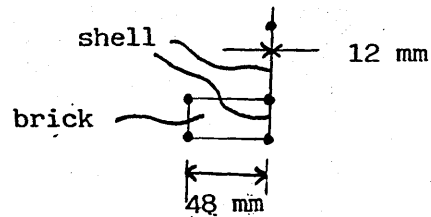
**Inlet Ring Structure**



**F.E. Model 1 Results  
(Sample)**

42  
158

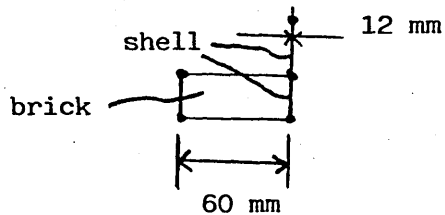
**Inlet Ring of  
F.E. Model 1**



**F.E. Model 2 Results  
(Sample)**

62  
187

**Inlet Ring of  
F.E. Model 2**

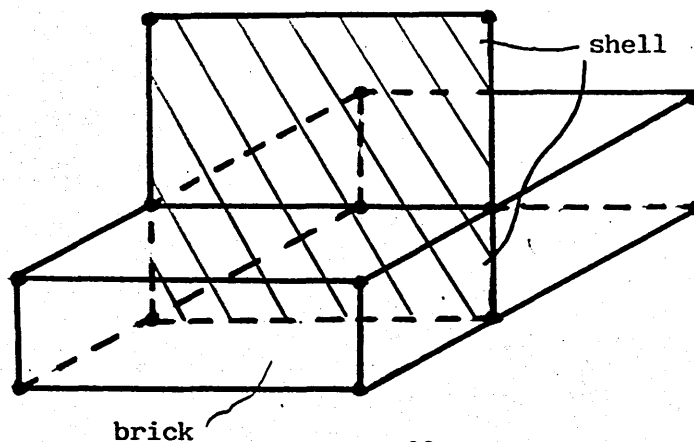


inlet ring is to model the brick elements as the full inlet ring thickness dimension and to add appropriate coupling shell elements of the same thickness as the sideplate. Although this may increase the local stiffness at this point the arrangement has been shown to produce acceptable results.

### Combination of Element Types

When using several element types in the same model cognaisance has to be taken of the fact that certain element types are incompatible, or require special consideration. In the PAFEC versions of the recommended 2D thin shell element ,3D brick element and 1D beam element there are 5 degrees of freedom, 3 degrees of freedom and 6 degrees of freedom respectively at each node. The resulting problem is to link rotational degrees of freedom on plates and beams to brick elements containing only translational degrees of freedom. The rigorous method of coupling the relevant freedoms would be to write the appropriate constraint equation for the interaction expressing the rotations in terms of displacements of adjoining nodes. However it may not be possible to do this in some packages and a suitable 'method' has to be found. Acceptable results were obtained in the impeller models analysed by using thin shell elements as coupling elements and the method adopted and recommended is shown below :

#### Plates to bricks

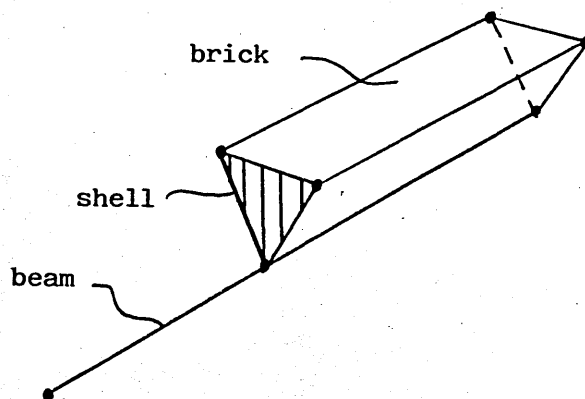


have to be linked to translational freedoms on the bricks. The insertion of a plate between the adjoining bricks removes the 'hinge' effect of improperly coupled plates. This has been shown to be effective as it is the coupling method used in all the F.E. results presented and has shown no significant difference from models where appropriate coupling constraints have been written into the program. There is some local stiffening of the section the 'coupling' element was placed in but the effect has been shown to be negligible for the structure types considered in this investigation.

To prevent numerical errors caused by very stiff elements joining very flexible elements, the recommended thickness of the coupling element is the same thickness as the shell element whose rotations require coupling.

#### Beams to Bricks

Again the recommended method of coupling the beam rotations to the brick translations in the context of joining the beam element shaft to the solid element hub section, is to place a coupling shell element over the face of the brick as shown below.



shown that for acceptable coupling the thickness of the shell element should be the thickness of the impeller centreplate.

~~CONFIDENTIAL~~

In the larger F.E. packages commonly used today there are often many solution methods available and consultation of the software literature should be made in order to provide a recommendation based on the type of results required. Also with some packages interaction with the solution mechanism is available to steer the solution in the direction the user wishes it to go, for example to provide a more accurate or faster analysis.

Complex structures usually involve large (in terms of numbers of degrees of freedom) models which in turn require large amounts of computing effort to solve. Customising the solution to suit the model and analysis type may often be possible and can actually make the difference between being physically able to find a solution using the computing resource available, or not .

By highlighting below some of the possibilities available with 1 analysis type on 1 structure type using 1 software package and computer, the intention is to stimulate the type of thinking that should be given to any complex analysis to ensure it is done most efficiently. The example used is the natural frequency analysis of a centrifugal impeller using the PAFEC suite on a Prime 2550 computer.

Software packages often suggest 'user-friendly' formats which claim to eliminate such problems but the truth is that the more automatic the features are the more difficult it becomes to cover every eventuality as efficiently as possible. Every analysis should be considered on its own merits to ensure that it will be carried out by the package in the most effective manner.

1. Can the accuracy of the solution be affected by the method of analysing the model ?
2. Can the time taken to perform the analysis be influenced by the user ?
3. Can the job be restarted if the computer 'goes down' ?

With reference to the aforementioned impeller analysis using PAFEC these questions are now addressed.

1. Natural frequency analysis of F.E. structures using an Eigenvalue solution method such as in PAFEC - see appendix A - can result in a large numerical problem for complex models. For example a numerically exact solution of a model containing 4000 degrees of freedom requires solution of 4000 simultaneous equations - ( to provide the Eigenvalues). Thus packages have to employ numerical techniques to reduce the problem to a manageable proportion. In PAFEC the method used is to utilise those degrees of freedom which best describe the dynamic characteristics of the model, providing a reduced set of Eigenvalues to solve for. As the user is able to select which freedoms should be chosen he can exert great power over the accuracy of the solution.

2. Referring to the above point , obviously the greater the number of equations to be solved , the longer it takes to do. Within the PAFEC package redundant degrees of freedom can normally be restrained by the user to remove them from the calculation and thus decrease the computer effort required without affecting the results obtained in any way.

3. In the engineers environment machines do break down, or computing time is only available at certain times each day. It is therefore imperative that the user knows if and where the

as PAFEC it is only possible to re-start a calculation at certain points, which can cause problems where time available is limited.

#### Examples of Effects of 'Considering How Analysis is Done'

##### A. Use of Symmetry :-

In the previous section, the use of cyclic symmetry and the RABBITS package in conjunction with PAFEC was recommended to reduce the size of the model. A feature of the RABBITS package is to apply a particular set of directional axes to those degrees of freedom lying on a symmetry interface and to keep all those freedoms in the main calculation procedure to simplify the addition of boundary conditions necessary to solve for all the natural frequencies. For a small model such as the flat disc in figure 1, use of a 60 segment of the disc and the RABBITS package results in an analysis which takes longer to perform than one on the full model! The reason is that freedoms which would normally be removed from the calculation due to redundancy remain in the segment model due to the action of the RABBITS package and result in a larger problem for the computer to solve.

Cognaisance of this fact was noted on the centrifugal impeller models and it was found that the calculation was storing a set of redundant freedoms on the symmetry interfaces which increased the calculation size with no gain in accuracy. When these freedoms were restrained manually an overall reduction of 30% in computing time was achieved to produce the same results.

B. If a full model of the impeller is constructed and analysed using PAFEC then both symmetric and assymmetric mode shapes are produced, in ascending order of frequency and descending accuracy. Use of the RABBITS package separates the analysis into

... application of several sets of boundary conditions. This can be useful in terms of modes of interest to the user , as by applying only the boundary conditions which provide the modes of interest (eg. symmetric modes shapes only) the calculation is speeded up .

The above results show that it is clearly beneficial not to regard solution mechanisms of F.E. packages as 'black boxes' , as the user can often tailor the solution to produce the results wanted with the best accuracy and least computer effort possible.

Frequencies of interest

An analysis of a structure's natural frequencies is normally done - certainly in the case of the centrifugal impeller - to ensure that natural frequencies do not coincide with known exciting force frequencies which may cause fatigue problems. Exciting force frequencies of interest to the centrifugal fan manufacturers are the running speed of the impeller and associated multiples (usually 2x, 3x and 4x running speed), and the blade passing frequency - frequency with which a blade passes the inlet to the impeller, eg. 11x running speed for an 11 bladed impeller. Thus the natural frequencies of interest will be all those between 0Hz. and say 110% of blade passing frequency. Coincidence between a natural frequency and blade passing frequency or running speed could potentially be catastrophic to the life of the impeller, and knowledge of the natural frequency and the associated mode shape is required to consider remedial action. It is the evaluation of this information from the F.E. results that this section is concerned with.

In the ideal world , the F.E. modeller's job is completed when the computer has finished its analysis , and the relevant , correct results are fed out in a form usable immediately by the modeller. Unfortunately this level of sophistication has not yet been reached by the software suppliers , and even the simplest analysis results require interpretation and moulding into a form suitable for presentation.

The results below in Table 8, are the PAFEC natural frequency results for the fixed disc in Figure 1.

	<u>Frequency (Hz.)</u>
1.	-0.0078
2.	206.2
3.	215.2
4.	454.8
5.	668.1
6.	669.2
7.	1571.7

Table 8

If these results were simply taken as being the first 7 natural frequencies of the disc , they would not be correct. Obviously frequency number 1. is not a natural frequency of the disc due to the negative quantity. In fact examination of the associated mode shape shows that it is a whole body rotation obtained by the calculation method due to the lack of rotational restraint on the F.E. model, and should have a frequency value of 0 Hz. The non-zero value of the frequency is a feature of the numerical calculation method. Frequencies 2 and 3 refer in fact to the same mode shape , shown schematically in figure 13. This

duplication of mode shapes is a mathematical representation of the fact that this mode shape (1 nodal diameter) has an infinite number of possible positions on the disc, and that a mathematical combination of two modes (vectors) can produce any other possible mode (vector). A similar reasoning exists for the duplicate mode shapes in frequencies 5. and 6.

Therefore correct interpretation of the F.E. results would produce the results of Table 9 below, which are then directly comparable to the theoretical results of Table 10.

Mode	Frequency (Hz.)
1 Nodal Dia.	210.7
0 Nodal Circles	454.8
2 Nodal Dia.'s	668.7
3 Nodal Dia.'s	1571.7

Table 9

Mode	Frequency (Hz.)
1 Nodal Dia.	Not Calculated
0 Nodal Circles	467.5
2 Nodal Dia.'s	654.6
3 Nodal Dia.'s	1524.5

Table 10

positively identify the F.E. mode shapes' uniqueness. Theoretical results however are usually only available for the simplest of structures and often measured results are the yardstick to which F.E. results are compared.

It is this feature which stretches the expertise of the modeller in identifying mode shapes of complex structures and comparing like with like in real structures in order to determine the accuracy of F.E. produced natural frequencies. The problem is increased when 2 further points are considered :

1. F.E. results of natural frequencies of the type considered here do not consider damping by the very nature of the free vibration calculation. Real-life measurements of structure natural frequencies can fail to record frequencies that are highly damped or have not been excited by the excitation methods used.

2. The F.E. model is a conceptualisation of the structure, and features such as non-perfect symmetry or dimensional discrepancies may cause natural frequencies /mode shapes in the real structure to be different from the F.E. results both in terms of appearance and non-appearance of mode shapes.

This investigation shows that empirical work on structures of similar types is the only reliable method, at present, to resolve such problems at reasonable cost. In this respect for the centrifugal impeller structures, the comparison of F.E. produced results with natural frequency results obtained by the calibrated hammer technique is now considered. The calibrated hammer technique is a simple reliable method of obtaining a structure's natural frequencies and is described in Appendix B. Use of a twin channel spectrum analyser to obtain mode shape information is

extremely time consuming for complex mode shapes, with numerous test points required.

The natural frequency results of the impeller in figure 10 are shown below in Table 11.

Frequency (Hz.)

---

.006

.22

41

82

135

198

203

306

323

331

401

( 'Double' frequencies omitted for clarity )

Table 11

the natural frequencies identified in the resonance tests using the calibrated hammer technique, for the impeller in figure 10, are listed below in Table 12.

Resonance Test Frequencies (Hz.)  
-----

42  
72  
140  
190  
296  
376

Table 12

Figure 14 shows the output from the spectrum analyser, highlighting the problem where a mode with a large transfer function 'swamps' out the other modes. Figure 15 shows the benefit of reducing the range analysed by the spectrum analyser, although this requires extra man-effort to carry out further tests on the structure.

Comparison of Tables 11 and 12 illustrates the problem that more natural frequencies were identified in the F.E. analysis than in the resonance tests. As explained before, the problem is to correlate mode shapes in the F.E. analysis to the mode shapes from the resonance test natural frequencies. In practice it would be very difficult to gain sufficient information from the resonance test, to determine the modal deflections throughout the structure. However examination of the F.E. mode shapes (such as figures 2 and 3) show that axial displacements of the back and sideplates give a great deal of information about the mode shapes - similar to the nodal patterns of circles and multiple diameters

on the flat disc of figure 1. The method used to identify the resonance test natural frequency mode shapes, was to use transfer function and phase information from an accelerometer placed on the side or centreplate of the impeller and from the load cell on the hammer.

For the double-inlet type centrifugal impeller, shown in figure 16, 24 test points were required on the sideplate and 48 test points on the centreplate to produce developed circumference plots of the mode shapes. Figure 17 shows examples of the type of plot produced by this method. Such plots can be used to identify and characterise relatively simple mode shapes and can be used to compare with F.E. produced mode shapes. The number of test points represents a measurement on and between a blade, and it requires a considerable amount of man-effort to correlate each of the mode shapes. The man-effort involved in Resonance Test work clearly highlights the benefits of being able to predict a structure's natural frequencies and mode shapes consistently with known accuracy.

#### F.E. Produced Mode Shapes

Standard methods of producing F.E. results are : numeric values of displacements of nodal points - normalised displacements for free vibration calculations and graphical representations of the deflected shape. Interpretation of a complex 3D mode shape from a 2D screen or hard copy can be very difficult - figure 18 shows views of F.E. produced mode shapes of a cyclically symmetric portion of a centrifugal impeller. Colour (shaded) or animated graphics can ease the problem in terms of categorising the mode shape for comparison with a real structure. For the purpose of this work a simple BASIC program was written to extract from the

displacements of circumferential centre and sideplate nodes, to enable a plot to be prepared which could then be used in direct comparison to the Resonance Test plots. The program with sample output is contained in Appendix C.

Strategic placing of nodal points during the construction of the model allows direct comparison between nodal points on the model and Resonance Test points on the impeller. The type of plot produced is shown in figure 19.

This method of comparison worked well for simple impellers such as the single inlet impeller of figure 10 and only for the simpler mode shapes of the more complex double-inlet impellers such as that in figure 16. The type of accuracy and correlation that can be expected in a single-inlet impeller is shown below in Table 13.

F.E. (Hz.)	Resonance Test
41	42
82	72
135	140
198	190
331	296
401	376

Table 13

Based on the above results and the investigations of this work in

1. simpler structures - such as flat discs and discs on shafts
2. More complex structures - such as two different double-inlet type impellers ; an expected accuracy band of +14% to -3.5% for a natural frequency analysis of a single-inlet type centrifugal

resonance tests to be recognised. In view of the lack of information that the static Resonance Test tells us about the in-service impeller , the recommendation would be to record the extra frequencies as natural frequencies of the impeller. Extra work on more sophisticated Resonance Tests would be required to determine if they were actually natural frequencies, but their inclusion, if in error, errs on the safe side.

The double inlet type centrifugal impeller results were, as mentioned, part of the basis for placing the accuracy limits detailed above for the single inlet impeller. The complexity of the double-inlet impeller type mode shapes , examples of which are shown in figures 20 and 21, were such that only the simplest F.E. mode shapes could be positively correlated to Test Results mode shapes using the method described above. However the accuracy that they exhibit as shown below in Table 14, would suggest that the other natural frequencies would exhibit similar accuracy. The proviso to this is of course that it is in the nature of the PAFEC F.E. calculation method to calculate higher value frequencies with reducing accuracy.

Resonance Test Results	Natural Frequency Results
64	62
176	187

Table 14

... into the  
results of the F.E. analysis, is that where actual test work on a structure is not possible - eg. pre-manufacture stage - the F.E. modeller with confidence in his analysis technique can create a model of the structure along objective guidelines, analyse it, and using the results, present a set of values with an associated tolerance, to which design criteria can be checked. The results of this particular investigation should enable an engineer to construct a model of a single-inlet type impeller, carry out a natural frequency analysis and have sufficient confidence in the results to determine if exciting force frequencies are liable to coincide with any natural frequencies of the impeller, and be able to characterise and recognise the associated mode shapes.

~~CONFIDENTIAL~~

The results of this investigation enabled a Design Guide to be produced for James Howden and Co. Ltd. In conjunction with the computing facilities and the PAFEC F.E. software package available at James Howden, an engineer with limited F.E. experience is able to utilise this Design Guide to create a model of a centrifugal-type impeller, carry out a natural frequency analysis on it and obtain results within known confidence levels. The work has also formed a basis for James Howden further research into dynamic analyses of their products.

It is useful therefore to discuss the material contained in the Design Guide with reference to the work described in this report in preceding sections.

The Design Guide covered the four basic parts of an analysis as covered by the earlier sections, namely :-

- A. Initial Steps
- B. Modelling the Impeller
- C. Analysing the Impeller
- D. Interpreting the Results

In order to give the engineer an appreciation of the solution mechanism, a brief description of its relevance to natural frequency analysis of cyclically symmetric structures was given. The concept of boundary conditions and master degrees of freedom were highlighted as was their effect on the accuracy of the frequencies obtained. i.e. approximately one third of the number of masters used is the number of frequencies that can be expected to be accurate for each set of boundary conditions applied. This is a function of the numerical reduction method used in PAFEC.

The initial steps described in Section 1. of this report were identified in the Design Guide, including a checklist of the

information required about the impeller before beginning to create the model. It was stressed that the recommendations only pertained to the natural frequency analysis of impellers and were not applicable to other analyses such as stress analyses.

It was recommended in the Design Guide to analyse the impeller as a stationary structure. The effect of gyroscopic forces and other factors such as centrifugal stiffening were considered, but due to the relatively slow operational speed these effects were thought to be small. In order to prove this, however, substantial work would be required needing sophisticated F.E. software and computing resources not available in James Howden. The Design Guide instructs the user which parts of the PAFEC suite to use, and estimates how long the analysis can be expected to take on the Prime 2550 computer.

Section B of the Guide is concerned with modelling the impeller. In order to obtain accurate results for the diaphragming and diametral type modes, shown in figures 2 and 3, the Guide instructs the user to include the shaft in the model, restraining it in the vertical plane at the bearing centres. As the flexibility in the real impeller shaft supports is ignored, those modes in which the shaft displaces will not have the correct natural frequencies. The Prohl method is used routinely in James Howden to calculate shaft whirling frequencies and therefore the complexity of analysing an F.E. model with flexible supports is not required.

Section B of the Guide identifies those impeller features which should be modelled, and describes the methods to be used. The Guide recommends that the shaft be modelled using one-dimensional beam elements, simply supported at the appropriate

span corresponding to the bearing centres. This ensures that all the modes of the impeller/shaft combination are produced, whilst also minimising the degrees of freedom used to describe the shaft.

The simplest method of obtaining the natural frequencies of a real impeller structure is to carry out a resonance test on a simply supported stationary impeller - this is then analagous to the F.E. analysis. The Design Guide can be used to obtain information on an impeller design prior to manufacture and remove the need for time consuming and costly resonance testing after manufacture.

A description of how to model a shrink-fitted hub in the impeller model was given in Section 2 of this report. The effect of this approximation on the natural frequency results was found to be small. Section B of the Guide instructs the user to use this method for impellers with shrink-fitted hubs. This approximation is achieved by connecting the shaft to the hub at the hub ends only as in figure 6. and provides for fewer degrees of freedom in the model and hence takes less time than the fully connected hub/shaft in figure 5. The connection in figure 6 simulates the very high local stresses found at the hub/shaft interface during operation of shrink-fitted hubs.

This investigation showed that acceptable results for natural frequency can be obtained using simple four-noded shell elements in general and with triangular shell elements to describe complex geometry. Thus in the impeller models, platework was described using these simple elements. In order for these straight-sided elements to describe the bending deformations of the platework between blades it is necessary to place a nodal point between the blades as in the mesh in figure 10. The Guide quantifies the mesh

density in different areas of the impeller. For example, two shell elements are recommended between each blade in order to produce acceptable results. Following the Guide's instructions would produce a mesh similar to the coarse mesh model in figure 11. The natural frequency results from that model are shown in Section 3, Table 13. The use of curved elements with mid-side nodes would result in many more degrees of freedom in the model with little gain in accuracy of results as Table 7 in section 2. shows. By quantifying the number and type of elements to be used in each particular area of the impeller model, the Guide obtains an accurate solution economically.

The combination of element types suggested in Section 2. requires a method of coupling degrees of freedom which would not otherwise be coupled by the normal PAFEC procedures, and highlights situations where coupling is required. The Guide specifically states where coupling is required in the impeller model -

1. At the shaft (beam element) / hub (solid element) interface
2. At the side/centreplate (shell element) / hub (solid element) interface
3. At the sideplate (shell element) / inlet ring (solid element) interface

In each case the method of inserting a coupling shell element, as described in Section 2. , is recommended. The justification for this coupling method is not rigorous mathematically, but comparison between the rigorous coupling equation and the 'coupling shell element' method proved it to perform well. The thickness of shell element to be used was determined by the incorporation of different thicknesses in various models and comparing them with the more time-consuming but rigorous coupling

... effect of the extra local stiffness imparted by the use of an extra 'coupling shell element' would not be expected to alter the stiffness distribution greatly as the areas suggested for its use in the Design Guide are areas where the connections on either side have greater magnitudes of stiffness than the coupling element itself.

Section 3 considered the analysis of the F.E. model, discussing opportunities which the F.E. analyst has to ensure that the software package carries out the analysis in the most efficient manner possible. Unless the user of even the most 'user-friendly' F.E. package is conversant with its operation it may be difficult to use efficiently. Therefore, the Guide instructs the user how to utilise the PAFEC package for natural frequency analysis without assuming prior knowledge. Normally the PAFEC package continues to try and complete the analysis in one sweep after it is instructed to begin - no matter how much computing time is required. This is obviously of little use in a computing environment such as can be sustained in an engineering company where interactive use of the computing facilities is normally required during the day, and large batch computing is done during the night. The Design Guide thus instructs the user on how to customise the solution procedure in order that it can be carried out in parts which can be stopped and re-started, and also estimates the time that will be required for the computer to produce results for each part. This is achieved by breaking into the software (according to instructions given in the Guide) and changing certain parameters. The time required for each portion was determined by comparing the model sizes in terms of degrees of freedom and the relative time taken for these analyses during this investigation.

The master degrees of freedom described in Section 3. are the reduced set of degrees of freedom which are solved to produce the natural frequencies. The Design Guide recommends that the PAFEC automatic facility for master selection is used. This is because inappropriate choices of masters - for example two masters very close to one another and in the same direction - can cause numerical problems in the calculation procedure leading to inaccurate results.

The Design Guide describes how to remove 'redundant' freedoms from the cyclic symmetry interface, and thereby save up to 30% on a typical natural frequency analysis on an impeller. This is dealt with in Section 3. These 'redundant' freedoms are the in-plane rotations of the shell elements recommended for use in modelling the platework of the impeller. The element has no in-plane rotation at the element level but the cyclic symmetry routines in RABBITS extract all 6 degrees of freedom at each nodal point on a symmetry interface in order to apply boundary conditions to them at a later point in the calculation. This stores the 6th degree of freedom for the shell elements in the calculation unnecessarily and increases the time required to obtain the solution. By indicating in the Design Guide which degrees of freedom to restrain - i.e. remove from the calculation - the calculation is made more economic.

Section 4. describes work done on interpreting the results of an F.E. analysis to correlate them to the behaviour of a real structure. If the F.E. analysis predicts a natural frequency which coincides with a known exciting force then remedial action is necessary. If the mode shape of the impeller is known for the natural frequency in question then examination of it can indicate

action might be appropriate. As Section 4. shows, the F.E. produced results for natural frequencies can be confusing for those not experienced in F.E. analysis, with rigid body modes and 'double' frequencies produced. The Design Guide explains the occurrence of such frequencies and also indicates in which sections of the results they would be found. Rigid body modes will be found in the section where the boundary conditions applied produce mode shapes that are cyclically symmetrical, and will have frequencies numerically close to 0 Hz. They can have negative values due to the numerical calculation method.

The extraction of useful information from the output of an F.E. analysis can be a difficult task as Section 4. describes. The Design Guide utilises the BASIC program written during this investigation to extract as hard copy, only the information required. An example of the information produced by this program is contained in Appendix C. This allows storage of the complete displacement information, in the software medium. It can be appreciated that hard copy of every displacement of every degree of freedom in a model such as in figure 10, for every natural frequency identified, is a large mixture of useful and useless information. The problems in identifying the complex modes of an impeller is eased for the user of the Design Guide by providing examples of what types of mode shapes to expect from which sets of boundary condition in the cyclic symmetry analysis. For example the shaft flexure modes are obtained by the application of boundary conditions producing the results of 'Harmonic 1' in the PAFEC RABBITS analysis.

The comparison of F.E. produced natural frequency results with resonance tested impellers is described in Section 4. It is this

comparison which gives the accuracy predictions present in that section and which are also contained in the Design Guide. Section 4 considered the fact that there are some 'extra' frequencies which can appear in only one of either the F.E. results or Resonance Test results. The fact however that the most distinct resonance test peaks with high transfer functions do have comparable mode shapes and natural frequencies to the F.E. results, and that the modes found in F.E. results and not in Resonance Tests are higher frequency modes within each set of boundary conditions, supports the case presented in Section 4. that they are not significant to the accuracy of the results obtained. However this does represent an area for further research to determine whether it is a function of the imperfect F.E. model or the imperfect (i.e damped) free resonance tests, that produces these 'extra' frequencies.

Graphical representations of complex structures can enhance the viewers understanding of the structure if viewed at an appropriate angle. The Design Guide suggests a viewing angle which ensures repeatability for comparison of different mode shapes, as in figures 20 and 21.

The appearance of natural frequencies both above and below the 'true' values obtained from the resonance tests, is a useful illustration of the dangers in taking the theory of Finite Elements beyond practical limits. Following the theory of the PAFEC solution technique, an F.E. model of a real structure should produce results which will always be greater than those of the real structure, decreasing towards those of the real structure as the mesh density and hence the number of degrees of freedom used to describe the model increases. The practical

approximations in modelling and the use of economic mesh arrangements, produce complex models which can produce results for natural frequency which are both above and below their respective 'true' values. Thus Section 4. stated limits for results for the natural frequency analysis of the centrifugal impeller following the method outlined in this report as +14% to -3.5% .

No stage of an F.E. analysis should be considered in isolation from the others if meaningful results are to be obtained. When an F.E. model is being constructed, the analysis to be performed on it must be kept in mind. If for example a stress analysis is to be performed on a centrifugal impeller to determine stress during operation of the impeller then the shaft need not be modelled, and the respective loadings applied to the impeller. If however all the natural frequencies of the impeller are required then the shaft must be included as described in Section 2.

Complex F.E. analyses involving many degrees of freedom to be solved require large amounts of computing power. However the creation of a meaningful model is more important than having access to sophisticated computing facilities, as no computer could obtain correct results from an incorrect model. For example the disc on shaft model described in Section 2. could not produce correct results due to the inability of the brick elements to describe the bending deformation accurately.

Mesh generation aids should be utilised where available as the construction of an F.E. model can take longer than the analysis and production of results. The F.E. model of figures 2 and 3 took 5 man days to construct and 4 man days of computing time to produce its natural frequencies.

For natural frequency analyses the mesh should be regular throughout the model. This prevents numerical instability problems caused by elements with differing magnitudes of stiffness. However in practice this has to be balanced against modelling major structural features in complex geometries such as in figure 10.

high order elements with mid-side nodes are not required, provided that the elements used in the shaft region can undergo bending across their length. The use of simple elements reduces the number of degrees of freedom in the model. The flexure of the side/centreplate is achieved with these straight-sided elements by placing a nodal point between the blades as shown in figure 10. The necessity for flexural elements in the shaft was shown in Section 2. where the higher order 6 noded brick elements produced incorrect results whilst simple 2 noded beam elements produced accurate results.

Use of cyclic symmetry reduces the effort required for complex models but not for simple analyses. This is due to the fact that degrees of freedom lying on a symmetry interface are not automatically reduced out of the main calculation phase as they would be in the full structure model. Boundary conditions have to be applied to these interface freedoms to produce natural frequency results of the complete structure from a cyclically symmetric portion of it. The simple disc in figure 1 took less time to analyse than using the cyclic symmetry package RABBITS and 1/6th of the disc. However the F.E. model of one segment of a centrifugal impeller shown in figure 11, and analysed using RABBITS was the only method of obtaining the impeller natural frequencies, as the computing facilities at James Howden were not sufficient to analyse a model of the complete impeller.

Engineering intuition will always be required when modelling a real structure. This is because F.E. models have to be approximate for analyses to be solvable on practical computing resources. For example to model a real impeller complete with balance patches, dimensional discrepancies, dynamic forces and

flexible supports and then perform a natural frequency analysis would be impractical for impeller manufacturers to perform routinely.

The effect on the natural frequencies of modelling a shrink-fitted impeller on its shaft is negligible. However it does reduce the number of degrees of freedom in the model as described in Section 2. The method used was to connect the hub to the shaft at the ends only simulating the effect of the very high local stresses found at the hub/shaft interface during operation. This done only 1 shaft element need be placed along the length of the hub in place of the four or more for a fully connected hub, as figures 5 and 6 show.

Many different types of element can be used in a large complex model provided their formulations are understood and thus can be coupled correctly. The recommendations in Section 2. include using 1,2 and 3 dimensional elements in the same model, and indicate methods to ensure that they are coupled correctly.

F.E. packages should be checked to ensure that 'foolproof' mechanisms are not creating unnecessarily lengthy solutions. Interaction with the PAFEC program on a natural frequency analysis as described in Section 3. reduced the analysis time by 30%. This was due to the fact that the cyclic symmetry package - RABBITS - retained redundant freedoms in the solution.

The F.E. modeller's job is not complete when the computer analysis is finished as interpretation of the results is required. For example section 4 shows a sample of natural frequency results which includes frequencies that are a product of the numerical solution procedure and not of the impeller structure.

to F.E. model results as the impeller mode shapes in figures 19 and 20 indicate. This is due to the practical difficulties of obtaining comprehensive mode shape information of real,damped structures and the imperfections of the F.E. representations. However for centrifugal impellers the method detailed in Section 4. allows a simple comparison to be performed between F.E. results and Resonance Tests results. Figures 17 and 19 indicate the comparison that can be obtained.

F.E. model construction and analysis is largely a subjective exercise and not easy for the inexperienced analyst. This is due to the fact that large F.E. packages although simple to use do require detailed knowledge of the structural behaviour , element formulations, and analysis types contained in the package. Through the results of this investigation a Design Guide was written for James Howden which can lead an inexperienced engineer to model, analyse and produce natural frequency results of impellers in an objective manner to produce results which are in an accuracy range of +14 to -3.5%.

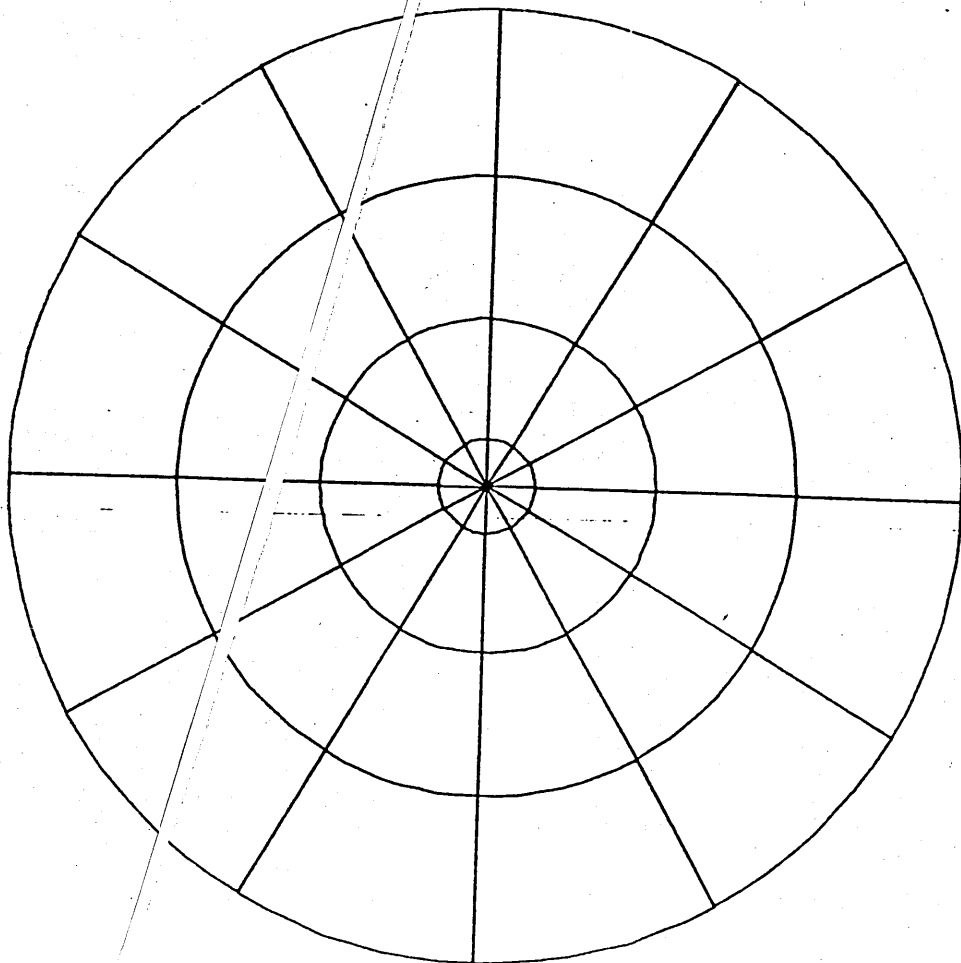


Figure 1

ROTATION  
X: 90  
Y: 0  
Z: 0  
Y: AXI  
OUTWARD  
Z

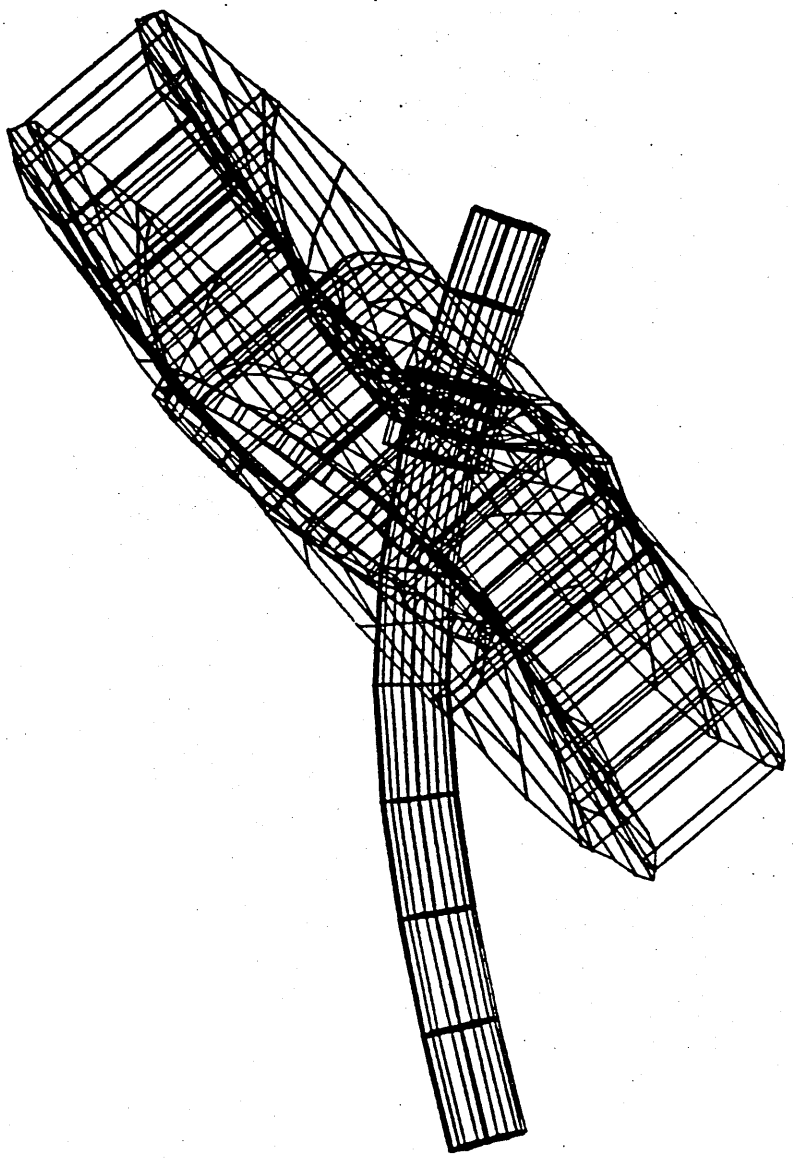
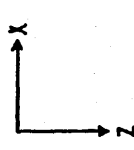


Figure 2

ROTATIONS:  
X: 90.  
Y: 0.  
Z: 0.

Y: AXLS.  
OUTWARDS.



A small diagram showing a coordinate system with a vertical arrow labeled 'X' and a horizontal arrow labeled 'Z' pointing to the right.

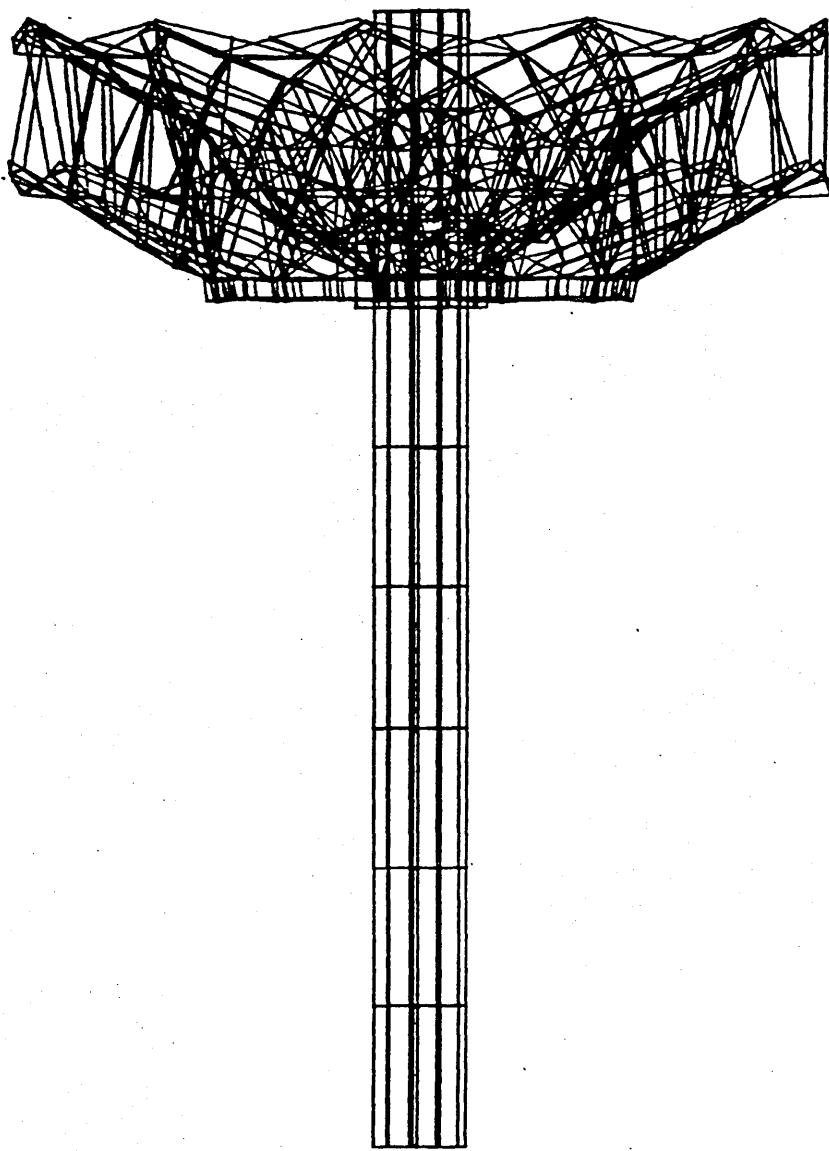


Figure 3

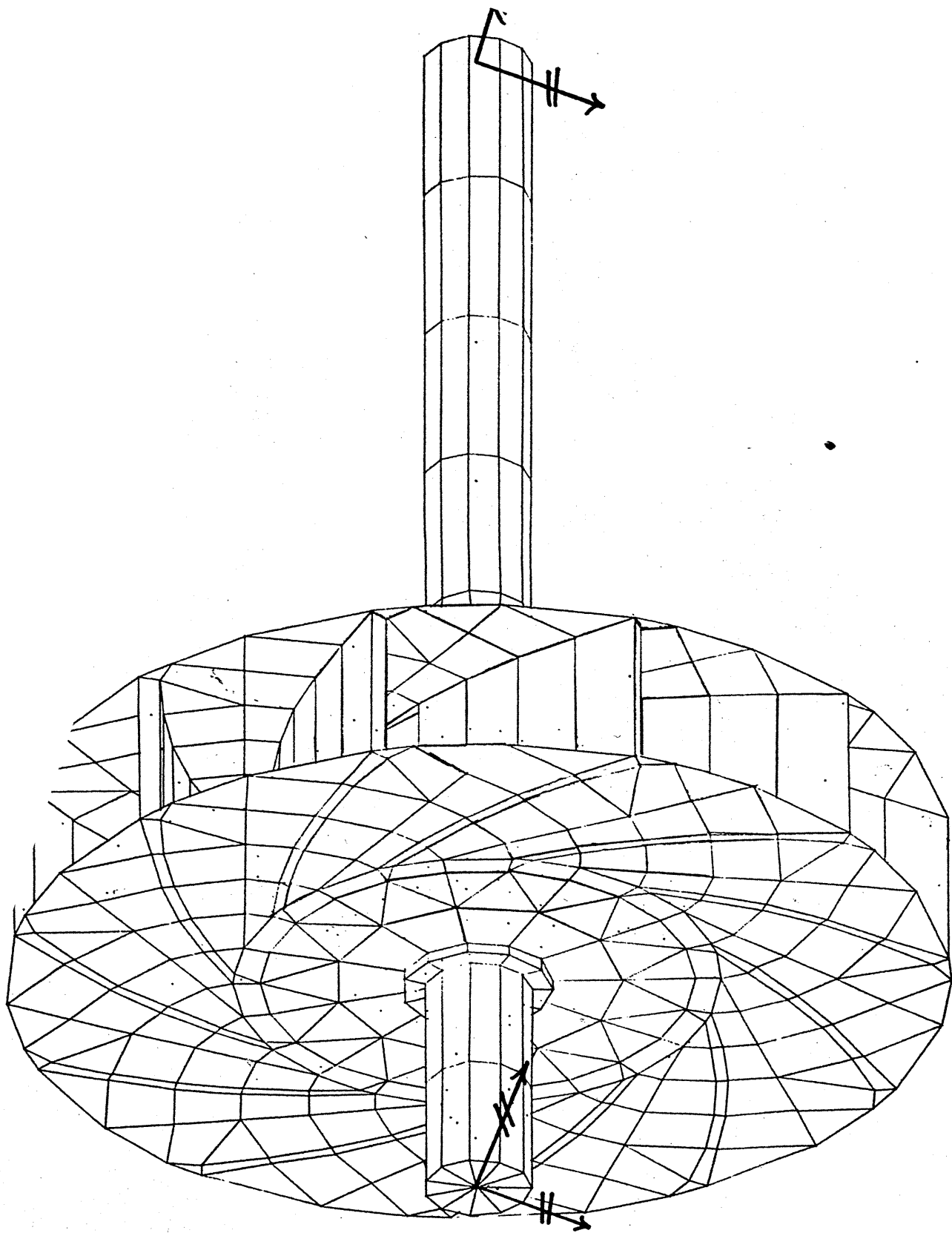


Figure 4

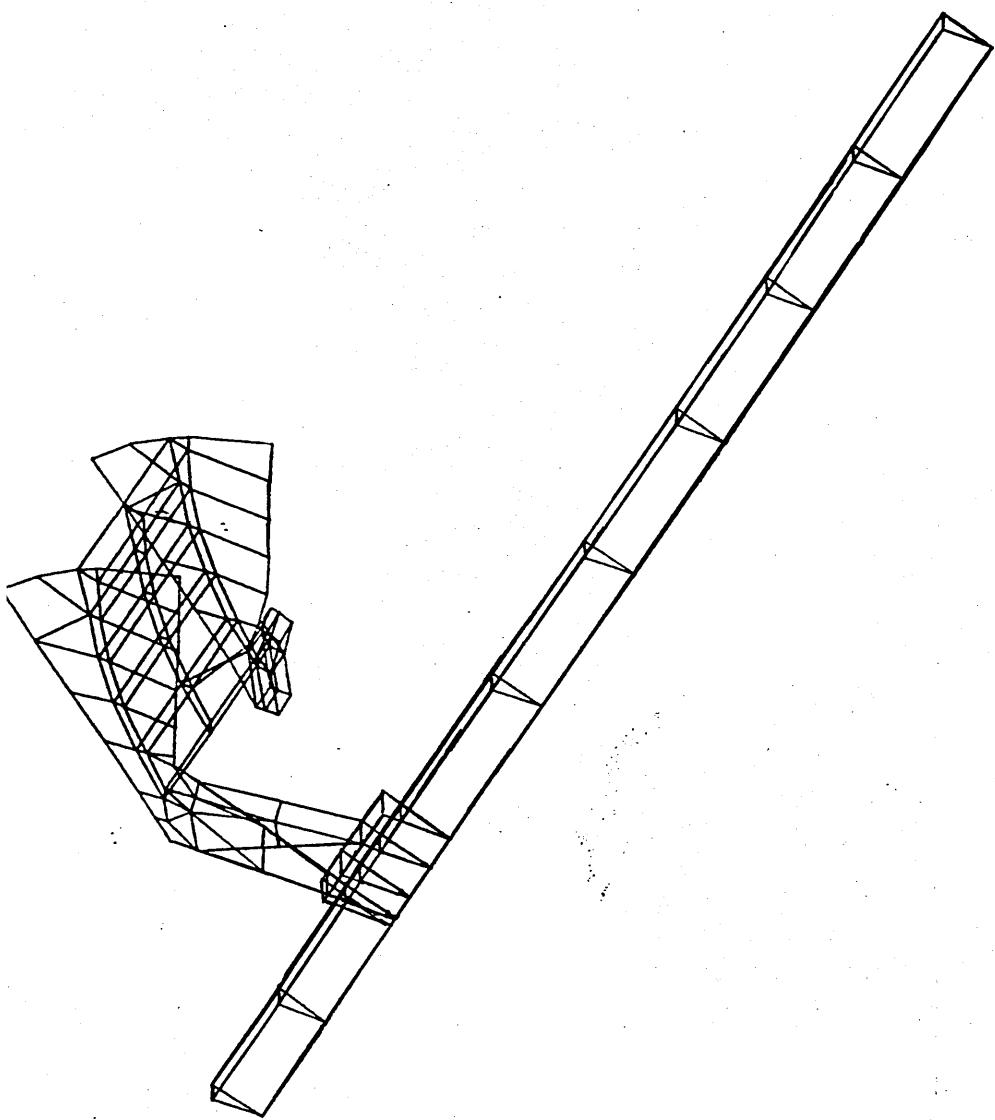


Figure 5

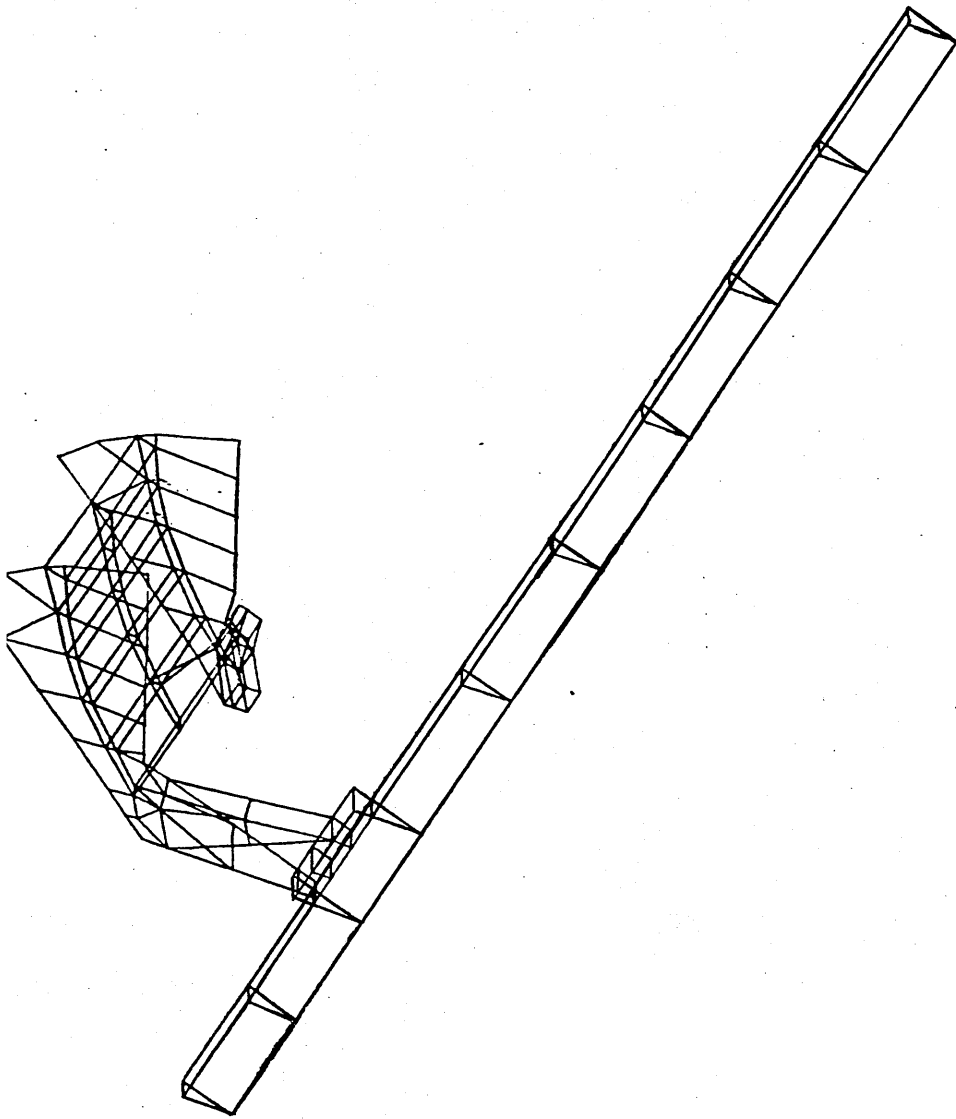


Figure 6  
B

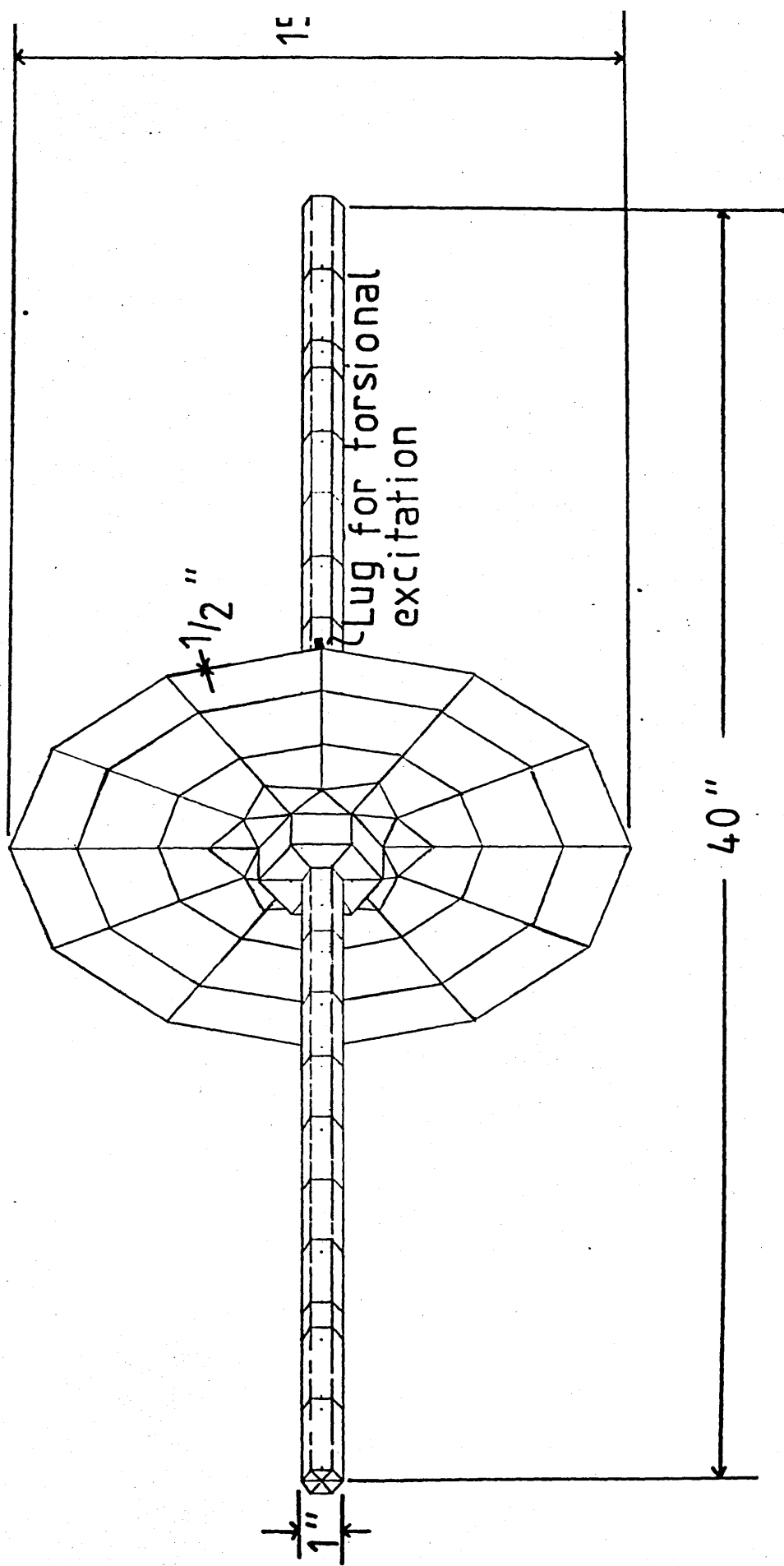
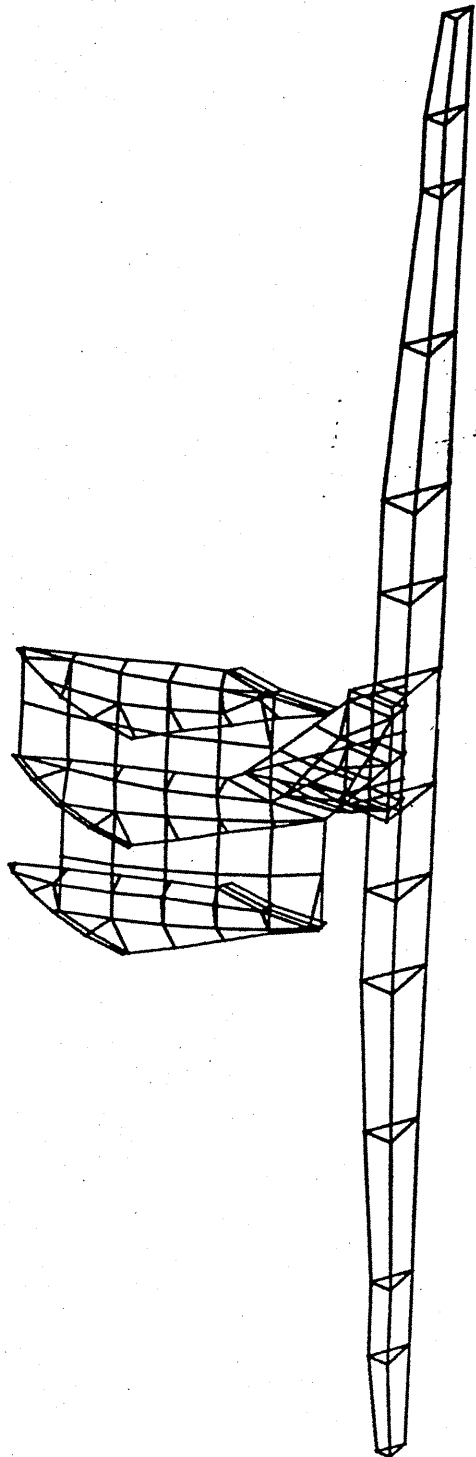


Figure 7



1  
2  
3  
4  
5  
6  
7  
8  
9  
10  
11  
12  
13  
14  
15  
16  
17  
18  
19  
20  
21  
22  
23  
24  
25  
26  
27  
28  
29  
30  
31  
32  
33  
34  
35  
36  
37  
38  
39  
40  
41  
42  
43  
44  
45  
46  
47  
48  
49  
50  
51  
52  
53  
54  
55  
56  
57  
58  
59  
60  
61  
62  
63  
64  
65  
66  
67  
68  
69  
70  
71  
72  
73  
74  
75  
76  
77  
78  
79  
80  
81  
82  
83  
84  
85  
86  
87  
88  
89  
90  
91  
92  
93  
94  
95  
96  
97  
98  
99  
100

Figure 8

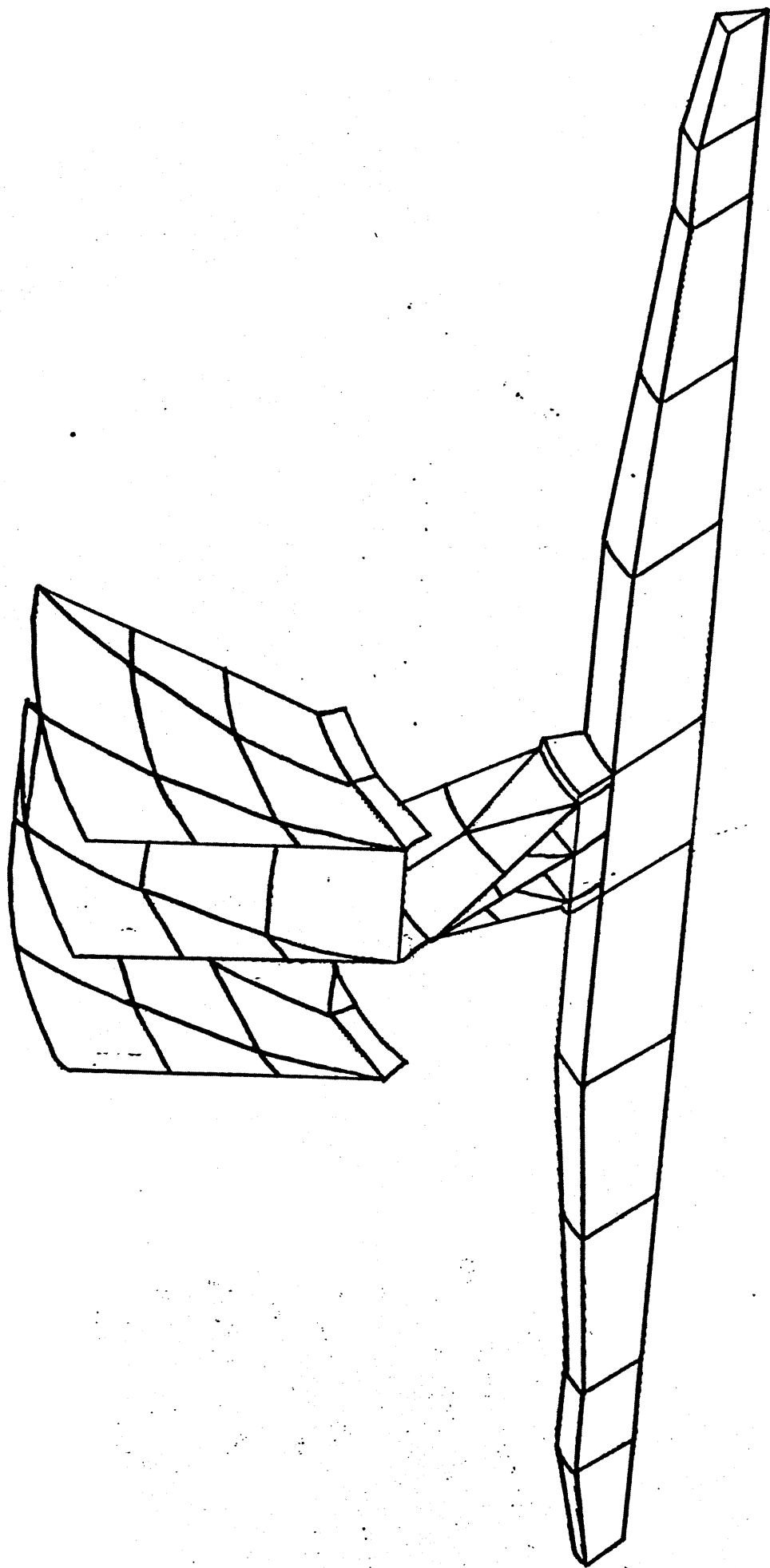


Figure 9

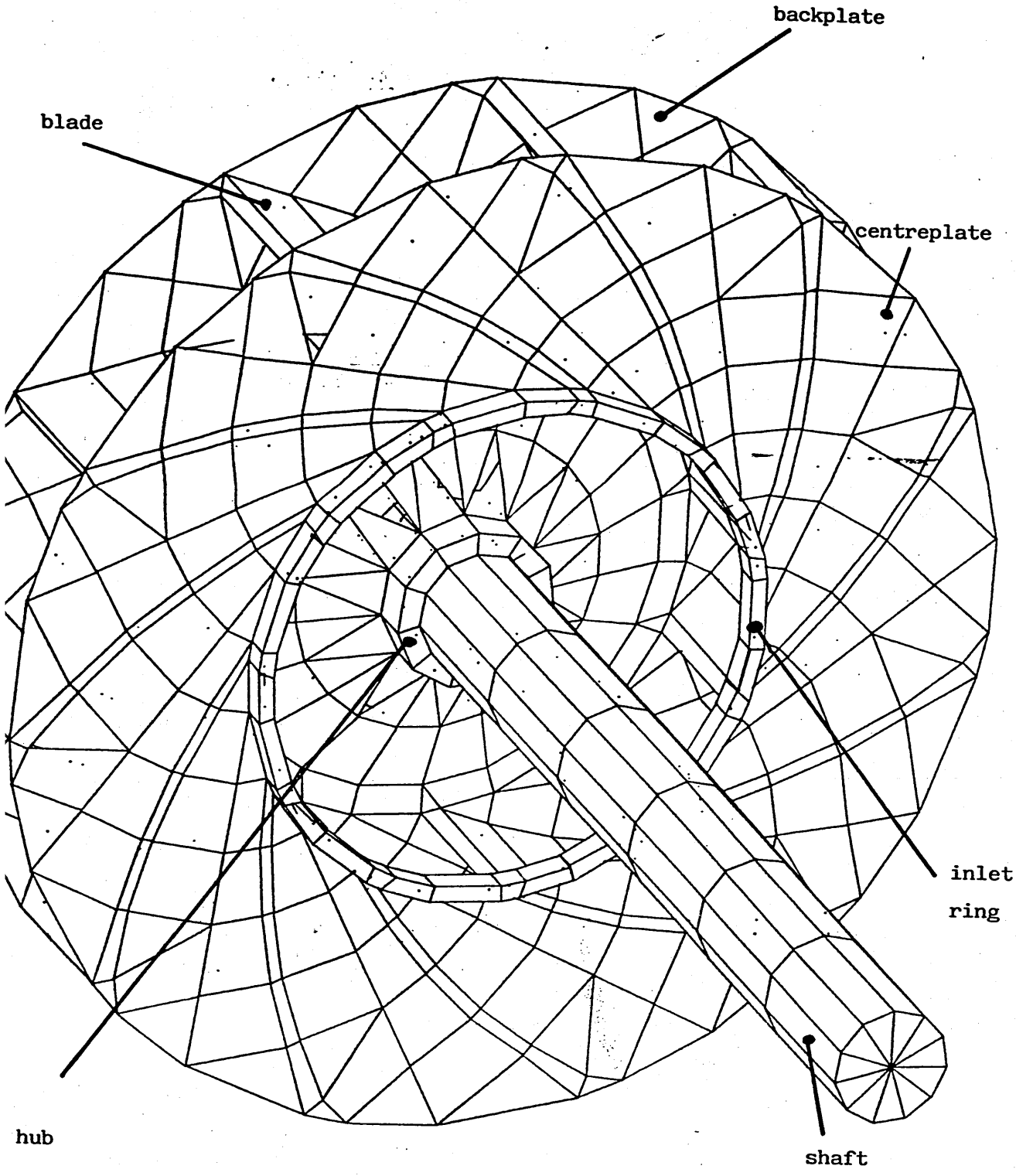


Figure 10

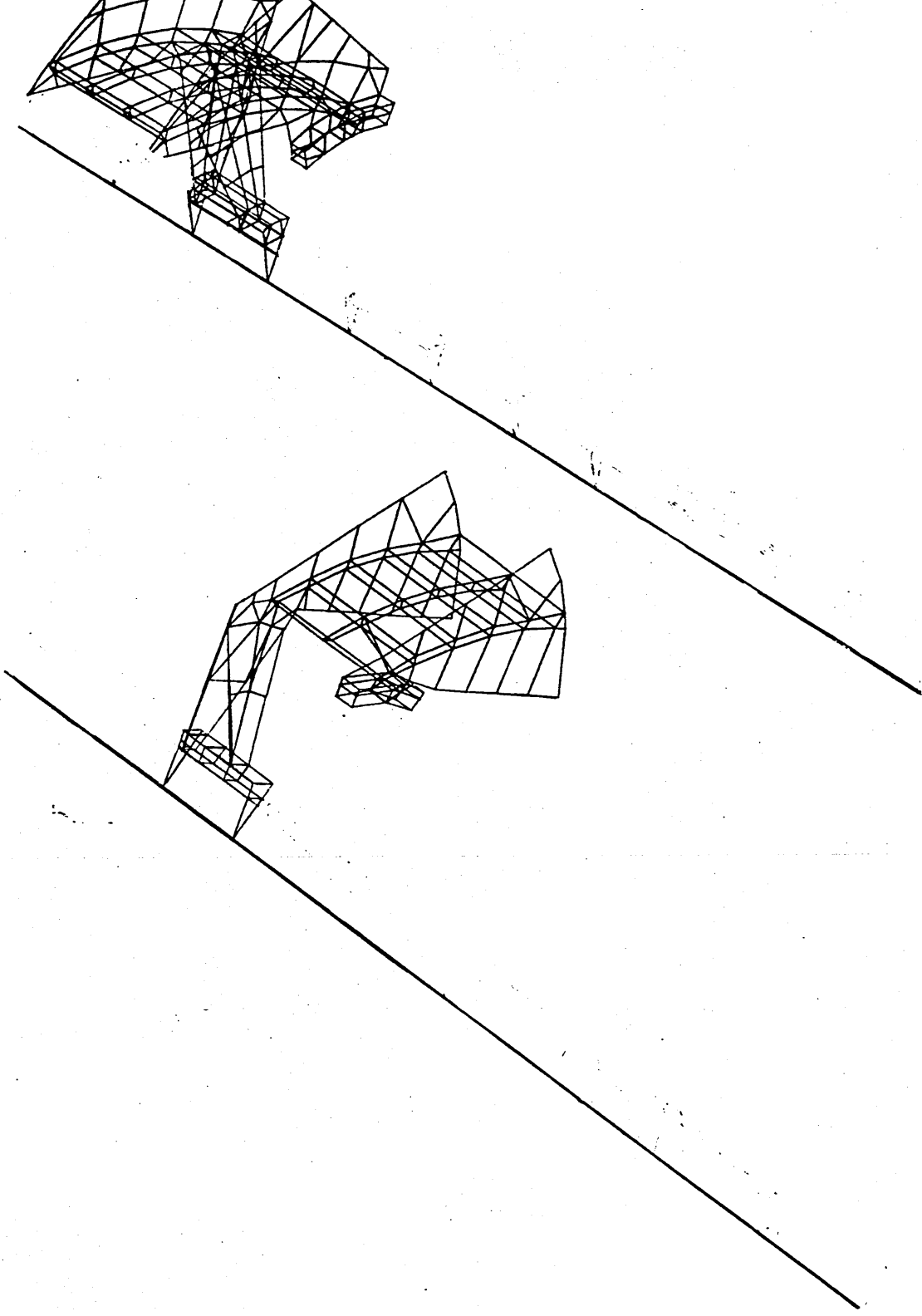


Figure 11

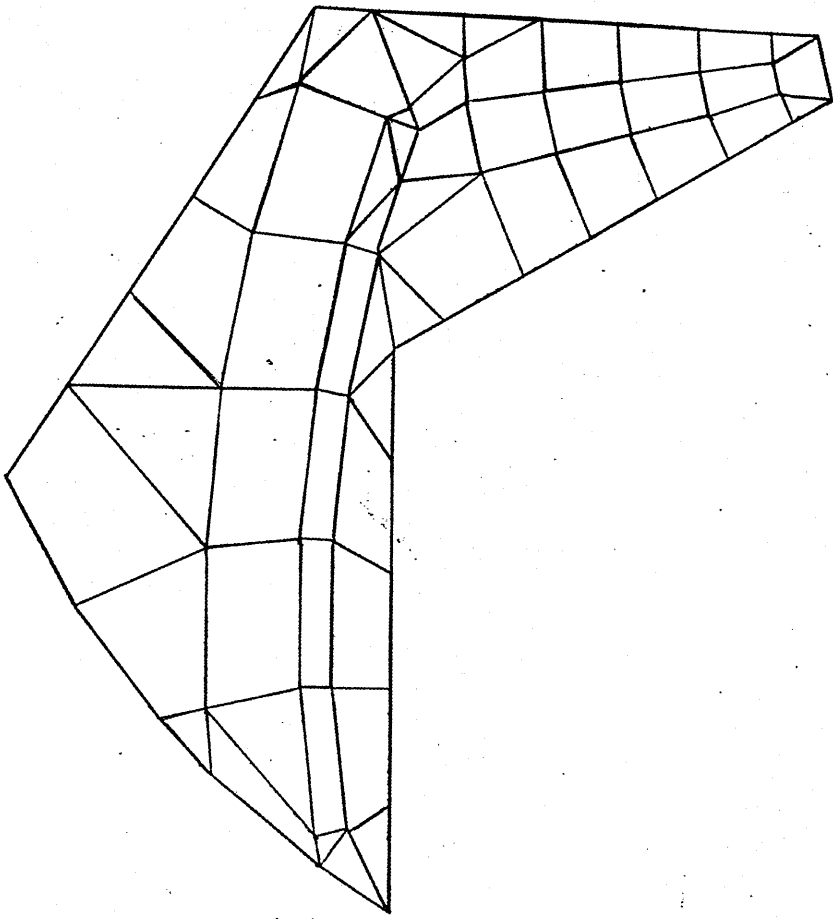
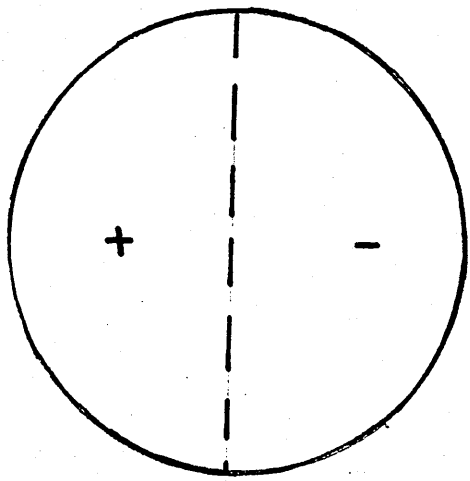
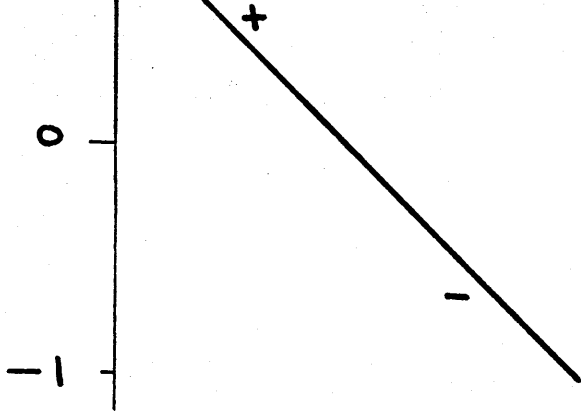
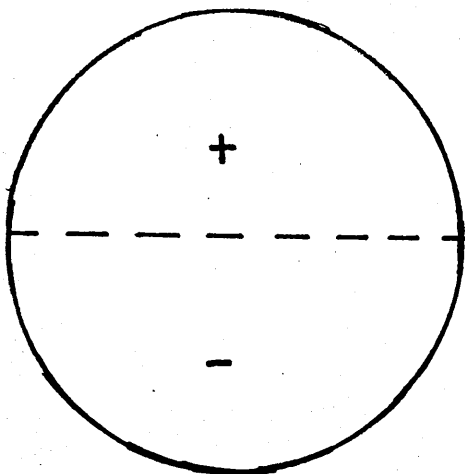
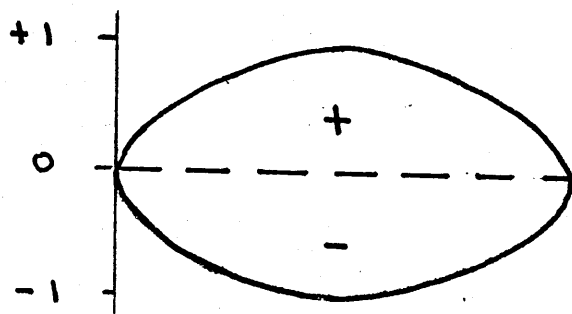


Figure 12



206.2 Hz.



215.2 Hz.

Figure 13

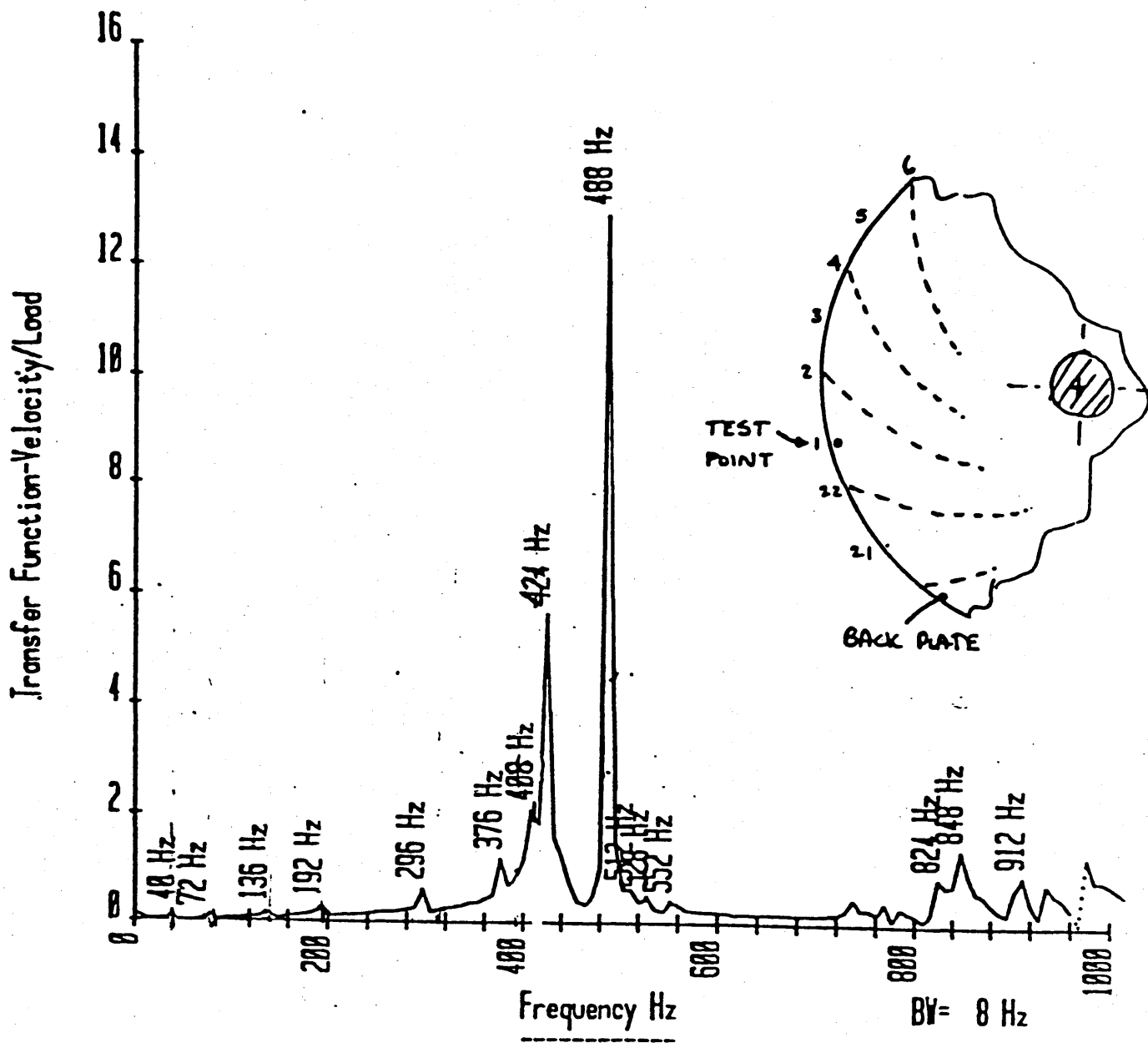


Figure 14

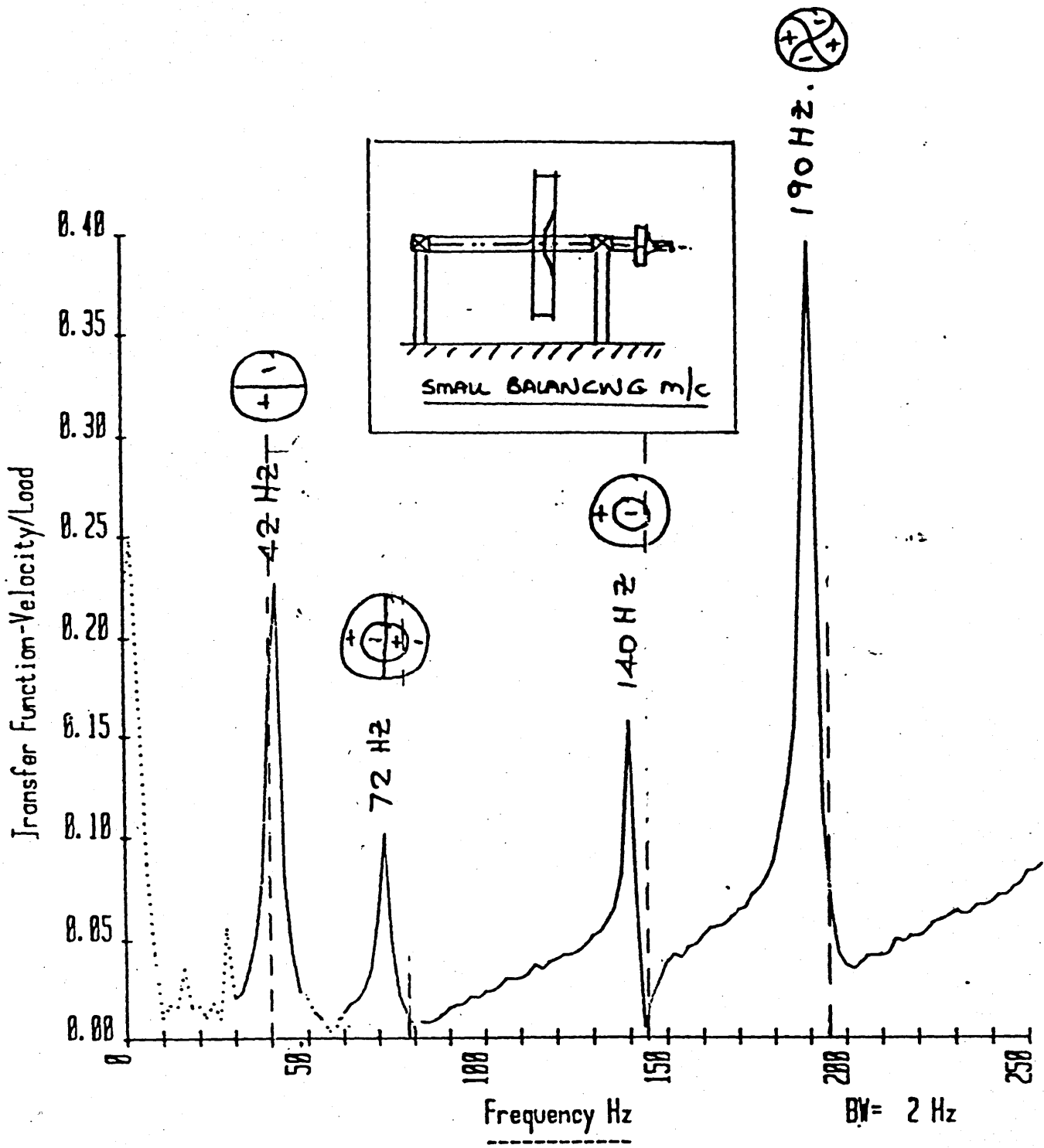
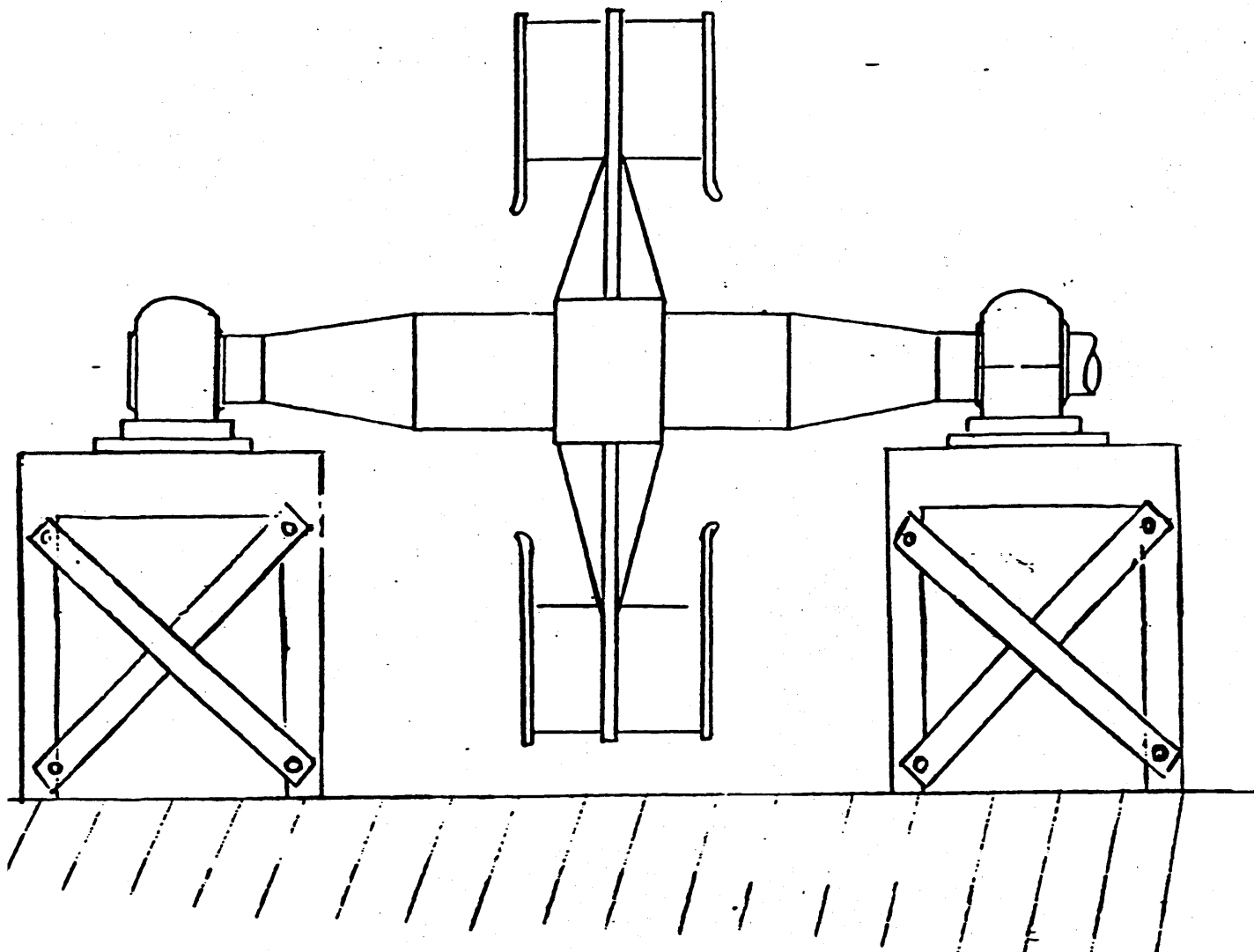


Figure 15



TEST ARRANGEMENT FOR  
FREQUENCY RESPONSE TESTS

Figure 16

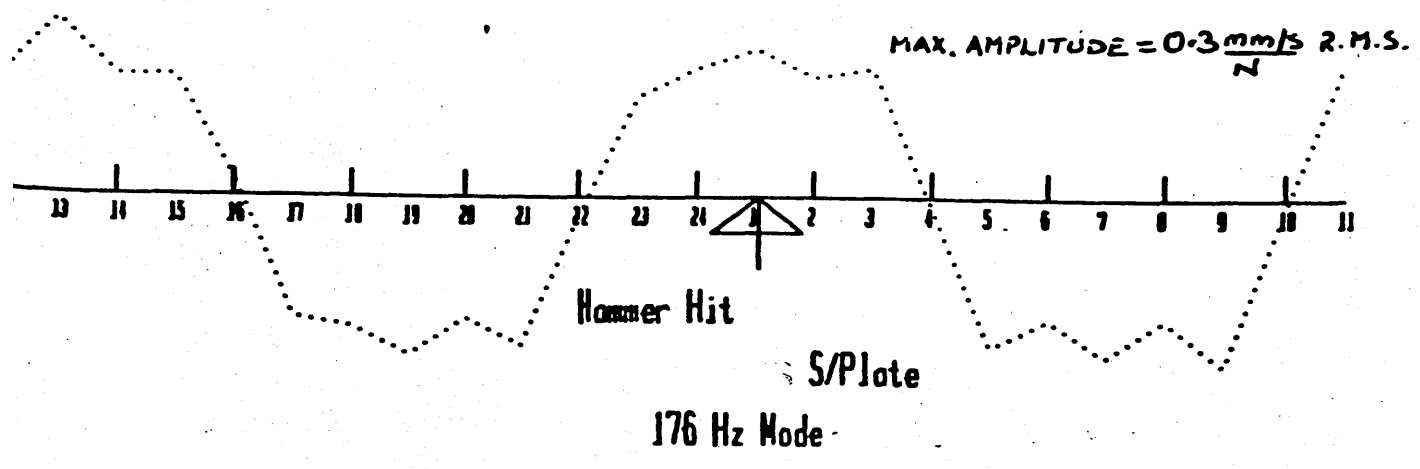
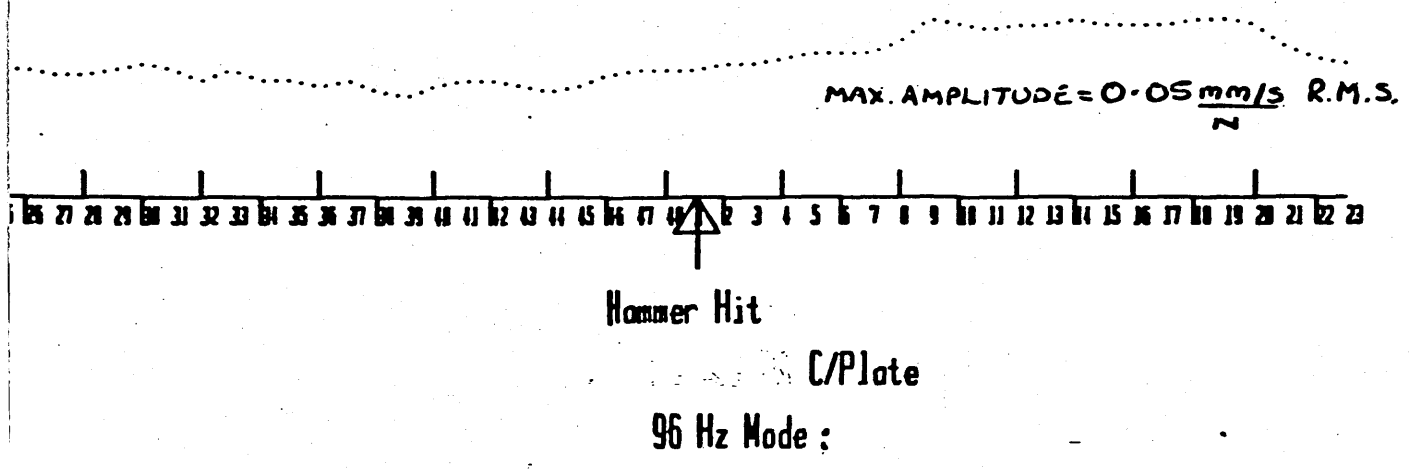
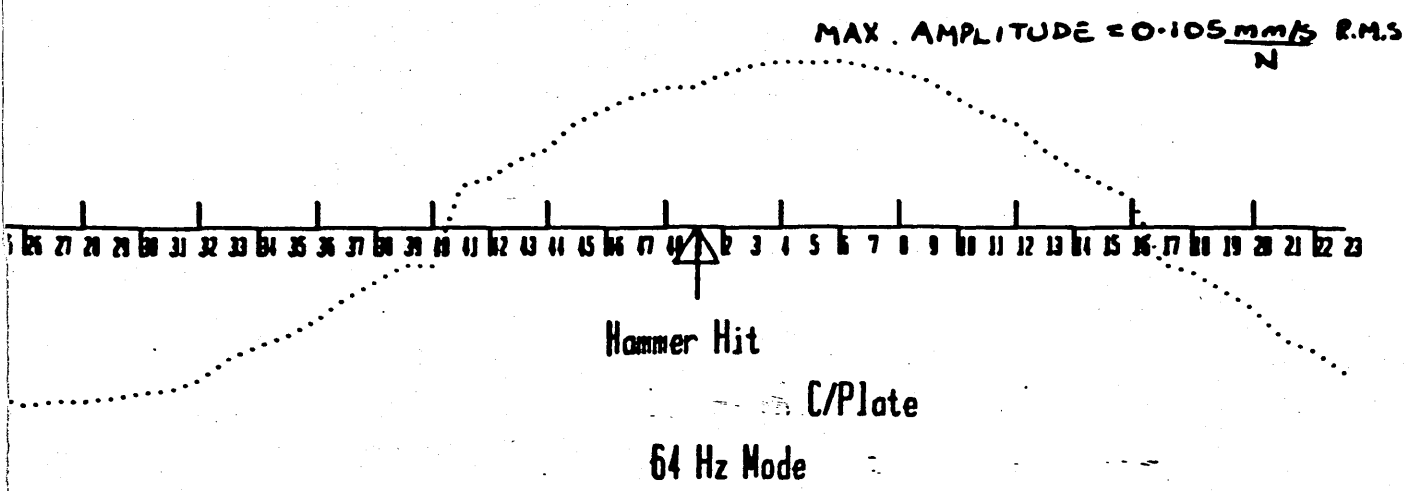


Figure 17

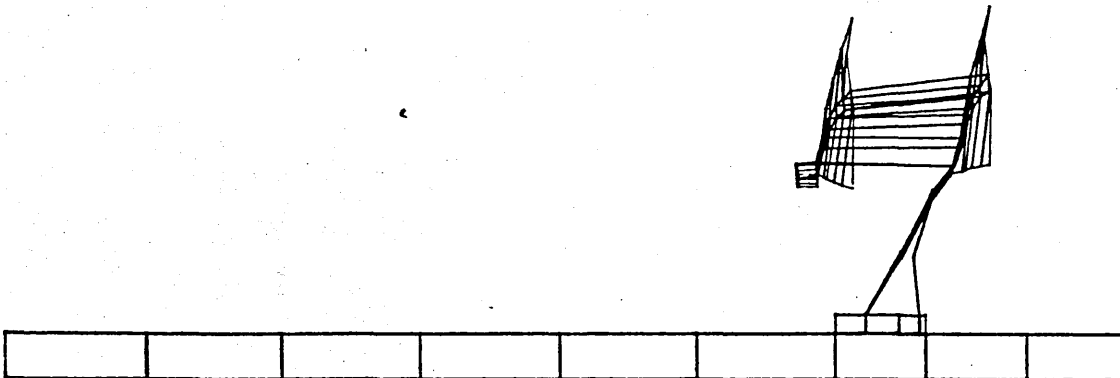
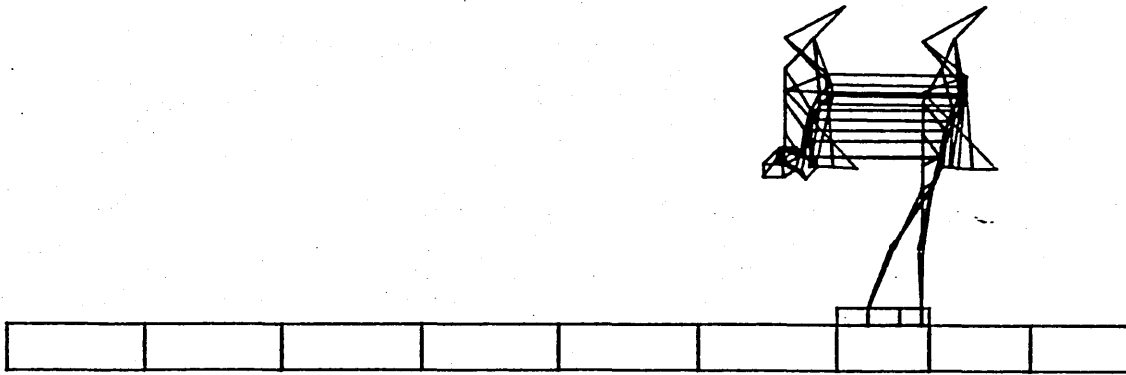
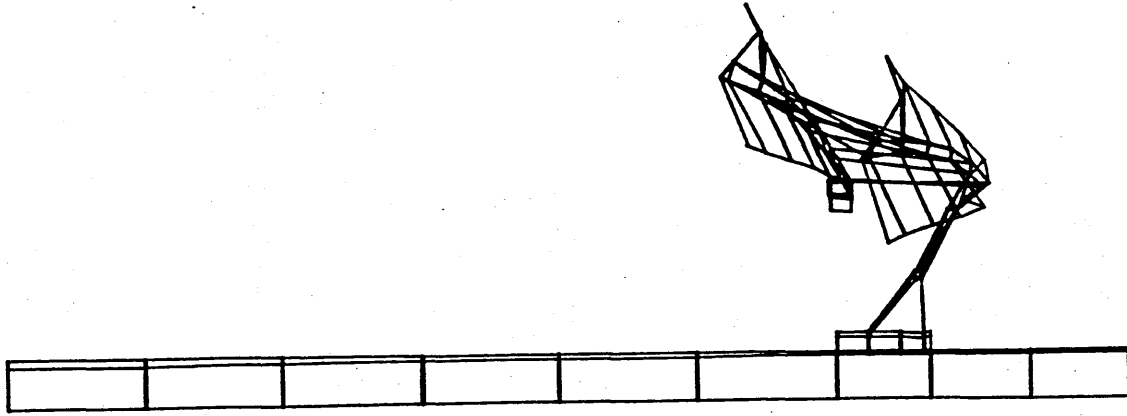


Figure 18

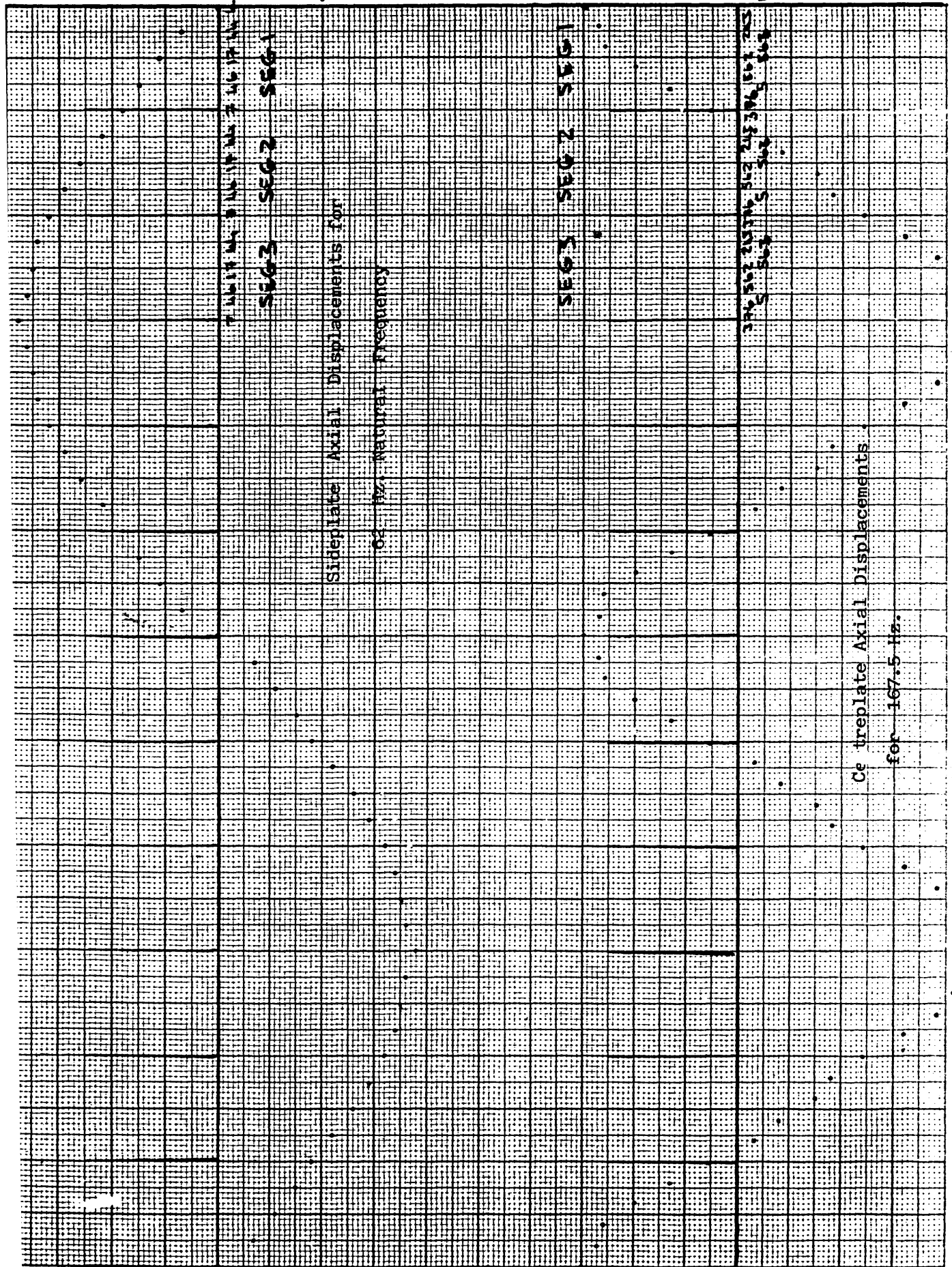


Figure 19  
71

W  
 P  
 Q  
 X /  
 INVAJ  
 Y  
 FREQ  
 227

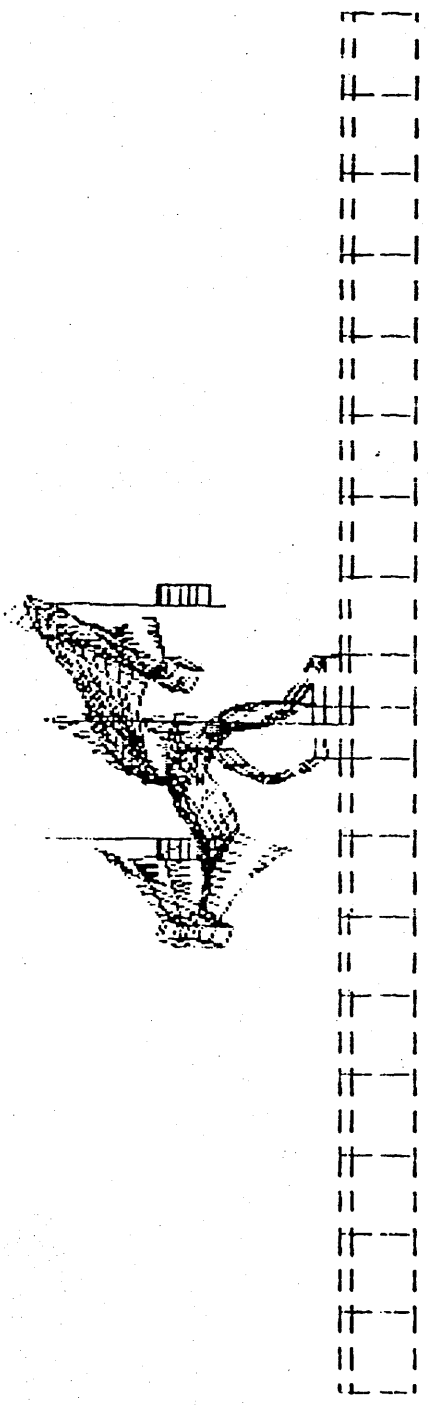
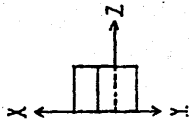


Figure 20

ROTATIONS  
X...270.  
Y...210.  
Z...270.



FREQ. HZ  
4.56E+2

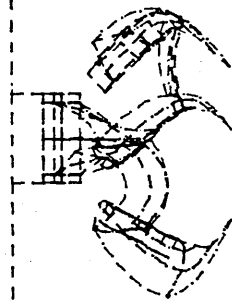


Figure 21

## REFERENCES

- 1 Den Hartog, J.P.  
'Mechanical Vibrations'  
McGraw-Hill, 1934
  
- 2 Morrision, D.  
'Influence of Plain Journal Bearings on the Whirling Action of an  
Elastic Rotor'  
Inst. Mech. Eng., 1961
  
- 3 White, D.J., Humpherson, J.  
'Finite Element Analysis of Stresses in Shafts Due  
to Interference-Fit Hubs'  
Journal of Strain Analysis, Vol.4 No.2, 1969
  
- 4 Andreev, G.Ya., Shat'ko, I.I.  
'Distribution of the Contact Pressure in Interference Fits'  
Russian Engineering Journal, Vol. XLVII, No. 5
  
- 5 'Guidelines to Finite Element Practice'  
National Agency for Finite Elements and Standards  
DTI, 1984
  
- 6 Timoshenko, S.  
'Vibration Problems in Engineering'  
4th Edition New York London  
Wiley 1974

A P P E N D I X A

---

Reproduced with kind permission of PAFEC Ltd

# 1 A SIMPLE VIEW OF THE FINITE ELEMENT METHOD.

This section is based upon the notes used in various PAFEC courses. The treatment is simple and is not mathematically rigorous. When the new reader has studied this section the outline of most of the other sections should be comprehensible. Some aspects of finite element theory will, however, only be meaningful after the more rigorous section 2 has been studied.

We start the theory with a development of the stiffness matrices for one of the most simple kinds of finite element - that of a beam subjected to bending loads. Before any analysis is started we shall decide what assumptions have to be made. These are as follows:

- (1) The beam is to lie with its neutral axis along the  $x$  coordinate axis.
- (2) the cross-section of the beam is to be uniform and is to be arranged so that the  $y$  and  $z$  directions are principal bending directions and so that bending in the  $y$  direction is not coupled with torsion.
- (3) The cross-sectional dimensions of the beam are to be small in relation to the length so that there is no warping and all the deformation is due to bending and none is due to shear.
- (4) The first three assumptions relate to the original undeflected element. One further assumption is needed in order to describe the manner in which deflection varies along the length of the beam. We shall only concern ourselves with the displacement  $u_y$  in the  $y$  direction and we shall assume that it varies along the length of the beam according to

$$u_y = \alpha_1 + \alpha_2 x + \alpha_3 x^2 + \alpha_4 x^3 \quad (1)$$

where the  $\alpha$ 's are arbitrary constants. Equation (1) may also be written in matrix form as:

$$u_y = [P]\{\alpha\} \quad (2)$$

where  $\{\alpha\}$  is a list of constants

and  $[P]$  is the polynomial matrix  $[P] = [1 \ x \ x^2 \ x^3]$

When different finite elements are connected together it will be necessary to join them at their nodal points which are situated at their ends. At this joining stage the displacements of two beams which meet will need to be identical. To enforce this continuity the equation (1) must be rewritten so that it involves the end displacements on the elements and not the constants  $\alpha_1$ ,  $\alpha_2$ , etc.

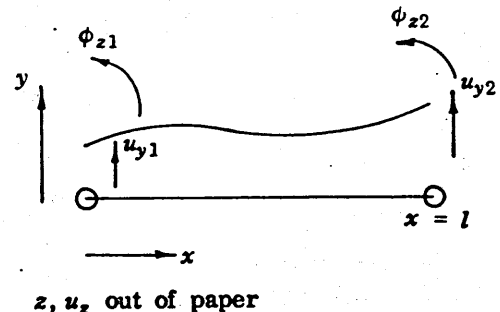


Fig. 1 Sign convention

We write down expressions for the nodal displacements in terms of the  $\alpha$ 's as

$$\left. \begin{aligned} u_{y1} &= \alpha_1 \\ \phi_{z1} &= \alpha_2 \\ u_{y2} &= \alpha_1 + \alpha_2 l + \alpha_3 l^2 + \alpha_4 l^3 \\ \phi_{z2} &= \alpha_2 + 2\alpha_3 l + 3\alpha_4 l^2 \end{aligned} \right\} \quad (3)$$

or in matrix form

$$\{u_e\} = [A]\{\alpha\} \quad (4)$$

where

$$[A] = \begin{bmatrix} 1 & 0 & 0 & 0 \\ 0 & 1 & 0 & 0 \\ 1 & l & l^2 & l^3 \\ 0 & 1 & 2l & 3l^2 \end{bmatrix}$$

and  $\{u_e\}$  is the listing of nodal displacements on the element  $u_{y1}$ ,  $\phi_{z1}$ ,  $u_{y2}$ ,  $\phi_{z2}$  written in a column vector.

From equation (4) the matrix  $[A]$  may be inverted and the value of  $\{\alpha\}$  substituted in equation (2) to give

$$u_y = [P][A]^{-1}\{u_e\} \quad (5)$$

Sometimes  $[P][A]^{-1}$  is written as  $[N]$  which is a row matrix containing the shape functions

$$[P][A]^{-1} = [N] = \left[ 1 - \frac{3x^2}{l^2} + \frac{2x^3}{l^3}, x - \frac{2x^2}{l} + \frac{x^3}{l^3}, \frac{3x^2}{l^2} - \frac{2x^3}{l^3}, -\frac{x^2}{l} + \frac{x^3}{l^2} \right] \quad (6)$$

The finite element method is based upon energy. For this reason we write down the strain energy stored in the beam finite element. It is

$$S.E. = \int \frac{1}{2} EI \left( \frac{\partial^2 u_y}{\partial x^2} \right)^2 dx \quad (7)$$

In equation (7)  $\frac{\partial^2 u_y}{\partial x^2}$  is the curvature of the beam and may be written in terms of the nodal displacements as:

$$\frac{\partial^2 u_y}{\partial x^2} = \frac{\partial^2}{\partial x^2} [P][A]^{-1}\{u_e\} \quad (8)$$

Since  $[A]^{-1}$  and  $\{u_e\}$  are not functions of  $x$  we may write:

$$\frac{\partial^2 u_y}{\partial x^2} = \left[ \frac{\partial^2 P}{\partial x^2} \right] [A]^{-1}\{u_e\} \quad (9)$$

where

$$\left[ \frac{\partial^2 P}{\partial x^2} \right] = [0 \quad 0 \quad 2 \quad 6x] \quad (10)$$

In the kernel of the integral in equation (7) the square of the scalar quantity  $(\partial^2 u_y / \partial x^2)$  arises. The scalar will be treated for the moment as a 1 by 1 matrix which may be transposed as follows:

$$\left( \frac{\partial^2 u_y}{\partial x^2} \right)^2 = \left[ \frac{\partial^2 u_y}{\partial x^2} \right]^T \left[ \frac{\partial^2 u_y}{\partial x^2} \right] \quad (11)$$

$$\left(\frac{\partial^2 u_y}{\partial x^2}\right)^T = \{u_e\}^T [A]^{-T} \left[\frac{\partial^2 P}{\partial x^2}\right]^T \left[\frac{\partial^2 P}{\partial x^2}\right] [A]^{-1} \{u_e\} \quad (12)$$

Examination of equations (7) and (12) shows that most of the quantities underneath the integration sign are in fact constant and may be written outside as

$$S.E. = \frac{1}{2} EI \{u_e\}^T [A]^{-T} \int_0^l \left[\frac{\partial^2 P}{\partial x^2}\right]^T \left[\frac{\partial^2 P}{\partial x^2}\right] dx [A]^{-1} \{u_e\} \quad (13)$$

Using equation (10) the kernel of the integral in equation (13) is

$$\begin{bmatrix} 0 \\ 0 \\ 2 \\ 6x \end{bmatrix} \begin{bmatrix} 0 & 0 & 2 & 6x \end{bmatrix} = \begin{bmatrix} 0 & 0 & 0 & 0 \\ 0 & 0 & 0 & 0 \\ 0 & 0 & 4 & 12x \\ 0 & 0 & 12x & 36x^2 \end{bmatrix} \quad (14)$$

The integral of equation (14) is

$$\begin{bmatrix} 0 & 0 & 0 & 0 \\ 0 & 0 & 0 & 0 \\ 0 & 0 & 4l & 6l^2 \\ 0 & 0 & 6l^2 & 12l^3 \end{bmatrix} \quad (15)$$

The matrix in equation (15) is scaled by  $EI$  and pre-multiplied by  $[A]^{-1}$  and post-multiplied by  $[A]^{-1}$  to form a matrix  $[S_e]$  so that equation (13) may be rewritten as

$$S.E. = \frac{1}{2} \{u_e\}^T [S_e] \{u_e\} \quad (16)$$

with

$$[S_e] = EI \begin{bmatrix} 12/l^3 & \text{symmetric} & & & \\ 6/l^2 & 4/l & & & \\ -12/l^3 & -6/l^2 & 12/l^3 & & \\ 6/l^2 & 2/l & -6/l^2 & 4/l & \end{bmatrix} \quad (17)$$

There is a theorem due to Castigliano which states that the differential of strain energy with respect to a displacement gives the force in the direction of that displacement. The equation (16) may be differentiated in that way to yield forces and moments at the ends of the beam finite element. It is valid in fact to differentiate the strain energy with respect to the list of displacements  $\{u_e\}$ .

$$\{F_e\} = \frac{\partial(S.E.)}{\partial\{u_e\}} = [S_e] \{u_e\} \quad (18)$$

The product  $[S_e]\{u_e\}$  in equation (18) is the list of generalised forces which act upon the element. The term generalised is used because both forces and moments are included.

$\{F_e\} = \begin{Bmatrix} F_{y1} \\ M_{y1} \\ F_{y2} \\ M_{y2} \end{Bmatrix}$  are the forces applied to the nodes. Note that the order within  $\{F_e\}$  corresponds to the order within  $\{u_e\}$ .

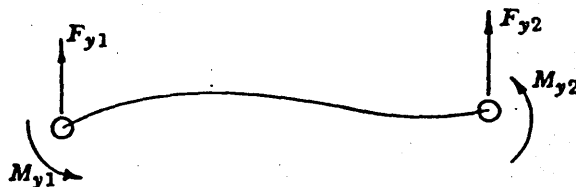


Fig. 2 Generalised forces at the ends of a beam finite element.

Equation (18) gives the generalised forces  $\{F_e\}$  on the element in terms of the generalised displacements  $\{u_e\}$  and the stiffness matrix  $[S_e]$  for the element. Since  $[S_e]$  is a function of geometric and material properties it is straightforward to write down this relationship for each element in the complete system.

To demonstrate this process we consider the structure shown in fig. 3 which is composed of two beam elements with a transverse load applied at one end of the structure and a clamped support at the other. There is an intermediate support at a point along the beam at which the section changes.

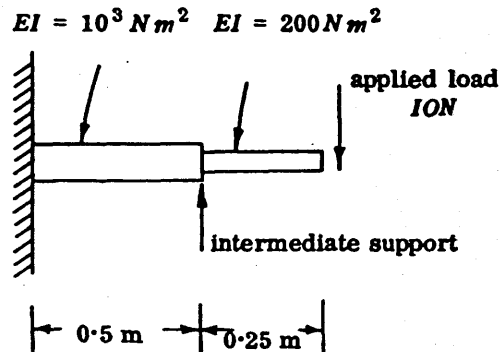


Fig. 3

The first task is to divide the structure into finite elements and the results of this is shown in fig. 4. The forces on the ends of the individual elements are also shown in fig. 4.

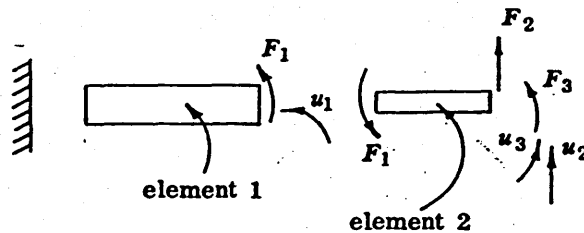


Fig. 4

Notice that there is no force shown wherever the problem is constrained. This does not mean that the force acting at the constraint is zero. We merely have no interest in the reaction loads at this stage. Each of the unknown displacements is numbered in the sequence  $u_1, u_2, u_3$ . In the direction of the first of these there are forces (actually generalised forces which can include moments) on each of the elements. It is obvious that  $F_1$  and  $F_1'$  are equal and opposite. We have left them as separate quantities at this stage since we wish for our approach to cater for a more general problem in which there are many elements meeting at a node. The subscript on each force is the same as the corresponding subscript on  $u$ .

Using the  $[S_e]$  matrix derived earlier we write down relations between the forces  $F_i$  and the displacements  $u_i$ .

For the element 1 we have the following:

$$\begin{Bmatrix} - \\ - \\ - \\ F_1 \end{Bmatrix} = \begin{bmatrix} - & - & - & - \\ - & - & - & - \\ - & - & - & - \\ - & - & - & 8000 \end{bmatrix} \begin{Bmatrix} 0 \\ 0 \\ 0 \\ u_1 \end{Bmatrix} \quad (19)$$

$$\begin{Bmatrix} F_1' \\ F_2 \\ F_3 \end{Bmatrix} = \begin{bmatrix} - & 3200 & -19200 & 1600 \\ - & -19200 & 153600 & -19200 \\ - & 1600 & -19200 & 3200 \end{bmatrix} \cdot \begin{Bmatrix} u_1 \\ u_2 \\ u_3 \end{Bmatrix} \quad (20)$$

The dashes in equations (19) and (20) indicate that the values of the terms are not needed in the analysis. The fact that the same displacement  $u_1$  appears in both the equations (19) and (20) shows that continuity between the two elements has been taken into account. We now consider equilibrium. The conditions of equilibrium are as follows:

$$F_1 + F_1' = 0, \quad F_2 = -10, \quad F_3 = 0. \quad (21)$$

The equations (21) are rewritten in terms of displacements by using the equations (19) and (20) to yield the following:

$$\left. \begin{array}{l} 8000 u_1 + 3200 u_1 - 19200 u_2 + 1600 u_3 = 0 \\ -19200 u_1 + 153600 u_2 - 19200 u_3 = -10 \\ 1600 u_1 - 19200 u_2 + 3200 u_3 = 0 \end{array} \right\} \quad (22)$$

Equation (22) may be rewritten in matrix form as:

$$\begin{bmatrix} 11200 & -19200 & 1600 \\ -19200 & 153600 & -19200 \\ 1600 & -19200 & 3200 \end{bmatrix} \cdot \begin{Bmatrix} u_1 \\ u_2 \\ u_3 \end{Bmatrix} = \begin{Bmatrix} 0 \\ -10 \\ 0 \end{Bmatrix} \quad (23)$$

or  $[S_s] \{u_s\} = \{F_s\} \quad (24)$

It is now clear that the equations (23) or (24) involve just the nodal displacements,  $\{u_s\}$ , as unknowns. The solution may be obtained as

$$u_1 = 0.0003125 \text{ rad}, \quad u_2 = 0.003385 \text{ m}, \quad u_3 = 0.001875 \text{ rad}.$$

Now that the solutions for the generalised displacements have been obtained we can go back to consider equation (5). For a particular point along the beam we know the value of  $[P]$ . The matrix  $[A]^{-1}$  contains only the length  $l$  of the beam which we know. The vector  $\{u_e\}$  of displacements on a particular element can be found from the system list of displacements  $\{u_s\}$ . Therefore we can find the value of  $u_y$  at any point along the beam.

Similarly we can use equation (9) to find the curvature at some point along the length of a particular beam element. From this we can find the bending moment.

$$M = EI \frac{\partial^2 u_y}{\partial x^2} \quad (25)$$

The shear force follows naturally by using the third derivative of the transverse displacement  $u_y$ .

### Summary of processes

We shall see that the derivation of stiffness matrices for a wide range of elements is similar to the development presented in this section which may be summarised in the following steps.

- (1) Design the finite element and list any relevant assumptions about the element geometry (e.g. the element is to be straight and one dimensional).
- (2) Make an assumption for the distribution of displacement within the element. If this assumption is in terms of arbitrary constants then these should be eliminated to give an interpolation for the displacement within an element in terms of the element nodal displacements.
- (3) Write down an expression for the strain energy in terms of the displacements and use the interpolation to express the energy in terms of nodal displacements. Carry out any necessary integration.
- (4) Use Castigliano's theorem by differentiating the strain energy with respect to displacements to give the forces at the nodes in terms of the displacements.
- (5) Write down equilibrium conditions between elements in terms of forces and then in terms of displacements. This yields a set of system equations for the displacements which can then be solved.
- (6) Knowing the nodal displacements on each element the bending moments or stresses can be found.

In the beam type element presented above there were only two degrees of freedom at each node and the element was one dimensional. There are many other types of finite element with one, two and three dimensions and these will be introduced in the sections that follow. We shall often want to introduce further degrees of freedom into the analysis in order to provide for other continuities. In general we shall consider six degrees of freedom at each node. They will be the three translations  $u_x$ ,  $u_y$ ,  $u_z$  in three perpendicular directions and also three rotations  $\phi_x$ ,  $\phi_y$ ,  $\phi_z$  about the three coordinate directions  $x$ ,  $y$ ,  $z$ . In fig. 5 these degrees of freedom are shown. The rotations are shown in two alternative ways by using a double headed arrow and by using a curved arrow. Note that the axis system is right handed and that a particular rotation  $\phi_i$  is in the right handed screw direction about the  $i$  axis.

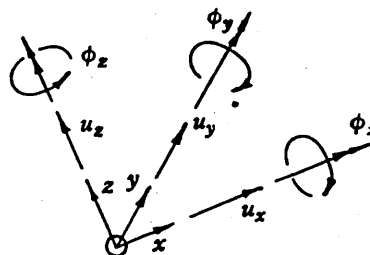


Fig. 5

More than six degrees of freedom at each node are possible but are not recommended for the solution of real engineering problems.

The different types of finite element may be categorised as follows:

- (1) Beam elements. Earlier in this section we studied a beam that had only two degrees of freedom at each node. If we consider a beam in which there is bending in two directions, axial motion and torsion we need all six degrees of freedom.
- (2) Membrane elements. Only in plane loads are carried. Two degrees of freedom  $u_x$ ,  $u_y$  only are needed at each node.
- (3) Three dimensional solid elements. Three degrees of freedom  $u_x$ ,  $u_y$ ,  $u_z$  are needed at each node.
- (4) Plate bending elements. The transverse displacement  $u_z$  and two rotations  $\phi_x$ ,  $\phi_y$  are needed.
- (5) Shell situations. There are various situations which will be dealt with separately later.
- (6) Combinations of structural elements. The general rule is to allow any degree of freedom which is required by any of the elements which is connected to a node.

(7) Temperature problems. In cases in which the temperature is unknown there is only one degree of freedom at each node.

The decision chart given in fig. 6 has been produced to assist the new user in deciding which type of finite element to use in a particular situation. (see pp. 2.8, 2.9)

## 2 A MORE RIGOROUS BASIS FOR THE FINITE ELEMENT METHOD

The theoretical basis for the finite element method which was described in the previous section is not rigorous. It was assumed that finite elements were joined together at nodes and that forces between elements are only transferred at these nodal points. This is of course impossible if the elements have line or surface contact. In fact the same theoretical results can be achieved if the finite element method is viewed in another way. It happens that nature chooses to arrange for the static equilibrium position of a linear elastic structure to be that position in which there is as little potential energy stored as possible. Now the potential energy of a structure is equal to the strain energy stored internally minus the work done on the structure by the externally applied loads.

$$\Pi_{PE} = S.E. - W.D. \quad (26a)$$

Thus the solution of the problem involves finding the minimum value of  $\Pi_{PE}$ . Since the S.E. term is always an integral involving unknown functions the problem has become a 'variational' one.<sup>551,552</sup> Corresponding to every variational problem there is one or perhaps a number of differential equation(s) known as the Euler equation(s) of the problem. It may be shown that the Euler equations obtained from the variational principle that  $\Pi_{PE}$  is a minimum happen to be the equations of equilibrium.

In applying the variational principle we write down the value of S.E. as a sum of the strain energies of the different elements. In the case where the applied loads are known the S.E. density is based upon the unknown displacements.

$$\Pi_{PE} = \sum_{\text{elements}} (S.E. \text{ density}) dV - W.D. \quad (26b)$$

or in tensor form

$$\Pi_{PE} = \int_{\text{volume}} \left( \frac{1}{2} u_{i,j} E_{ijkl} u_{k,l} - F_i u_i \right) dV - \int_{\text{surface } S_{\bar{\sigma}}} \bar{\sigma}_i \mu_j u_i dS \quad (26c)$$

where an overbar denotes a prescribed quantity

$E_{ijkl}$  is the modulus tensor

$\mu_j$  are the direction cosines of the surface element  $dS$

$F_i$  are prescribed body forces

$S_{\bar{\sigma}}$  is that part of the boundary on which stresses are prescribed

The integral is precisely the same as that which was obtained in the preceding section. However, the integral over one element in that instance was differentiated with respect to displacements in order to obtain the forces using Castigliano's Theorem. Instead of doing that we shall now write down the S.E. for each element as before.

$$S.E. = \frac{1}{2} \{u_e\}^T [S_{e1}] \{u_e\} \quad (27)$$

element  $i$

The sum of the strain energies over the whole structure can be obtained from equation (27) by first rearranging terms in  $[S_{ei}]$  and  $\{u_{ei}\}$  to give

$$S.E = \frac{1}{2} \{u_s\}^T [S_{ei}^*] \{u_s\} \quad (28)$$

element  $i$

Note that  $\{u_s\}$  is the list of unknown system displacements. The matrix  $[S_{ei}^*]$  is extremely sparse for practical problems because the list of displacements  $\{u_e\}$  is much smaller than the list  $\{u_s\}$

The strain energy summed over the elements can now be written as

$$S.E. = \frac{1}{2} \{u_s\}^T [S_s] \{u_s\} \quad (29a)$$

structure

where

$$[S_s] = \sum_i [S_{ei}^*] \quad (29b)$$

elements

The summation in fact represents the merging process. The individual  $[S_{ei}]$  matrices are transformed and added into the system matrix  $[S_s]$ .

In the variational principle which has been used above the displacements are unknown and the strain energy is written down in terms of these displacements. There are other variational principles in elasticity. One of the most complex is the Hu-Washizu principle in which stresses, strains and displacements are all unknown. The Euler equations derived from this principle state as follows:

- (1) Stresses must be related to strains by some equations that describe the material. In linear elastic analysis this corresponds to Hooke's law.
- (2) The stresses are in equilibrium.
- (3) The strains and displacements are related in the appropriate manner.

The Hu-Washizu principle (see equation (30) later) can be simplified by imposing the condition that the stress-strain relations are always satisfied. This yields the Hellinger-Reissner principle (see equation 31) later) which involves the stresses and displacements and as Euler equations yields the statements (2) and (3) above. Further, the condition (3) may be imposed so that only displacements are unknown. This yields the principle of minimum potential energy with which we have already dealt. Alternatively the displacements may be eliminated leaving just the stresses by imposing the condition that the stresses are in equilibrium. This yields the principle of minimum complementary potential energy (see equation (32) later). The Euler equations of this principle are the relations between strain and displacement.

The connections between the various variational statements is shown in fig. 2.7 (For further details see references 83, 92, 106).

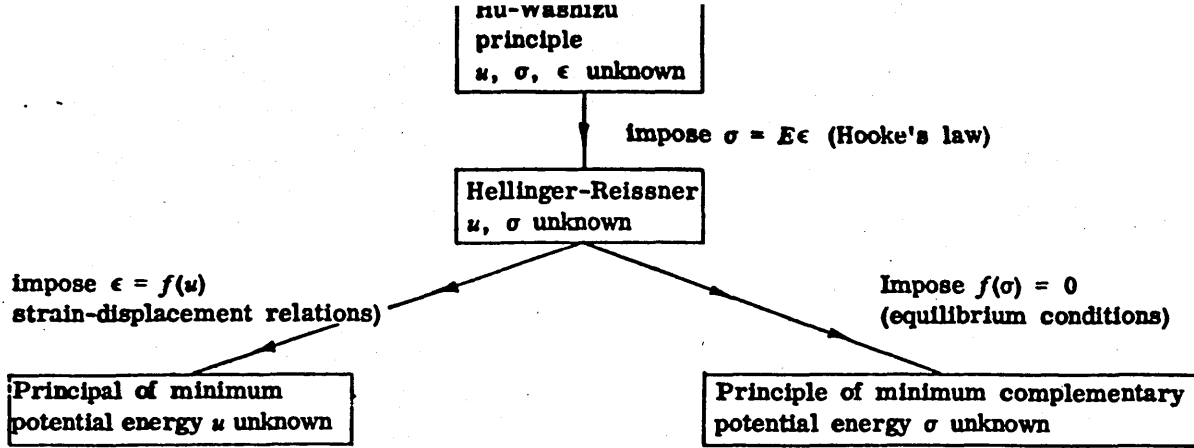


Fig. 2.7 Connections between variational principles

The variational statements described relate to a complete structure and the assumptions for the unknowns in each principle have to satisfy certain continuity requirements. When the finite element method is used the assumptions may be discontinuous across inter-element boundaries. In such situations extra terms within the variational statements will be needed. These so called jump terms are discussed in detail by Pian<sup>106</sup> and by Wolf<sup>83</sup>.

The Hu-Washizu variational principle discussed earlier in which  $\sigma_{ij}$ ,  $\epsilon_{ij}$  and  $u_i$  are all unknowns may be written as

$$\begin{aligned} \Pi_{HW} = \int_{\text{volume}} \left( \frac{1}{2} \epsilon_{ij} E_{ijkl} \epsilon_{kl} - F_i u_i + \left( \frac{1}{2} (u_{i,j} + u_{j,i}) - \epsilon_{ij} \right) \sigma_{ij} \right) dV \\ - \int_{\text{surface } S_{\tilde{\sigma}}} \tilde{\sigma}_{ij} \mu_j u_i dS - \int_{\text{surface } S_{\tilde{u}}} \sigma_{ij} u_j (u_i - \tilde{u}_i) dS \end{aligned} \quad (30)$$

The Hellinger-Reissner principle which is a function of  $\sigma_{ij}$  and  $u_i$  is given as

$$\begin{aligned} \Pi_{HR} = \int_{\text{volume}} \left( -\frac{1}{2} \sigma_{ij} C_{ijkl} \sigma_{kl} - F_i u_i + \frac{1}{2} \sigma_{ij} (u_{i,j} + u_{j,i}) \right) dV \\ - \int_{\text{surface } S_{\tilde{\sigma}}} \tilde{\sigma}_{ij} \mu_j u_i dS - \int_{\text{surface } S_{\tilde{u}}} \sigma_{ij} \mu_j (u_i - \tilde{u}_i) dS \end{aligned} \quad (31)$$

where  $C_{ijkl}$  is the compliance tensor.

The principle of minimum complementary potential energy is

$$\Pi_{CPE} = \int_{\text{volume}} \frac{1}{2} \sigma_{ij} C_{ijkl} \sigma_{kl} dV - \int_{\text{surface } S_{\tilde{\sigma}}} \sigma_{ij} \mu_j u_i dS \quad (32)$$

## 10.1 Element and system mass matrices

In the simple analysis presented in section 1 the expression for strain energy was differentiated with respect to displacements in order to obtain the forces on the element. We now present a dynamic analysis which is consistent with this level of mathematical rigour.

We assume that all displacements in a structure vary sinusoidally in time at frequency  $\omega$ . We shall omit the factor  $\sin \omega t$  or  $\exp(i\omega t)$  in the analysis which follows. We write down the kinetic energy of a single simple beam element as

$$K.E. = \int_0^l \frac{1}{2} \rho A u_y^2 \omega^2 dx \quad (307)$$

We use the fact that  $u_y$  may be rewritten in terms of the nodal values  $\{u_e\}$  from equation (5) and then the kinetic energy becomes

$$K.E. = \frac{1}{2} \omega^2 \{u_e\}^T [M_e] \{u_e\} \quad (308)$$

$[M_e]$  which is known as the element mass matrix is given by

$$[M_e] = \rho A [A]^{-T} \int_0^l [P]^T [P] dx [A]^{-1} \quad (309)$$

Differentiating the kinetic energy in equation (288) with respect to  $\{u_e\}$  yields the forces required to produce the acceleration. Since the acceleration is in the opposite direction to the displacements the forces required to overcome the inertia are

$$\{F_e\}_{\text{inertia}} = -\omega^2 [M_e] \{u_e\} \quad (310)$$

The total force acting on an element in order to overcome both stiffness and inertia is

$$\{F_e\} = [S_e] \{u_e\} - \omega^2 [M_e] \{u_e\} \quad (311)$$

These forces may be merged in exactly the same way as the stiffness forces were merged in section 1. The process yields a system set of equations as

$$[S_s] \{u_s\} - \omega^2 [M_s] \{u_s\} = (S_s - \omega^2 [M_s]) \{u_s\} = \{F_s\} \quad (312)$$

where  $[M_s]$  is the system mass matrix and  $\{F_s\}$  is a list of the harmonically varying forces which are applied to the system.

In the case of a vibrating beam in which we are concerned only with transverse  $u_y$  motion there is only one component of velocity to be considered. In a general three dimensional situation there will be velocities in all three directions and we can write the kinetic energy as

$$K.E. = \frac{1}{2} \int_{\text{volume}} \rho \omega^2 (u_x^2 + u_y^2 + u_z^2) dV \quad (313)$$

The development presented so far has not been mathematically rigorous. This remark applies to section 1 earlier but section 2 shows how variational statements can be made which are rigorously admissible. In dynamic situations the appropriate variational statement is that the Lagrangian.

$$L = K.E. - S.E. \quad (314)$$

is a minimum

The Euler equations of this variational statement are the equations of motion for infinitesimal elements of the continuum.

## 10.2 Lumped mass element

In most elastic structures the mass is distributed over the elastic elements and mass matrices for each of these elements can be found by the usual integration procedures. But in certain structures there are small concentrated masses that have no flexibility. We account for these by using lumped mass elements.

Let us consider a rigid body with its centre of mass at a point  $G$  where the displacements and rotations are  $u_{xG}, u_{yG}, \dots, \phi_{zG}$ . In sinusoidal conditions the kinetic energy of some other point on the body at distances  $x', y', z'$  along the cartesian directions from  $G$  is

$$K.E. = \frac{1}{2} \rho \cdot dV \cdot \omega^2 \cdot ((u_{zG} + z' \phi_y - y' \phi_z)^2 + (u_{yG} + x' \phi_z - z' \phi_x)^2 + (u_{xG} + y' \phi_x - x' \phi_y)^2) \quad (315)$$

$$\text{now } m = \text{the mass} = \int \rho dV$$

$$I_{xx}, I_{yy}, I_{zz} \text{ are the moments of inertia } \int \rho(x'^2 + z'^2) dV \text{ etc.} \quad (317)$$

$$I_{xy}, I_{yz}, I_{zx} \text{ are the products of inertia } \int \rho x' y' dV \text{ etc.} \quad (318)$$

When a lumped mass element is placed with its centre of mass at node at which the displacement listing  $\{u\}$  is given by equation (319) then the mass matrix has the form of equation (320).

$$\{u\} = \{u_{xG}, u_{yG}, u_{zG}, \phi_{xG}, \phi_{yG}, \phi_{zG}\} \quad (319)$$

$$[M_e] = \begin{bmatrix} m & & & & & & \\ 0 & m & & & & & \\ 0 & 0 & m & & & & \\ 0 & 0 & 0 & I_{xx} & & & \\ 0 & 0 & 0 & -I_{xx} & I_{yy} & & \\ 0 & 0 & 0 & -I_{zx} & -I_{yz} & I_{zz} & \end{bmatrix} \quad (320)$$

Now let us suppose that the lumped mass element is placed at distances  $e_x, e_y, e_z$  along the cartesian directions from a node at which the displacements are  $u_x$  to  $\phi_z$  as shown in fig. 2.43. From the geometrical considerations we find that

$$u_{xG} = u_x + e_x \phi_y - e_y \phi_z \text{ etc.} \quad (321)$$

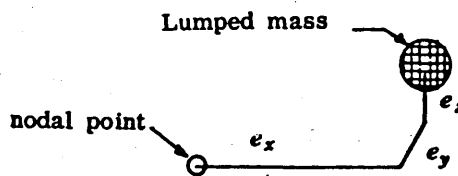


Fig. 43.

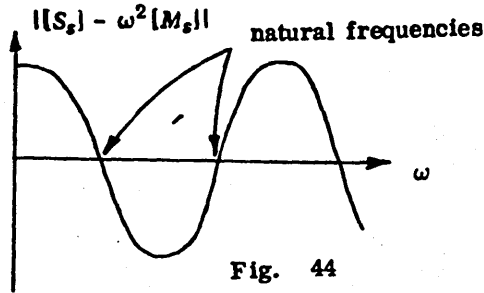
Using equation (321) in equation (316) gives the effective element mass matrix at node  $N$  as

$$[M_e] = \begin{bmatrix} m & & & & & & \\ 0 & m & & & & & \\ 0 & 0 & m & & & & \\ 0 & -m e_z & m e_y & I_{xx} + m(e_y^2 + e_z^2) & & & \\ m e_z & 0 & -m e_x & -I_{xy} - m e_x e_y & I_{yy} + m(e_x^2 + e_z^2) & & \\ -m e_y & m e_x & 0 & -I_{yz} - m e_z e_x & -I_{yz} - m e_y e_z & I_{zz} + m(e_x^2 + e_y^2) & \end{bmatrix} \quad (322)$$

with the commonly occurring problem of natural frequency determination we wish to find the frequencies  $\omega_1, \omega_2$  etc. at which the structure will vibrate naturally without external loads being applied. Accordingly we consider equation (312) and set  $\{F\} = \{0\}$

$$([S_s] - \omega^2[M_s])\{u_s\} = \{0\} \quad (323)$$

Equation (323) would be satisfied if  $\{u_s\}$  were a null vector but of course this would represent a trivial solution with no vibration at all. We therefore choose  $\omega$  for the square matrix  $([S_s] - \omega^2[M_s])$  to have a zero determinant. A typical variation of  $|[S_s] - \omega^2[M_s]|$  is shown in fig. 44. The values where the curve crosses the  $\omega$  axis are the natural frequencies of the system.



It would be possible, but extremely expensive to evaluate  $|[S_s] - \omega^2[M_s]|$  enough times to obtain a graph and hence the natural frequencies. A better technique is to transform the equation (323). We proceed by factorizing  $[M_s]$  to obtain

$$[M_s] = [L][L^T] \quad (324)$$

where  $[L]$  is a lower triangular matrix and of course  $[L]^T$  is its upper triangular transpose. We then transform the degrees of freedom  $\{u_s\}$  using

$$\{u'\} = [L]^T\{u_s\} \quad (325)$$

Equation (325) is substituted into equation (323) and  $\{u_s\}$  is eliminated. On premultiplying by  $[L]^{-1}$  we obtain

$$([S'] - \omega^2[I])\{u'\} = \{0\} \quad (326)$$

where  $[S']$  is the symmetric matrix  $[S'] = [L]^{-1}[S_s][L]^{-T}$  (327)

and  $[I]$  is a unit matrix

Equation (326) will be recognised by numerical analysts as a symmetric real eigenvalue problem. There are many efficient methods available for finding the eigenvalues  $\omega^2$  and the corresponding vectors  $\{u'\}$  which satisfy equation (326). From a  $\{u'\}$  vector the corresponding  $\{u_s\}$  is calculated using equation (325).

#### 10.4 Eigenvalue economisation

Although the eigenvalue process is considerably faster than the determinant search method, it is still prohibitively expensive for systems with more than about 100 degrees of freedom. It happens that almost all the degrees of freedom in a very large eigenvalue problem have little effect on the mass matrix. The stiffness matrix is found from strains which are obtained as differentials of the displacements or degrees of freedom. A large number of degrees of freedom are essential since differentiation is a process which introduces 'noise' and inaccuracy. This is not so with the mass matrix (see equation (313)). Thus we can eliminate in some way the mass aspects of certain degrees of freedom provided that we leave the stiffness intact. This can be achieved by neglecting the inertia effects of certain freedoms (see refs. 97,98,121,123,124). We consider equation (323) and we partition the

vector  $\{u_s\}$  into

$$\{u_s\} = \{\{u_m\}, \{u_r\}\} \quad (328)$$

In equation (328)  $\{u_m\}$  are the master degrees of freedom which will be retained whereas  $\{u_r\}$  are the slave displacements which are to be reduced out. Equation (323) now becomes

$$\left( \begin{bmatrix} [S_{mm}] & [S_{mr}] \\ [S_{rm}] & [S_{rr}] \end{bmatrix} - \omega^2 \begin{bmatrix} [M_{mm}] & [M_{mr}] \\ [M_{rm}] & [M_{rr}] \end{bmatrix} \right) \begin{Bmatrix} \{u_m\} \\ \{u_r\} \end{Bmatrix} = \begin{Bmatrix} \{0\} \\ \{0\} \end{Bmatrix} \quad (329)$$

The lower partition of this equation represents the statement that there is to be equilibrium at the slave degrees of freedom  $\{u_r\}$  which are to be reduced out. The inertia terms are neglected in this statement and we have

$$[S_{rm}] \{u_m\} + [S_{rr}] \{u_r\} = \{0\} \quad (330)$$

This is constraint on the degrees of freedom. It may be rewritten as an equation for  $\{u_m\}$ . We cannot use this expression directly in the upper partition of equation (329). We must remember that the finite element method is based upon energy and rewrite the strain and kinetic energies using equation (330) in order to eliminate  $\{u_r\}$ .

After development we find that

$$S.E. = \frac{1}{2} \{u_m\}^T \left( [S_{mm}] - [S_{mr}] [S_{rr}]^{-1} [S_{rm}] \right) \{u_m\} \quad (331)$$

$$= \frac{1}{2} \{u_m\}^T [S_m] \{u_m\} \quad (332)$$

$$K.E. = \frac{1}{2} \{u_m\}^T \left( [M_{mm}] - [M_{mr}] [S_{rr}]^{-1} [S_{rm}] - [S_{mr}] [S_{rr}]^{-1} [M_{rm}] + [S_{mr}] [S_{rr}]^{-1} [M_{rr}] [S_{rr}]^{-1} [S_{rm}] \right) \{u_m\} \quad (333)$$

$$= \frac{1}{2} \{u_m\}^T [M_m] \{u_m\} \quad (334)$$

The terms in round brackets in equations (331) and (333) represent the effective stiffness and mass matrices of the reduced system, and the system equations are now

$$\left( [S_m] - \omega^2 [M_m] \right) \{u_m\} = \{F_m\} \quad (335)$$

where the subscript  $m$  represents master degrees of freedom and  $\{F_m\}$ , the force vector, is zero for natural frequency calculation. It would be difficult to carry out the matrix operations implied in these equations because of the great demand on computer core store. In practice the elimination of the terms in the  $\{u_r\}$  vector is part of the frontal process which will be described later. (section 2.14). When the reduced stiffness and mass matrices have been found the eigenvalue process described earlier is used.

An important question that arises is how to choose which degrees of freedom are to be reduced out and which are to be kept. The master degrees of freedom should be those which are important in describing the kinetic energy. Therefore the masters should be concentrated in the region of heavy areas in the structure and free ends of components which can be expected to vibrate easily should contain masters. Even with a number of guidelines the choice of masters is not easy and an automatic method for their selection has been developed.

In essence the automatic method of master selection involves studying the ratio between  $S_{ii}$  and  $M_{ii}$ , the leading diagonal stiffness and mass terms for degree of freedom  $i$ .

When  $S_{ii}/M_{ii}$  is large then either the mass at degree of freedom  $i$  is small or its stiffness is large and hence it is well connected into the structure; it is unwise to keep degree of  $i$  as a master. On the other hand if  $M_{ii}$  is large and/or  $S_{ii}$  is small then the degree of freedom  $i$  is likely to give rise to appreciable inertia effects. The automatic selection technique involves keeping as masters the degrees of freedom from which  $S_{ii}/M_{ii}$  is small.

## 14 SOLUTION METHODS

### 14.1 Introduction

We wish to solve the problem

$$[S]\{u\} = \{F\} \quad (411)$$

where  $[S]$  is the square symmetric system stiffness matrix

$\{F\}$  is the list of applied nodal forces

$\{u\}$  is a list of the unknown displacements

Note that the system symbol,  $s$  has been dropped since no confusion can arise.

Often there will be a number of different loading cases and therefore the right hand side of equation (411) will be a rectangular matrix  $[F]$  and the unknowns will be written in columns in a matrix  $[u]$  of the same size. The following analysis can be extended to cover this more general situation without difficulty.

The static problem involves finding the solution to equation (411) as

$$\{u\} = [S]^{-1}\{F\} \quad (412)$$

In the following sections we shall consider various methods of doing this. The methods of solution which can be used are capable of division into two classes as (1) direct methods and (2) indirect methods. With direct methods the only approximations which arise are due to errors in arithmetical operations since computers work to a finite number of decimal places. Indirect methods usually involve making a guess at the solution and improving this guess until it is adequately accurate. We shall only be concerned in the following sections with direct methods.

### 14.2 Full [S]

The full system stiffness matrix, which is square and symmetric, is assembled and the solution is obtained by solving the equations in the computer core. The method is only feasible if the number of degrees of freedom in the structure is very small indeed (for example 50).

### 14.3 Banded [S]

The system stiffness matrix  $[S]$  is banded if the degrees of freedom are ordered carefully. A typical  $[S]$  is shown on the left of fig. 2.57. It is very wasteful to store the whole of  $[S]$  as is the case in the full  $[S]$  method. We only store the lower part of the band by replacing  $[S]$  by a rectangular array as shown. With the matrix stored in this revised form it is possible to solve the set of equations economically by factorising  $[S]$  to give

$$[S] = [L][L]^T \quad (413)$$

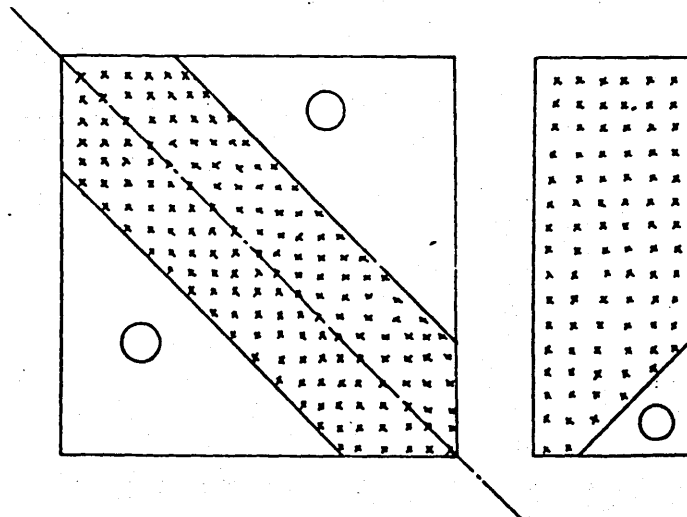


Fig. 2.57

visualise the process which is used to obtain [L] the first few terms of [S] and [L] will be written in conventional rather than banded form as

$$\begin{bmatrix} S_{11} & \text{symmetric} & & & \\ S_{21} & S_{22} & & & \\ S_{31} & S_{32} & S_{33} & & \\ \dots & \dots & \dots & \dots & \\ \dots & \dots & \dots & \dots & \\ \dots & \dots & \dots & \dots & \end{bmatrix} = \begin{bmatrix} L_{11} & 0 & 0 & 0 & \\ L_{21} & L_{22} & 0 & 0 & \\ L_{31} & L_{32} & L_{33} & 0 & \\ \dots & \dots & \dots & \dots & \\ \dots & \dots & \dots & \dots & \\ \dots & \dots & \dots & \dots & \end{bmatrix} \cdot \begin{bmatrix} L_{11} & L_{21} & L_{31} & & \\ 0 & L_{22} & L_{32} & & \\ 0 & 0 & L_{33} & & \\ \dots & \dots & \dots & \dots & \\ \dots & \dots & \dots & \dots & \\ \dots & \dots & \dots & \dots & \end{bmatrix} \quad (414)$$

The  $S_{11}$  term on the left of equation (414) can be written as

$$S_{11} = L_{11}^2 \quad (415)$$

From equation (415) we can find the value of  $L_{11}$  as  $\sqrt{S_{11}}$ . Let us now consider some other terms

$$S_{21} = L_{21} \cdot L_{11} \quad (416)$$

$$S_{31} = L_{31} \cdot L_{11} \quad (417)$$

$$S_{22} = L_{21}^2 + L_{22}^2 \quad (418)$$

$$S_{32} = L_{31}L_{21} + L_{32}L_{22} \quad (419)$$

$$S_{ii} = \sum_{j=1}^i L_{ij}^2 \quad (420)$$

$$S_{ki} = \sum_{j=1}^i L_{kj}L_{ij} \quad \text{for } k > i \quad (421)$$

Since the value of  $L_{11}$  can be obtained from equation (415) the values of  $L_{21}$  and  $L_{31}$  can be found from equations (416) and (417). At this stage,  $L_{22}$  is the only unknown in equation (418) which may therefore be rewritten as

$$L_{22} = \sqrt{(S_{22} - L_{21}^2)} \quad (422)$$

The only unknown in equation (419) is then  $L_{32}$  which may be calculated.

The general equations are given by (420) and (421). We can always use the first of these to find the diagonal entries in [L] and the second equation to find the off-diagonal terms.

Let us take the semi-bandwidth of [S] = 0 for all  $i, j$  such that

$$|i-j|+1 > w \quad (423)$$

From equations (416) and (417) it is apparent that the bandwidth down column 1 of [L] will be identical to that of [S]. A careful consideration of equation (414) shows this is indeed the case for all columns of [L].

By forming the [L] matrix column by column we can show that no  $S_{ij}$  term is required after the corresponding  $L_{ij}$  term has been evaluated. This consideration together with the statements above concerning bandwidth show that [L] may be formed in the [S] array which is therefore destroyed by the process.

Equation (420) can be used to find the leading diagonal terms of  $[L]$  as

$$L_{ii} = \sqrt{S_{ii} - \sum_{j=1}^{i-1} L_{ij}^2} = \sqrt{Z} \quad (424)$$

For structural problems in which a deformation always causes positive strain energy to be stored we say that the stiffness matrix  $[S]$  is positive definite. It is possible to prove that the quantity,  $Z$ , within the square root sign in equation (424) is always positive. If a structure has rigid body modes then zero strain energy states are possible and there will be as many values of  $i$  for which  $Z = 0$  as there are independent rigid body modes. In practice there will be numerical errors in the evaluation of the  $[S]$  and  $[L]$  matrices. Hence the value of  $Z$  may turn out to be slightly negative resulting in a program failure. The practical way out of this difficulty is to change  $Z$  to a small positive number, print a warning and proceed.

If there is a gross error in the data for a mesh, such as incorrect ordering of element topologies then an element may effectively have some negative area and hence negative stiffness. In such cases the algorithm for evaluating  $[L]$  encounters a large negative value of  $Z$  at some stage. The calculation is stopped and a diagnostic is printed.

After the factorization is complete the matrix equation (413) which is to be solved can now be rewritten as

$$[L][L]^T \{u\} = \{F\} \quad (425)$$

We make the substitution

$$\{v\} = [L]^T \{u\} \quad (426)$$

Now we rewrite the first few simultaneous equations in (426) as

$$L_{11} v_1 = F_1 \quad (427)$$

$$L_{21} v_1 + L_{22} v_2 = F_2 \quad (428)$$

Since  $[L]$  is a lower triangular matrix it is straightforward to obtain  $v_1$  from equation (427) and when this is done  $v_2$  can be found directly from equation (428). The remainder of the terms in  $\{v\}$  can be found just as easily. This ease of solution always arises if a set of equations has a triangular coefficient matrix.

Now that the  $\{v\}$  terms are known the  $\{u\}$  terms can be found from equation (426) which also has a triangular coefficient matrix. In this case the evaluation of the  $\{u\}$  terms starts with the last and works backwards.

If we consider an idealisation with 1000 degrees of freedom and one loading case the full  $[S]$  method of solution requires the storage of a full 1000 by 1000 stiffness matrix together with a loading vector containing 1000 terms. This requires 978K of computer storage (1K = 1024 words). This amount of storage rules out the full  $[S]$  solution method for this example problem which must be considered as small to medium in size. The amount of storage required for the banded method obviously depends upon the bandwidth  $w$  as defined earlier. For many types of structure we find that the bandwidth is approximately equal to the total number of degrees of freedom raised to the power 0.6 plus about half the number of degrees of freedom on one element. For the problem with 1000 degrees of freedom we shall take  $w = 70$ . The storage required for the stiffness matrix and the loading vector is 69K which is just acceptable for a large modern computer. Since the whole of the stiffness and loading matrices are stored in core there are no expensive transfers from core store to backing store. Therefore the banded  $[S]$  method is highly suited to problems of small to medium size whereas the full  $[S]$  method is only appropriate for the academic type of tests which are made during the development of a new element.

For large problems the storage requirements of the banded [S] method increase approximately as the total number of degrees of freedom raised to the power 1.6. We soon reach a situation in which a banded solution within a computer core is impossible. The frontal solution method uses far less core store than the banded method but it does so at the expense of some use of backing store. At the present time it is the best solution method for most practically occurring problems. Changes in computer architecture, operating systems, or the types of problem to be solved may of course change the optimum solution method. Indeed it may be that some of the common solution methods of the future will be indirect rather than direct.

In the front solution method we assemble the system stiffness matrix relating to the first element of a structure. In the case of the structure shown in fig. 2.58 this means assembling some of the parts of the stiffness matrix which relate to nodes 2, 7 and 8. The information relating to node 1 will be complete since there are no other elements meeting at that point. Let us assume that there are two displacements  $u_1$  and  $u_2$  at node 1; the first part of the system stiffness matrix S will be

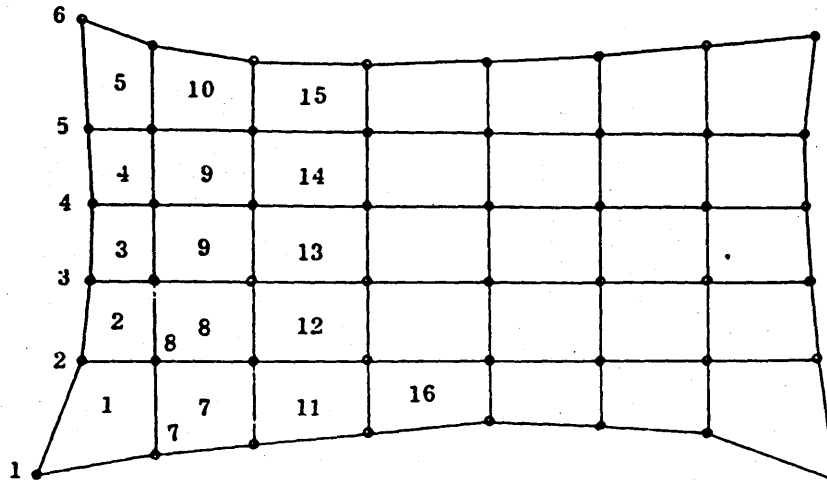


Fig. 58 Element numbers and nodes

$$S_{11}u_1 + S_{12}u_2 + \text{other terms} \tag{429}$$

$$S_{21}u_2 + S_{22}u_2 + \text{other terms} \tag{430}$$

other equations

where the 'other terms' are complete but the 'other equations' are incomplete.

We can rewrite the first equations as

$$u_1 = (F_1 - S_{12}u_2 - \text{other terms})/S_{11} \tag{431}$$

This equation can be used as a substitution for  $u_1$  in terms of the other variables and therefore  $u_1$  may be eliminated completely from the set of equations. Of course we shall eventually need to know the value of  $u_1$  which can be found from equation (431).

When  $u_1$  has been eliminated the second equation, (430), will have different coefficients and a different right hand side. It can then be rewritten in a similar manner to equation (431) except that  $u_2$  will be on the left. The equation can be used to eliminate  $u_2$  wherever it occurs in the remainder of the set of equations.

We have eliminated the degrees of freedom  $u_1$  and  $u_2$  immediately after the first element stiffness matrix has been assembled into the system stiffness matrix. The second element can now be assembled and the system matrix will now contain terms due to the nodes 2, 3, 7, 8 and 9. At this stage the degrees of freedom at node 2 can be eliminated.

Further elements are merged and at each stage any nodes which do not appear in later elements can be reduced out. The solution is proceeding as a 'front' through the structure. After element 16 has been assembled and the necessary elimination has been performed the degrees of freedom represented within the system matrix are all along the line A on fig. 2.59. As element 17 is assembled we need the degrees of freedom at the nodes indicated by line B. After the eliminations which follow the assembly of element 17 we need the degrees of freedom indicated by line C. The solution front has moved from line A to the line C as element 17 was assembled. It is easy to imagine what would happen to it if the next element were assembled. The system stiffness matrix need only be large enough to hold the stiffness terms represented by the largest number of degrees of freedom on the front at any stage of the elimination process. In the case of the structure shown in figs. 2.58 and 2.59 the 'maximum instantaneous front size' is nearly constant as the solution proceeds. It is represented by the line B shown in fig. 2.59.

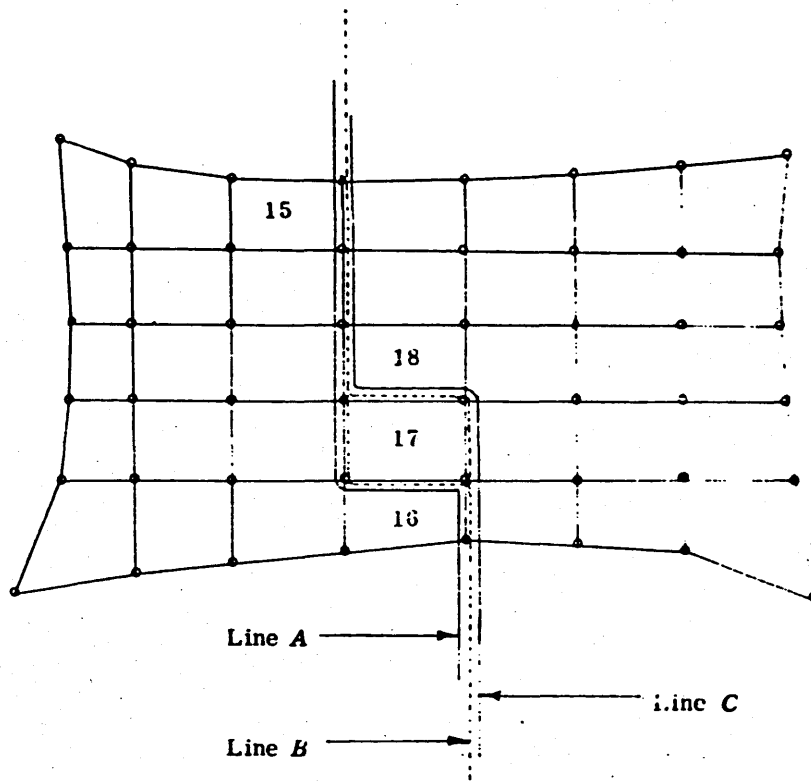


Fig. 59 The progress of a solution front

When all the elements have been merged into the system matrix the final eliminations can proceed until there is just one degree of freedom,  $u_n$ , left in the matrix. The equation for it will be of the form

$$S_{nn} u_n = F_n \quad (432)$$

From this equation  $u_n$  can be found numerically as  $F_n/S_{nn}$ . The preceding elimination for  $u_{n-1}$  enables this quantity to be found. Then other degrees of freedom eliminated earlier can be obtained. This 'back-substitution' calculation proceeds in the reverse order compared with that of the forward elimination phase.

Having outlined the frontal solution philosophy we now give the precise mathematical details. At any stage the  $k^{\text{th}}$  equation may be written as

$$\sum_{j=1}^n S_{kj} u_j = F_k \quad (433)$$

or alternatively by rearrangement

$$u_k = F_k/S_{kk} - \sum_{j=1}^n S_{kj} u_j / S_{kk} \quad (434)$$

except  $j = k$

$$\sum_{j=1}^n S_{ij} u_j = F_i \quad (435)$$

or

$$\sum_{j=1}^n S_{ij} u_j + S_{ik} F_{kk} / S_{kk} - (S_{ik} / S_{kk}) \cdot \sum_{j=1}^n S_{kj} / u_j = F_i \quad (436)$$

except  $j = k$  except  $j = k$

and hence

$$\sum_{j=1}^n (S_{ij} - S_{ik} \cdot S_{kj} / S_{kk}) u_j = F_i - F_{kk} \cdot S_{ik} / S_{kk} \quad (437)$$

except  $j = k$

Thus when the  $k^{\text{th}}$  variable is eliminated the  $S_{ij}$  and  $F_i$  terms are changed as

$$S_{ij} \rightarrow S_{ij} - S_{ik} \cdot S_{kj} / S_{kk} \text{ and } F_i \rightarrow F_i - F_{kk} \cdot S_{ik} / S_{kk} \quad (438)$$

This process can be achieved efficiently by setting up a vector  $\{V\}$  with

$$V_i = S_{ik} / \sqrt{S_{kk}} \quad (439)$$

then the modifications are

$$S_{ij} \rightarrow S_{ij} - V_i \cdot V_j \text{ and } F_i \rightarrow F_i - F_{kk} V_i / \sqrt{S_{kk}} \quad (440)$$

The backsubstitution is achieved by forming the vector

$$\{W\} = \{V\} / \sqrt{S_{kk}} \quad (441)$$

The  $\{W\}$  is stored on backing store and is used as follows to obtain  $u_k$  from

$$u_k = F_{kk} \cdot W_k - \sum_{j=1}^n W_j u_j \quad (442)$$

except  $j = k$

The system stiffness matrix is never completely formed when the front solution is used. The area that is used to store the lower triangle of the currently active part of the stiffness matrix is used over and over again to store the coefficients relating to many different equations. It is of course imperative to keep a proper account of the identity of the equations that are kept in the  $[S]$  array. The details of the housekeeping are given in the systems manual.

In certain non-linear problems such as creep and plasticity a single forward elimination is required followed by a number of separate back-substitutions each with a different load vector. From the theoretical standpoint the resolution method as it is called is identical to the normal front solution.

A P P E N D I X B

## Hammer Technique

### Instrumentation

A block diagram of the instrument layout is shown in figure 1.

### Test Layout

The shafted impeller is assembled on a temporary support structure such as is shown in figure 2.

The vibration measuring equipment is set up and calibrated .

The force link load cell is calibrated. A suitable head is fitted to the impact hammer. Teflon heads are suitable for vibration tests of large impellers.

### Test Procedure

#### DE Sideplate

The drive end sideplate is marked off into sections, as shown in figure 3. Test points are located opposite blade attachments and midway between blades.

The accelerometer is attached to the sideplate at position 1. Four impacts are made at point 1 with the load cell. The spectrum analyser is set to average these four tests. If the coherence is satisfactory the results are recorded on the microcomputer. A transfer function chart is recorded on the X-Y plotter.

The accelerometer is moved to position 2 and a further four impacts made at position 1. The averaged results are recorded. This procedure is repeated until the accelerometer has been placed at each test point. A print-out of all test data is obtained from the computer.

#### Centreplate

The centreplate is marked off into equal sections as shown in

figure 4 . Half of the points are located opposite blade attachments and the remaining half midway between blades.

A similar test procedure to the one previously described for the sideplate is then carried out.

A number of points are marked across a diameter of the centreplate. The point at the circumference is selected for the impact position. Transfer function vibration measurements are recorded at all the points on the centreplate diameter by moving the accelerometer while impacting at the single location.

### Results

Forced vibration tests by the calibrated hammer technique are a reliable method of obtaining frequency response characteristics for structures such as fan impellers. The accuracy of the resonant frequency measurements depend on the spectrum analyser bandwidth. For frequency ranges of 0 to 500 and 0 to 100 Hz. the measured natural frequencies should be accurate to 2 and 4 Hz. respectively.

### Blade Passing Frequency

The blade passing frequency of a double inlet impeller with staggered blades is

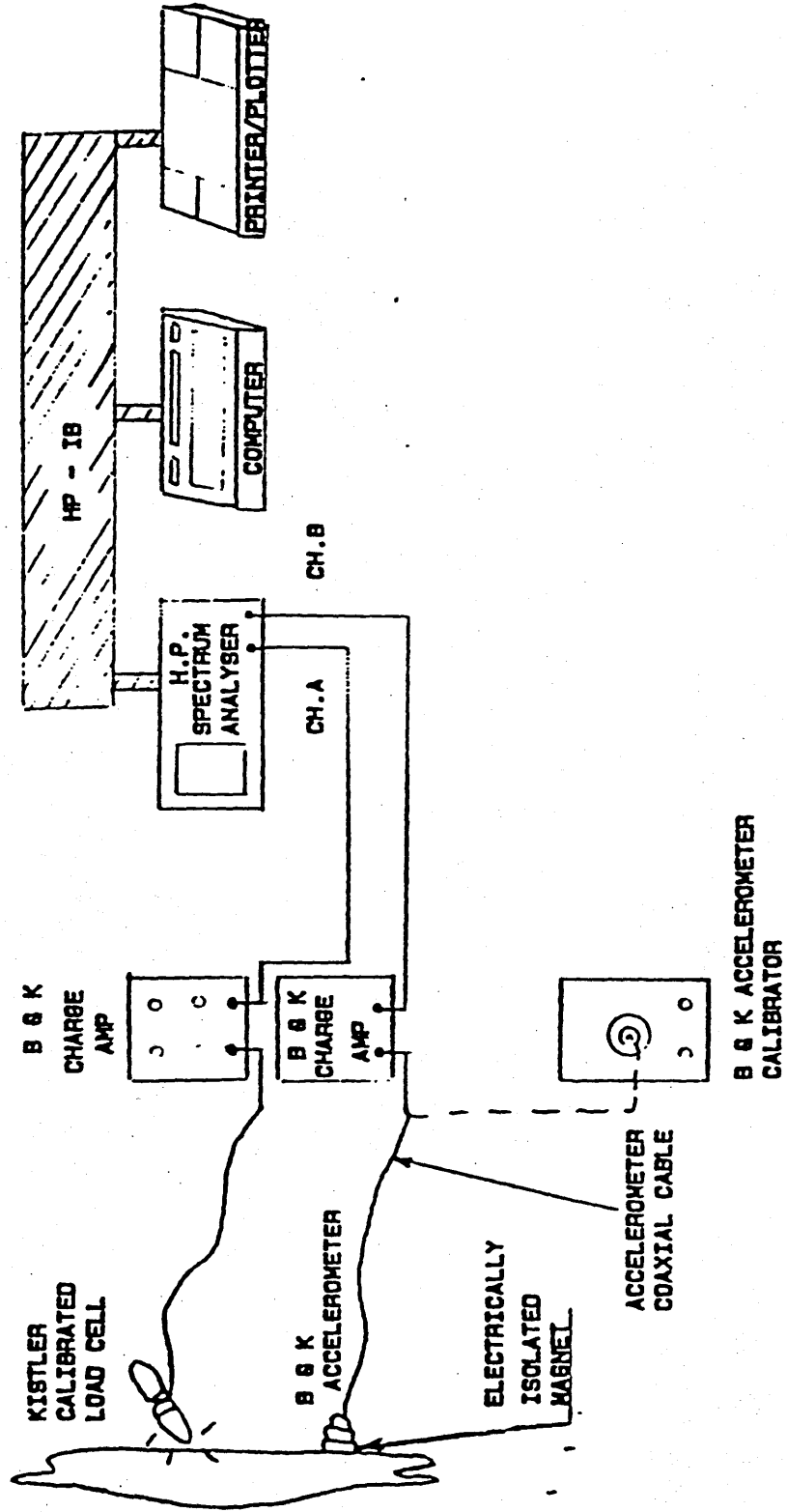
$$\frac{N \times \text{RPM}}{2 \times 60} \quad \text{Hz.}$$

Where N = total number of blades for both inlets.

Many engineers incorrectly consider the double inlet impeller as a single sound source. This misconception leads to the view that the blade passing frequency for a double inlet impeller with staggered blades is twice the frequency of a single inlet impeller.

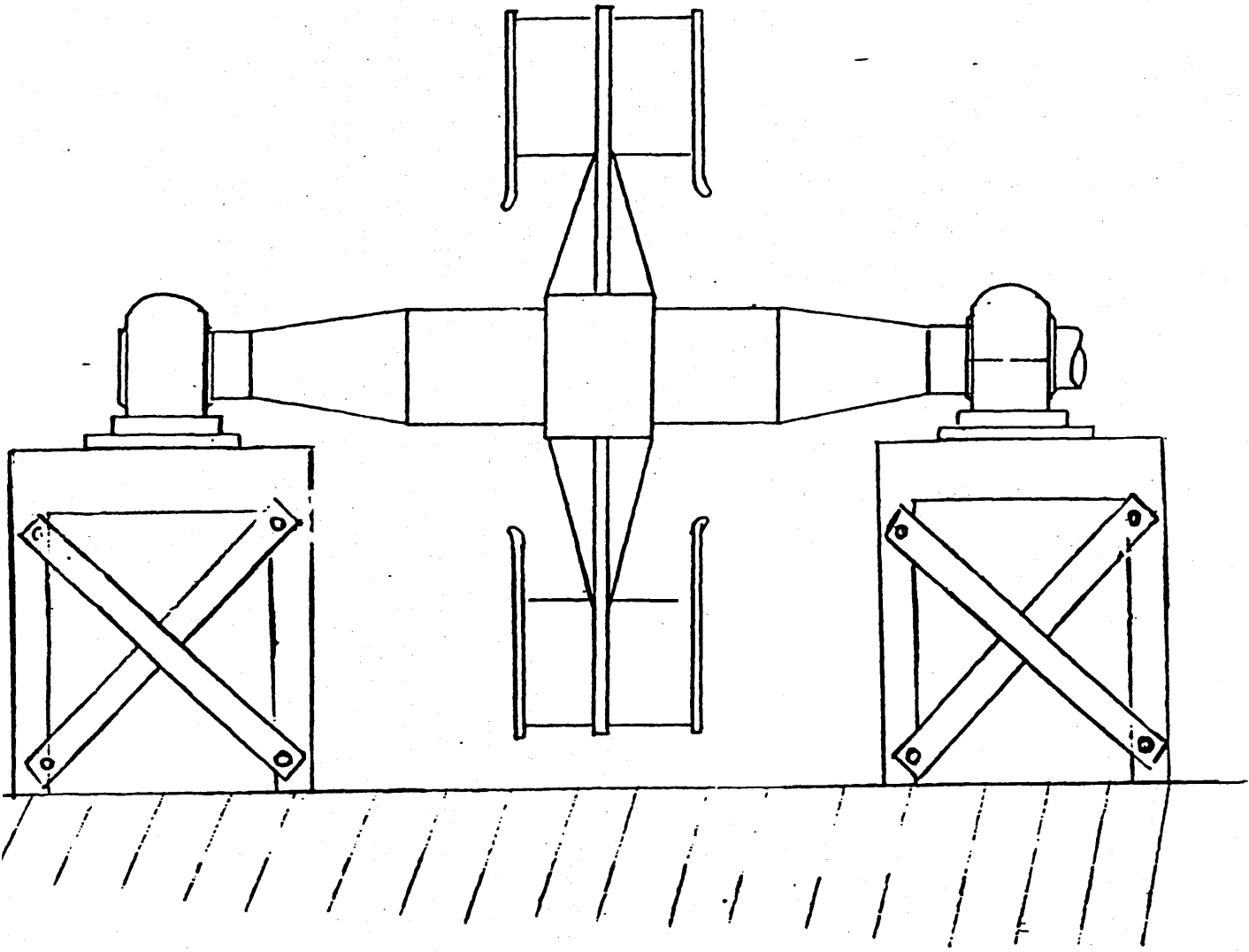
The best way to understand how to calculate the true B.P.F. of a double inlet impeller is to imagine two single inlet impellers coming together and that a double inlet impeller is in fact two sound sources.

Say the B.P.F. of both single inlet impellers is 300 Hz. When these single inlet impellers are joined back to back to form a double inlet impeller the B.P.F. of the combined system of two sound sources is still 300 Hz. irrespective of whether the blades are inline or staggered. The amplitudes of the discrete tones at B.P.F. and harmonics depend on the phase relationship of the separate tones generated by each of the single inlet impellers. For staggered blades there is normally a degree of active noise cancellation which reduces the discrete sound pressure level amplitude. For inline blades the tones at B.P.F. are in phase and the double inlet discrete tone at 300 Hz. could be up to 6 dB higher than for the single inlet impeller.

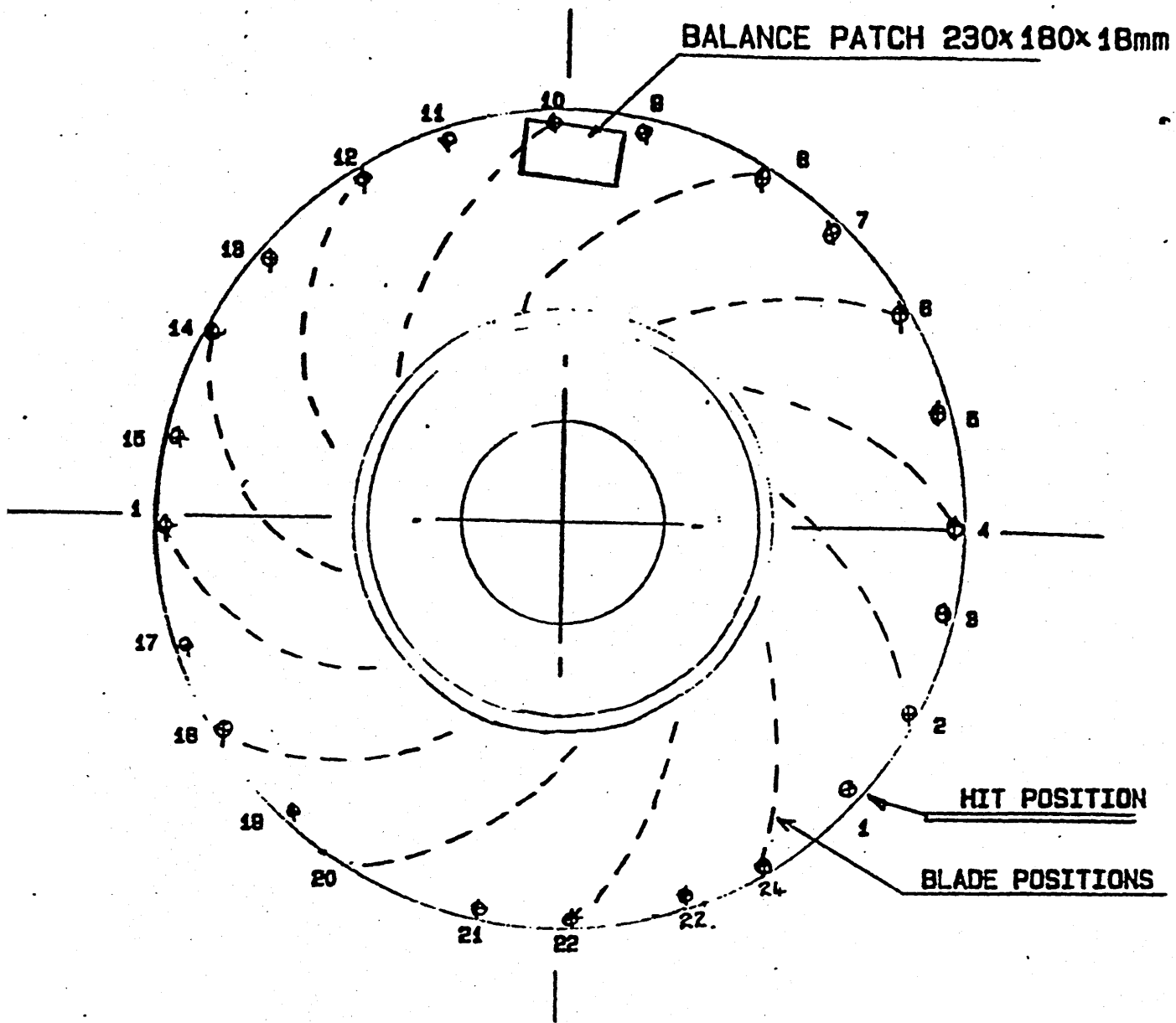


EQUIPMENT SET-UP FOR..

VIBRATION TESTS

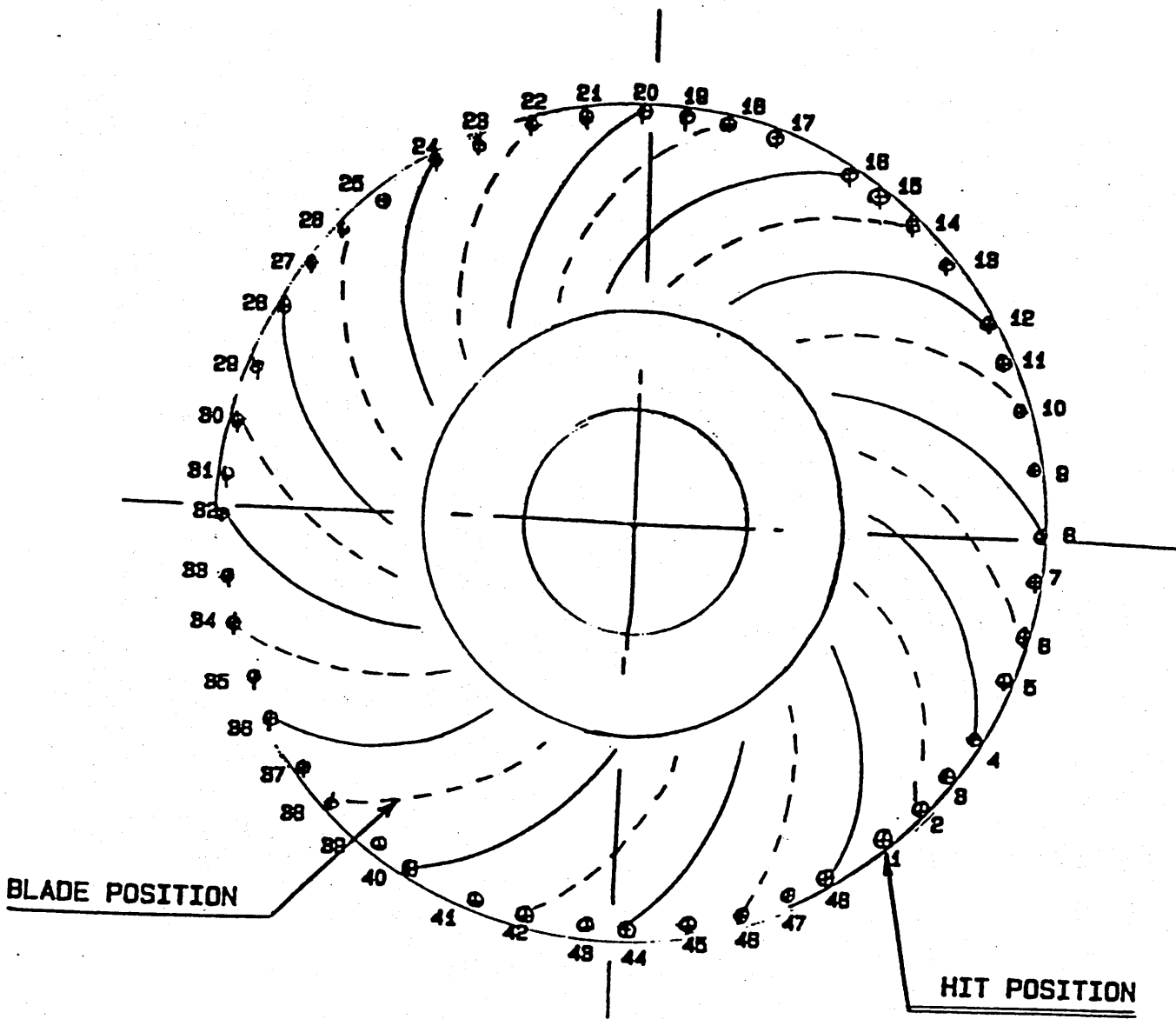


TEST ARRANGEMENT FOR  
FREQUENCY RESPONSE TESTS



D.E. SIDEPLATE SHOWING TEST POSITIONS

(VIEWED FROM D.E. BEARING SIDE)



CENTREPLATE SHOWING TEST POSITIONS  
 (VIEWED FROM D.E. BEARING SIDE)

A P P E N D I X C

SEGMENT 1

3D DISPLACEMENTS FOR MODE SHAPE 1

3D DISPLACEMENTS AT NODES

NUMBER	UX	UY	UZ	PHIX	PHIY	PHIZ	U	HISTOGRAM			
3	0.0186	0.9228	0.7504	1.292	1.242	-0.209	9.7510	*****	0.00	1.08	0.00
9L	-0.0200	0.0066	-0.1503	5.750	-5.237	-0.094	0.1518	*	0.28	1.04	0.00
13L	0.0200	-0.0066	0.1503	-5.750	5.237	0.094	0.1518	*	-0.28	1.04	0.00
21	0.0066	-0.0018	0.4576	3.650	2.720	*	0.4576	****	0.14	1.07	0.00
22	0.0034	0.0287	0.6947	-1.536	-2.294	*	0.6954	*****	-0.14	1.07	0.00
47L	0.0193	-0.0013	0.2166	5.122	-3.978	-0.000	0.2175	**	0.28	1.04	0.29
59L	-0.0193	0.0013	-0.2166	-5.122	3.978	0.000	0.2175	**	-0.28	1.04	0.29
60	-0.0153	-0.0148	0.7327	-0.930	-1.518	0.103	0.7330	*****	0.00	1.08	0.29
63	-0.0067	-0.0259	0.3856	-2.215	-3.685	*	0.3865	***	-0.14	1.07	0.29
69	-0.0074	0.0060	0.7070	2.086	1.614	*	0.7071	*****	0.14	1.07	0.29
83L	-0.0230	0.0105	-0.9878	-7.585	6.342	0.064	0.0914	*	0.28	1.04	-0.29
95L	0.0230	-0.0105	0.9878	7.585	-6.342	-0.064	0.0914	*	-0.28	1.04	-0.29
96	0.0047	-0.0101	-1.2563	-3.879	-0.043	*	1.2564	*****	0.00	1.08	-0.29
99	0.0067	0.0058	-0.8713	1.561	5.019	*	0.8713	*****	-0.14	1.07	-0.29
105	-0.0053	-0.0218	-0.9236	-7.120	-3.336	*	0.9238	*****	0.14	1.07	-0.29

3D DISPLACEMENTS FOR MODE SHAPE 2

3D DISPLACEMENTS AT NODES

NUMBER	UX	UY	UZ	PHIX	PHIY	PHIZ	U	HISTOGRAM			
3	-7.115	-15.435	90.126	-3.603	-3.871	-0.011	91.715	*	0.00	1.08	0.00
9L	-16.386	14.372	505.06	0.584	-0.540	0.150	505.53	*****	0.28	1.04	0.00
13L	16.386	-14.372	-505.06	-0.584	0.540	-0.150	505.53	*****	-0.28	1.04	0.00
21	-12.956	-18.138	457.48	-1.023	-1.292	*	458.02	*****	0.14	1.07	0.00
22	3.843	-1.536	-329.93	-1.785	-2.465	*	329.96	***	-0.14	1.07	0.00
47L	7.752	3.786	-1000.0	0.151	2.267	0.000	1000.0	*****	0.28	1.04	0.29
59L	-7.752	-3.786	1000.0	-0.151	-2.267	-0.000	1000.0	*****	-0.28	1.04	0.29
60	-4.524	-13.475	46.211	4.619	5.167	0.084	48.348		0.00	1.08	0.29
63	1.858	-14.603	674.97	4.039	4.458	*	675.14	*****	-0.14	1.07	0.29
69	-5.086	-1.404	-627.93	1.613	3.560	*	627.95	*****	0.14	1.07	0.29
83L	14.663	-16.033	495.91	-0.877	0.352	-0.116	496.39	*****	0.28	1.04	-0.29
95L	-14.663	16.033	-495.91	0.877	-0.352	0.116	496.39	*****	-0.28	1.04	-0.29
96	0.060	18.788	-126.22	-2.150	-3.707	*	127.62	*	0.00	1.08	-0.29
99	-9.584	3.658	-484.50	-0.733	-1.430	*	484.60	*****	-0.14	1.07	-0.29
105	12.429	21.792	290.67	-1.368	-2.067	*	291.76	***	0.14	1.07	-0.29

0D ISPLACEMENTS FOR NODE SHAPE 3

0DISPLACEMENTS AT NODES

NUMBER	UX	UY	UZ	PHIX	PHIY	PHIZ	U	HISTOGRAM			
3	0.0066	-0.0008	0.2077	0.741	1.247	-0.059	0.2078	**	0.00	1.08	0.00
9L	0.0059	-0.0182	0.0588	-0.314	1.676	-0.013	0.0618		0.28	1.04	0.00
13L	-0.0059	0.0182	-0.0588	0.314	-1.676	0.013	0.0618		-0.28	1.04	0.00
21	0.0112	-0.0017	0.0565	-0.086	0.703	*	0.0577		0.14	1.07	0.00
22	-0.0030	-0.0015	0.1632	-0.309	-1.131	*	0.1632	*	-0.14	1.07	0.00
47L	0.0049	-0.0008	0.4867	1.706	-2.738	-0.000	0.4867	****	0.28	1.04	0.29
59L	-0.0049	0.0008	-0.4867	-1.706	2.738	0.000	0.4867	****	-0.28	1.04	0.29
60	-0.0096	-0.0054	0.2286	-1.628	-2.113	0.033	0.2289	**	0.00	1.08	0.29
63	-0.0044	-0.0068	-0.1175	-2.599	-2.955	*	0.1178	*	-0.14	1.07	0.29
69	-0.0042	0.0012	0.4744	0.571	-1.009	*	0.4744	****	0.14	1.07	0.29
83L	0.0005	0.0209	0.0583	6.191	-4.373	-0.009	0.0619		0.28	1.04	-0.29
95L	-0.0005	-0.0209	-0.0583	-6.191	4.373	0.009	0.0619		-0.28	1.04	-0.29
96	-0.0065	0.0040	1.2597	4.469	1.148	*	1.2597	*****	0.00	1.08	-0.29
99	0.0049	0.0010	0.9290	-1.447	-5.013	*	0.9290	*****	-0.14	1.07	-0.29
105	-0.0133	0.0069	0.8089	7.373	3.602	*	0.8090	*****	0.14	1.07	-0.29

0D ISPLACEMENTS FOR NODE SHAPE 4

0DISPLACEMENTS AT NODES

NUMBER	UX	UY	UZ	PHIX	PHIY	PHIZ	U	HISTOGRAM			
3	-0.0174	-0.0100	-0.1056	-0.582	-0.268	0.068	0.1115	*	0.00	1.08	0.00
9L	0.0028	-0.0083	-0.2391	-0.999	0.233	-0.066	0.2393	**	0.28	1.04	0.00
13L	-0.0028	0.0083	0.2391	0.999	-0.233	0.066	0.2393	**	0.28	1.04	0.00
21	-0.0018	-0.0009	-0.1850	0.358	0.549	*	0.1850	**	0.14	1.07	0.00
22	-0.0124	-0.0085	0.0006	0.288	1.471	*	0.0150		-0.14	1.07	0.00
47L	-0.0090	0.0052	-1.0000	-1.047	0.537	0.000	1.0001	*****	0.28	1.04	0.29
59L	0.0090	-0.0052	1.0000	1.047	-0.537	-0.000	1.0001	*****	-0.28	1.04	0.29
60	0.0277	0.0135	-0.1134	2.602	3.345	-0.046	0.1176	*	0.00	1.08	0.29
63	0.0157	0.0153	0.4525	2.971	4.563	*	0.4530	****	-0.14	1.07	0.29
69	0.0099	-0.0016	-0.6601	1.609	3.054	*	0.6602	*****	0.14	1.07	0.29
83L	-0.0108	0.0140	-0.2584	2.083	-1.191	0.006	0.2599	***	0.28	1.04	-0.29
95L	0.0108	-0.0140	0.2584	-2.083	1.191	-0.006	0.2590	***	-0.28	1.04	-0.29
96	-0.0002	-0.0037	0.4082	2.704	2.570	*	0.4082	****	0.00	1.08	-0.29
99	0.0058	0.0029	0.5332	0.314	-0.558	*	0.5332	****	-0.14	1.07	-0.29
105	-0.0080	-0.0072	0.0399	2.781	2.154	*	0.0413		0.14	1.07	-0.29

SEGMENT 2

0D ISPLACEMENTS FOR NODE SHAPE 1

0DISPLACEMENTS AT NODES

#####

NUMBER	UX	UY	UZ	PHIX	PHIY	PHIZ	U	HISTOGRAM			
3	-0.0136	-0.0228	-0.7504	-1.293	-1.242	0.209	0.7510	*****	0.00	1.08	0.00
9L	0.0200	-0.0066	0.1503	-5.750	5.237	0.094	0.1518	*	0.28	1.04	0.00
13L	-0.0200	0.0066	-0.1503	5.750	-5.237	-0.094	0.1518	*	-0.28	1.04	0.00
21	-0.0066	0.0010	-0.4576	-3.651	-2.720	*	0.4577	****	0.14	1.07	0.00
22	-0.0084	-0.0287	-0.6947	1.536	2.294	*	0.6954	*****	-0.14	1.07	0.00
47L	-0.0193	0.0013	-0.2166	-5.122	3.978	0.000	0.2175	**	0.28	1.04	0.29
59L	0.0193	-0.0013	0.2166	5.122	-3.978	-0.000	0.2175	**	-0.28	1.04	0.29
60	0.0153	0.0148	-0.7327	0.930	1.518	-0.103	0.7330	*****	0.00	1.08	0.29
63	0.0069	0.0250	-0.3856	2.215	3.685	*	0.3864	***	-0.14	1.07	0.29
69	0.0074	-0.0060	-0.7070	-2.086	-1.614	*	0.7071	*****	0.14	1.07	0.29
83L	0.0230	-0.0105	0.0878	7.585	-6.342	-0.064	0.0914	*	0.28	1.04	-0.29
95L	-0.0230	0.0105	-0.0878	-7.585	6.342	0.064	0.0914	*	-0.28	1.04	-0.29
96	-0.0047	0.0101	1.2563	3.869	0.043	*	1.2564	*****	0.00	1.08	-0.29
99	-0.0069	-0.0058	0.8713	-1.562	-5.019	*	0.8713	*****	-0.14	1.07	-0.29
105	0.0053	0.0218	0.9236	7.120	3.336	*	0.9238	*****	0.14	1.07	-0.29

ND ISPLACEMENTS FOR NODE SHAPE 2

NDISPLACEMENTS AT NODES

NUMBER	UX	UY	UZ	PHIX	PHIY	PHIZ	U	HISTOGRAM			
3	7.110	15.432	-90.141	3.603	3.871	0.011	91.728	*	0.00	1.08	0.00
9L	16.386	-14.372	-505.06	-0.584	0.540	-0.150	505.53	*****	0.28	1.04	0.00
13L	-16.386	14.372	505.06	0.584	-0.540	0.150	505.53	*****	-0.28	1.04	0.00
21	12.954	18.137	-457.51	1.023	1.292	*	458.05	*****	0.14	1.07	0.00
22	-3.845	1.535	320.92	1.785	2.465	*	320.95	***	-0.14	1.07	0.00
47L	-7.752	-3.786	1000.0	-0.151	-2.267	-0.000	1000.0	*****	0.28	1.04	0.29
59L	7.752	3.786	-1000.0	0.151	2.267	0.000	1000.0	*****	-0.28	1.04	0.29
60	4.526	13.476	-46.230	-4.617	-5.167	-0.084	48.367		0.00	1.08	0.29
63	-1.857	14.602	-674.98	-4.039	-4.058	*	675.14	*****	-0.14	1.07	0.29
69	5.086	1.404	627.89	-1.614	-3.559	*	627.91	*****	0.14	1.07	0.29
83L	-14.663	16.033	-495.91	0.877	-0.352	0.116	496.39	*****	0.28	1.04	-0.29
95L	14.663	-16.033	495.91	-0.877	0.352	-0.116	496.39	*****	-0.28	1.04	-0.29
96	-0.060	-18.790	126.22	2.350	3.707	*	127.62	*	0.00	1.08	-0.29
99	9.584	-3.659	484.50	0.732	1.430	*	484.60	*****	-0.14	1.07	-0.29
105	-12.430	-21.794	-290.67	1.368	2.067	*	291.76	***	0.14	1.07	-0.29

ND ISPLACEMENTS FOR NODE SHAPE 3

NDISPLACEMENTS AT NODES

NUMBER	UX	UY	UZ	PHIX	PHIY	PHIZ	U	HISTOGRAM			
3	-0.0066	0.0008	-0.2077	-0.741	-1.247	0.059	0.2078	**	0.00	1.08	0.00
9L	-0.0059	0.0182	-0.0588	0.314	-1.576	0.013	0.0618		0.28	1.04	0.00
13L	0.0059	-0.0182	0.0588	-0.314	1.576	-0.013	0.0618		-0.28	1.04	0.00
21	-0.0112	0.0017	-0.0565	0.086	-0.703	*	0.0577		0.14	1.07	0.00
22	0.0030	0.0015	-0.1532	0.309	1.131	*	0.1632	*	-0.14	1.07	0.00
47L	-0.0049	0.0008	-0.4867	-1.706	2.738	0.000	0.4867	****	0.28	1.04	0.29
59L	0.0049	-0.0008	0.4867	1.706	-2.738	-0.000	0.4867	****	-0.28	1.04	0.29
60	0.0096	0.0054	-0.2286	1.628	2.113	-0.033	0.2289	**	0.00	1.08	0.29

\*\*\*\*\*

DISPLACEMENTS FOR NODE SHAPE 2

DISPLACEMENTS AT NODES

NUMBER	UX	UY	UZ	PHIX	PHIY	PHIZ	U	HISTOGRAM			
3	-7.115	-15.435	90.126	-3.603	-3.871	-0.011	91.715	*	0.00	1.08	0.00
9L	-16.386	14.372	505.06	0.584	-0.540	0.150	505.53	*****	0.28	1.04	0.00
13L	16.386	-14.372	-505.06	-0.584	0.540	-0.150	505.53	*****	-0.28	1.04	0.00
21	-12.756	-18.138	457.48	-1.023	-1.292	*	458.02	*****	0.14	1.07	0.00
22	3.843	-1.536	-320.93	-1.785	-2.465	*	320.96	***	-0.14	1.07	0.00
47L	7.752	3.786	-1000.0	0.151	2.267	0.000	1000.0	*****	0.28	1.04	0.29
59L	-7.752	-3.786	1000.0	-0.151	-2.267	-0.000	1000.0	*****	-0.28	1.04	0.29
60	-4.524	-13.475	46.211	4.619	5.167	0.084	48.348		0.00	1.08	0.29
63	1.858	-14.603	674.97	4.039	4.058	*	675.14	*****	-0.14	1.07	0.29
69	-5.086	-1.404	-627.93	1.613	3.560	*	627.95	*****	0.14	1.07	0.29
83L	14.663	-16.033	495.91	-0.877	0.352	-0.116	496.39	*****	0.28	1.04	-0.29
95L	-14.663	16.033	-495.91	0.877	-0.352	0.116	496.39	*****	-0.28	1.04	-0.29
96	0.060	18.788	-126.22	-2.350	-3.707	*	127.62	*	0.00	1.08	-0.29
99	-9.584	3.658	-484.50	-0.733	-1.430	*	484.60	*****	-0.14	1.07	-0.29
105	12.429	21.792	290.67	-1.368	-2.067	*	291.76	***	0.14	1.07	-0.29

DISPLACEMENTS FOR NODE SHAPE 3

DISPLACEMENTS AT NODES

NUMBER	UX	UY	UZ	PHIX	PHIY	PHIZ	U	HISTOGRAM			
3	0.0066	-0.0008	0.2077	0.741	1.247	-0.059	0.2078	**	0.00	1.08	0.00
9L	0.0059	-0.0182	0.0588	-0.314	1.676	-0.013	0.0618		0.28	1.04	0.00
13L	-0.0059	0.0182	-0.0588	0.314	-1.676	0.013	0.0618		-0.28	1.04	0.00
21	0.0112	-0.0017	0.0565	-0.086	0.703	*	0.0577		0.14	1.07	0.00
22	-0.0030	-0.0015	0.1632	-0.309	-1.131	*	0.1632	*	-0.14	1.07	0.00
47L	0.0049	-0.0008	0.4867	1.706	-2.738	-0.000	0.4867	****	0.28	1.04	0.29
59L	-0.0049	0.0008	-0.4867	-1.706	2.738	0.000	0.4867	****	-0.28	1.04	0.29
60	-0.0076	-0.0054	0.2286	-1.628	-2.113	0.033	0.2289	**	0.00	1.08	0.29
63	-0.0044	-0.0068	-0.1175	-2.590	-2.955	*	0.1178	*	-0.14	1.07	0.29
69	-0.0042	0.0012	0.4744	0.571	-1.009	*	0.4744	****	0.14	1.07	0.29
83L	0.0005	0.0209	0.0583	6.191	-4.373	-0.009	0.0619		0.28	1.04	-0.29
95L	-0.0005	-0.0209	-0.0583	-6.191	4.373	0.009	0.0619		-0.28	1.04	-0.29
96	-0.0065	0.0040	1.2597	4.469	1.148	*	1.2597	*****	0.00	1.08	-0.29
99	0.0049	0.0010	0.9290	-1.447	-5.013	*	0.9290	*****	-0.14	1.07	-0.29
105	-0.0133	0.0039	0.8099	7.373	3.602	*	0.8090	*****	0.14	1.07	-0.29

DISPLACEMENTS FOR NODE SHAPE 4

DISPLACEMENTS AT NODES

NUMBER	UX	UY	UZ	PHIX	PHIY	PHIZ	U	HISTOGRAM
--------	----	----	----	------	------	------	---	-----------

69	0.0042	-0.0012	-0.4744	-0.571	1.009	z	0.4744	****	0.14	1.07	0.29
83L	-0.0005	-0.0207	-0.6583	-6.191	4.373	0.009	0.6619		0.28	1.04	-0.29
95L	0.0005	0.0207	0.6583	6.191	-4.373	-0.009	0.6619		-0.28	1.04	-0.29
96	0.0065	-0.0040	-1.2597	-4.470	-1.148	z	1.2597	*****	0.00	1.08	-0.29
99	-0.0049	-0.0010	-0.9290	1.446	5.013	z	0.9290	*****	-0.14	1.07	-0.29
105	0.0133	-0.0057	-0.8089	-7.374	-3.602	z	0.8090	*****	0.14	1.07	-0.29

DISPLACEMENTS FOR MODE SHAPE 4

DISPLACEMENTS AT NODES

NUMBER	UX	UY	UZ	PHIX	PHIY	PHIZ	U	HISTOGRAM			
3	0.0174	0.0109	0.1096	0.592	0.268	-0.066	0.1115	z	0.00	1.08	0.00
9L	-0.0028	0.0023	0.2391	0.990	-0.233	0.066	0.2393	**	0.28	1.04	0.00
13L	0.0028	-0.0023	-0.2391	-0.990	0.233	-0.066	0.2393	**	-0.28	1.04	0.00
21	0.0018	0.0009	0.1850	-0.358	-0.549	z	0.1850	**	0.14	1.07	0.00
22	0.0123	0.0035	-0.0006	-0.298	-1.471	z	0.0150		-0.14	1.07	0.00
47L	0.0090	-0.0052	1.0000	1.047	-0.537	-0.000	1.0001	*****	0.28	1.04	0.29
59L	-0.0090	0.0052	-1.0000	-1.047	0.537	0.000	1.0001	*****	-0.28	1.04	0.29
60	-0.0277	-0.0135	0.1134	-2.603	-3.345	0.046	0.1176	z	0.00	1.08	0.29
63	-0.0157	-0.0153	-0.4525	-2.972	-4.563	z	0.4530	*****	-0.14	1.07	0.29
69	-0.0079	0.0016	0.6601	-1.610	-3.054	z	0.6602	*****	0.14	1.07	0.29
83L	0.0108	-0.0140	0.2584	-2.983	1.191	-0.006	0.2590	***	0.28	1.04	-0.29
95L	-0.0108	0.0140	-0.2584	2.983	-1.191	0.006	0.2590	***	-0.28	1.04	-0.29
96	0.0002	0.0037	-0.4082	-2.704	-2.578	z	0.4082	****	0.00	1.08	-0.29
99	-0.0058	-0.0029	-0.5332	-0.314	0.558	z	0.5332	*****	-0.14	1.07	-0.29
105	0.0080	0.0072	-0.0399	-2.781	-2.154	z	0.0413		0.14	1.07	-0.29

SEGMENT 3

DISPLACEMENTS FOR MODE SHAPE 1

DISPLACEMENTS AT NODES

NUMBER	UX	UY	UZ	PHIX	PHIY	PHIZ	U	HISTOGRAM			
3	0.0186	0.0228	0.7504	1.292	1.242	-0.209	0.7510	*****	0.00	1.08	0.00
9L	-0.0200	0.0066	-0.1503	5.750	-5.237	-0.094	0.1518	z	0.28	1.04	0.00
13L	0.0200	-0.0066	0.1503	-5.750	5.237	0.094	0.1518	z	-0.28	1.04	0.00
21	0.0066	-0.0018	0.4576	3.650	2.720	z	0.4576	****	0.14	1.07	0.00
22	0.0084	0.0287	0.6947	-1.536	-2.294	z	0.6954	*****	-0.14	1.07	0.00
47L	0.0193	-0.0013	0.2166	5.122	-3.978	-0.000	0.2175	**	0.28	1.04	0.29
59L	-0.0193	0.0013	-0.2166	-5.122	3.978	0.000	0.2175	**	-0.28	1.04	0.29
60	-0.0153	-0.0148	0.7327	-0.930	-1.518	0.103	0.7330	*****	0.00	1.08	0.29
63	-0.0069	-0.0250	0.3856	-2.215	-3.685	z	0.3865	***	-0.14	1.07	0.29
69	-0.0074	0.0060	0.7070	2.086	1.614	z	0.7071	*****	0.14	1.07	0.29
83L	-0.0230	0.0105	-0.0878	-7.585	6.342	0.064	0.0914	z	0.28	1.04	-0.29
95L	0.0230	-0.0105	0.0878	7.585	-6.342	-0.064	0.0914	z	-0.28	1.04	-0.29
96	0.0067	-0.0101	-1.2563	-3.870	-0.043	z	1.2564	*****	0.00	1.08	-0.29
99	0.0069	0.0058	-0.8713	1.561	5.019	z	0.8713	*****	-0.14	1.07	-0.29
105	-0.0053	-0.0218	-0.9236	-7.120	-3.336	z	0.9238	*****	0.14	1.07	-0.29

\*\*\*\*\*

9L	0.0028	-0.0083	-0.2391	-0.990	0.233	-0.066	0.2393	**	0.28	1.04	0.00
13L	-0.0028	0.0083	0.2391	0.990	-0.233	0.066	0.2393	**	-0.28	1.04	0.00
21	-0.0018	-0.0009	-0.1850	0.358	0.549	z	0.1850	**	0.14	1.07	0.00
22	-0.0124	-0.0085	0.0006	0.288	1.471	z	0.0150		-0.14	1.07	0.00
47L	-0.0090	0.0052	-1.0000	-1.047	0.537	0.000	1.0001	*****	0.28	1.04	0.29
59L	0.0090	-0.0052	1.0000	1.047	-0.537	-0.000	1.0001	*****	-0.28	1.04	0.29
60	0.0277	0.0135	-0.1134	2.602	3.345	-0.046	0.1176	z	0.00	1.08	0.29
63	0.0157	0.0153	0.4525	2.971	4.563	z	0.4530	****	-0.14	1.07	0.29
69	0.0099	-0.0016	-0.6601	1.609	3.054	z	0.6602	*****	0.14	1.07	0.29
83L	-0.0108	0.0140	-0.2584	2.083	-1.191	0.006	0.2590	***	0.28	1.04	-0.29
95L	0.0108	-0.0140	0.2584	-2.083	1.191	-0.006	0.2590	***	-0.28	1.04	-0.29
96	-0.0002	-0.0037	0.4082	2.704	2.578	z	0.4082	****	0.00	1.08	-0.29
99	0.0058	0.0029	0.5332	0.314	-0.558	z	0.5332	*****	-0.14	1.07	-0.29
105	-0.0080	-0.0072	0.0399	2.781	2.154	z	0.0413		0.14	1.07	-0.29

SEGMENT 4

DISPLACEMENTS FOR MODE SHAPE 1

DISPLACEMENTS AT NODES

NUMBER	UX	UY	UZ	PHIX	PHIY	PHIZ	U	HISTOGRAM			
3	-0.0186	-0.0228	-0.7504	-1.293	-1.242	0.209	0.7510	*****	0.00	1.08	0.00
9L	0.0200	-0.0066	0.1503	-5.750	5.237	0.094	0.1518	z	-0.28	1.04	0.00
13L	-0.0200	0.0066	-0.1503	5.750	-5.237	-0.094	0.1518	z	-0.28	1.04	0.00
21	-0.0066	0.0018	-0.4576	-3.651	-2.720	z	0.4577	****	0.14	1.07	0.00
22	-0.0084	-0.0287	-0.6947	1.536	2.294	z	0.6954	*****	-0.14	1.07	0.00
47L	-0.0193	0.0013	-0.2166	-5.122	3.978	0.000	0.2175	z	0.28	1.04	0.29
59L	0.0193	-0.0013	0.2166	5.122	-3.978	-0.000	0.2175	z	-0.28	1.04	0.29
60	0.0153	0.0111	-0.7327	0.930	1.518	-0.103	0.7330	*****	0.00	1.08	0.29
63	0.0069	0.0250	-0.3856	2.215	3.685	z	0.3864	***	-0.14	1.07	0.29
69	0.0074	-0.0060	-0.7070	-2.086	-1.614	z	0.7071	*****	0.14	1.07	0.29
83L	0.0230	-0.0105	0.0878	7.585	-6.342	-0.064	0.0914	z	0.28	1.04	-0.29
95L	-0.0230	0.0105	-0.0878	-7.585	6.342	0.064	0.0914	z	-0.28	1.04	-0.29
96	-0.0047	0.0101	1.2563	3.869	0.043	z	1.2564	*****	0.00	1.08	-0.29
99	-0.0069	-0.0058	0.8713	-1.562	-5.019	z	0.8713	*****	-0.14	1.07	-0.29
105	0.0053	0.0218	0.9236	7.120	3.336	z	0.9238	*****	0.14	1.07	-0.29

DISPLACEMENTS FOR MODE SHAPE 2

DISPLACEMENTS AT NODES

NUMBER	UX	UY	UZ	PHIX	PHIY	PHIZ	U	HISTOGRAM			
3	7.110	15.432	-90.141	3.603	3.071	0.011	91.728	z	0.00	1.08	0.00
9L	16.386	-14.372	-505.06	-0.584	0.540	-0.150	505.53	*****	0.28	1.04	0.00
13L	-16.386	14.372	505.06	0.584	-0.540	0.150	505.53	*****	-0.28	1.04	0.00
21	12.554	18.137	-457.51	1.023	1.292	z	458.05	*****	0.14	1.07	0.00
22	-3.345	1.535	320.92	1.785	2.465	z	320.95	***	-0.14	1.07	0.00
47L	-7.752	-3.786	1000.0	-0.151	-2.267	-0.000	1000.0	*****	0.28	1.04	0.29
59L	7.752	3.786	-1000.0	0.151	2.267	0.000	1000.0	*****	-0.28	1.04	0.29

53	-1.857	14.602	-674.78	-4.039	-4.058	±	675.14	*****	-0.14	1.07	0.29
67	5.086	1.404	627.89	-1.614	-3.559	±	627.91	*****	0.14	1.07	0.29
35L	-14.663	16.033	-495.91	0.877	-0.352	0.116	496.39	*****	0.28	1.04	-0.29
75L	14.663	-16.033	495.91	-0.877	0.352	-0.116	496.39	*****	-0.28	1.04	-0.29
75	-0.060	-18.790	126.22	2.350	3.707	±	127.62	±	0.00	1.08	-0.29
77	9.584	-3.659	484.50	0.732	1.430	±	484.60	*****	-0.14	1.07	-0.29
105	-12.430	-21.794	-290.67	1.368	2.067	±	291.76	***	0.14	1.07	-0.29

00 DISPLACEMENTS FOR NODE SHAPE 3

00 DISPLACEMENTS AT NODES

NUMBER	UX	UY	UZ	PHIX	PHIY	PHIZ	U	HISTOGRAM			
3	-0.0066	0.0008	-0.2077	-0.741	-1.247	0.059	0.2078	**	0.00	1.08	0.00
7L	-0.0059	0.0182	-0.0588	0.314	-1.676	0.013	0.0618		0.28	1.04	0.00
13L	0.0059	-0.0182	0.0588	-0.314	1.676	-0.013	0.0618		-0.28	1.04	0.00
21	-0.0112	0.0017	-0.0565	0.086	-0.703	±	0.0577		0.14	1.07	0.00
22	0.0030	0.0015	-0.1632	0.309	1.131	±	0.1632	*	-0.14	1.07	0.00
47L	-0.0049	0.0008	-0.4867	-1.706	2.738	0.000	0.4867	***	0.28	1.04	0.29
57L	0.0049	-0.0008	0.4867	1.706	-2.738	-0.000	0.4867	***	-0.28	1.04	0.29
60	0.0096	0.0054	-0.2286	1.628	2.113	-0.033	0.2289	**	0.00	1.08	0.29
63	0.0044	0.0068	0.1175	2.590	2.955	±	0.1178	±	-0.14	1.07	0.29
67	0.0042	-0.0012	-0.4744	-0.571	1.009	±	0.4744	****	0.14	1.07	0.29
63L	-0.0005	-0.0209	-0.0583	-6.191	4.373	0.009	0.0619		0.28	1.04	-0.29
75L	0.0005	0.0209	0.0583	6.191	-4.373	-0.009	0.0619		-0.28	1.04	-0.29
75	0.0065	-0.0040	-1.2577	-4.470	-1.148	±	1.2577	*****	0.00	1.08	-0.29
77	-0.0049	-0.0010	-0.9290	1.446	5.013	±	0.9290	*****	-0.14	1.07	-0.29
105	0.0133	-0.0069	-0.0039	-7.374	-3.602	±	0.0090	*****	0.14	1.07	-0.29

00 DISPLACEMENTS FOR NODE SHAPE 4

00 DISPLACEMENTS AT NODES

NUMBER	UX	UY	UZ	PHIX	PHIY	PHIZ	U	HISTOGRAM			
3	0.0174	0.0100	0.1096	0.582	0.268	-0.068	0.1115	±	0.00	1.08	0.00
7L	-0.0028	0.0083	0.2391	0.990	-0.233	0.066	0.2393	**	0.28	1.04	0.00
13L	0.0028	-0.0083	-0.2391	-0.990	0.233	-0.066	0.2393	**	-0.28	1.04	0.00
21	0.0018	0.0009	0.1850	-0.358	-0.549	±	0.1850	**	0.14	1.07	0.00
22	0.0123	0.0085	-0.0006	-0.288	-1.471	±	0.0150		-0.14	1.07	0.00
47L	0.0090	-0.0052	1.0000	1.047	-0.537	-0.000	1.0001	*****	0.28	1.04	0.29
57L	-0.0090	0.0052	-1.0000	-1.047	0.537	0.000	1.0001	*****	-0.28	1.04	0.29
60	-0.0277	-0.0135	0.1134	-2.603	-3.345	0.046	0.1176	±	0.00	1.08	0.29
63	-0.0157	-0.0153	-0.4525	-2.972	-4.563	±	0.4530	****	-0.14	1.07	0.29
67	-0.0099	0.0016	0.6601	-1.610	-3.054	±	0.6602	*****	0.14	1.07	0.29
63L	0.0108	-0.0140	0.2584	-2.083	1.191	-0.006	0.2590	***	0.28	1.04	-0.29
75L	-0.0108	0.0140	-0.2584	2.083	-1.191	0.006	0.2590	***	-0.28	1.04	-0.29
75	0.0002	0.0037	-0.4082	-2.704	-2.578	±	0.4082	****	0.00	1.08	-0.29
77	-0.0058	-0.0029	-0.5332	-0.314	0.558	±	0.5332	*****	-0.14	1.07	-0.29
105	0.0080	0.0072	-0.0379	-2.781	-2.154	±	0.0413		0.14	1.07	-0.29

